CODING FOR SATELLITE CHANNELS WITH CO-CHANNEL AND INTERSYMBOL INTERFERENCE

by

Whay Chiou Lee

Submitted to the

DEPARTMENT OF ELECTRICAL ENGINEERING AND COMPUTER SCIENCE

in partial fulfillment of the requirements

FOR THE DEGREES OF

BACHELOR OF SCIENCE

and

MASTER OF SCIENCE

at the

MASSACHUSETTS INSTITUTE OF TECHNOLOGY

June, 1983

Signature of Author_____
Department of Electrical Engineering and Computer Science,
May 16, 1983

Certified by_____
Assoc. Prof. Pierre A. Humblet
Thesis Supervisor (academic)

Certified by_____
Dr. Russell J.F. Fang
Company Supervisor, COMSAT Laboratories

Accepted by_____
Prof. Arthur C. Smith
Chairman, Departmental Committee on Graduate Students

CODING FOR SATELLITE CHANNELS WITH CO-CHANNEL AND INTERSYMBOL INTERFERENCE

by

WHAY CHIOU LEE

Submitted to the Department of Electrical Engineering and Computer Science on May 16, 1983 in partial fulfillment of the requirements for the Degrees of Bachelor of Science and Master of Science in Electrical Engineering

ABSTRACT

This thesis presents a combined coding and modulation technique for four-dimensional satellite transmissions in the presence of interference and noise. Improved error performance is achieved by four-dimensional channel coding with expanded signal sets in a manner which increases free Euclidean distance. A power-efficient four-dimensionally coded phase-shift-keying system (PSK) is described. Convolutional coding with maximum likelihood decoding is used to further trade off bandwidth for power. Using Ungerboeck's rules for channel signal assignment, simple trellis codes are selected. Lower bounds are derived for the free Euclidean distance at the output of the modulator, and asymptotic performance is evaluated. It is shown that combining a rate 2/3 encoder with four-dimensionally coded quarternary phase-shift-keying yields an Eb/No gain of 3 to 4 dB over uncoded two-dimensional BPSK, at moderate signal-to-noise ratios.

The performance of the coded four-dimensional system in the presence of AWGN, co-channel interference, intersymbol interference, and other satellite channel non-linearities is simulated on the computer.

Thesis Supervisors: Dr. Pierre A. Humblet
Associate Professor of Electrical Engineering

Dr. Russell J.F. Fang
Director of Transmission Systems Laboratory
COMSAT Laboratories

ACKNOWLEDGMENTS

I would like to thank Professor Pierre Humblet for his invaluable guidance that made this thesis meaningful. Special thanks go to Dr. Russell Fang, who first introduced me to the subject and provided very helpful supervision during the course of my research.

I gratefully acknowledge the extensive industrial practice experience acquired in my co-op work assignments at COMSAT Laboratories. I have enjoyed working with my colleagues, in the Communications Systems Studies department, who have provided support, encouragement and constructive comments throughout my assignment. I am particularly indebted to Dr. Peter Chang who has patiently helped me learn to use and modify the "Channel Modeling Program". I have benefitted from my discussions with Dr. Walter Hagmann, Dr. Ken Mackenthun, Mr. Smith Rhodes, and Mr. William Sandrin, on various topics related to my research. I also want to thank Brenda Hichborn for her invaluable assistance in the final preparation of the report.

Last but not least, I would like to thank my parents, from whom I have learnt to persevere. This thesis is dedicated to them with love.

Table of Contents

Table of Contents (Cond't)

Table of Contents (Cond't)

Table of Contents (Cond't)

List of Illustrations

List of Illustrations (Cont'd)

List of Illustrations (Cont'd)

List of Tables

1. INTRODUCTION

Over the past few decades, there has been an exponential growth in the needs for communication services [1]. Continuous efforts have been made to improve and expand the capabilities of communication systems. Today, communication is no longer a generalization of telephony, radio and television transmissions. It also offers a whole new spectrum of services to mankind, such as navigation, weather-forecasting, astronomy, remote medical diagnosis, electronic mail, teleconferencing, and many other esoteric applications.

The rapid advancement in communications satellite technology has significantly lowered the costs of communications, and extended communication links to remote corners of the world. With the advent of the space shuttles, satellite deployment will soon become a routine in space. The geosynchronous orbit is already heavily congested with satellites operating in the commercial C-band frequency region (6/4-GHz). Bandwidth availability in this frequency region is limited to only about 500 MHz. Hence, if future demands for communication services are to be met, it is necessary to open up new spectral resources or to utilize the limited available spectrum more efficiently. Higher frequency bands are potentially available for satellite transmissions. Frequencies in the K-band frequency region (14/11-GHz) have already been employed by several commercial satellites such as the INTELSAT V satellites.

An alternative solution to the problem of limited spectral resources is multiple reuse of available frequency bands, which can be achieved by orthogonal polarization or by multiple exclusive spot beams [2]-[4]. Unfortunately, the utilization of these frequency-reuse systems is strongly contingent upon a

satisfactory level of antenna beam isolation or cross-polarization discrimination. Non-ideal antenna systems often impose a limit to the achievable level of beam isolation. Propagation difficulties such as attenuation and phase shifts due to rain, particularly severe at frequencies above 10 GHz, can significantly reduce the cross-polarization discrimination of a dual-polarized frequency-reuse system [5]. Imperfect isolation of channels utilizing the same frequency band results in co-channel interference. Although it is possible to design antenna systems with high directionality, or transmission systems with adaptive cross-polarization cancelling devices, it is often very costly and impractical to maintain perfect orthogonality between the frequency-reuse channels under all weather and operational conditions.

Besides co-channel interference (CCI), many other forms of interference and noise are present in the satellite channels. Additive white Gaussian noise is almost always present in any communication system. Imperfect transponder frequency isolation results in adjacent channel interference (ACI). Non-ideal channel filtering gives rise to intersymbol interference (ISI). Due to the presence of various inter-channel interference, satellite communication systems are often power-limited in the sense that increasing the signal power does not improve the signal-to-interference ratio without limit.

Given the power and bandwidth constraints, it is desirable to design and use modulation techniques with high resistance to interference. On top of that, improved coding techniques can also be used to protect the desired signals from interference and noise impairment. Over the past few years, coding and modulation have evolved to become a combined entity in the design of modern communication systems.

Communication data is often transmitted over multiple channels which, due to various interference, are not perfectly orthogonal. It is intuitively convincing that system performance is best if the coding and modulation problems are considered jointly for all the channels. However, this is usually not done in the current technology, where the transmission system for each channel is often designed separately. For instance, frequency-reuse channels have often been treated as independent channels. In addition co-channel interference is usually assumed to be some kind of additive Gaussian noise. Such assumptions have undoubtedly simplified the analysis and design of frequency-reuse communication systems. Nevertheless, they are not very realistic. Moreover, it appears to be possible and certainly an advantage to cooperatively process the signals that are to be transmitted through the channels employing the same frequency. Information theory shows that the channel capacity region of a multiple dimensional channel expands with increasing co-operation among the transmitters and receivers for all the component channels.

With ever increasing orbital overcrowding by communications satellites, [6] and with improved knowledge of the nature and statistics of rain depolarization [7], the problems of co-channel interference in frequency-reuse systems have become a greater concern of modern communications engineers. Advanced communications technology, especially in the area of coding and modulation, will enable future satellite systems to continue the trend of expanding capacities with greater frequency-reuse, and improving transmission reliability in the presence of interference and noise.

In this thesis, we study a combined coding and modulation technique for transmission systems with four dimensions, which

consist of the in-phase and quadrature components of two two-dimensional channels. Using the above technique, we then design four-dimensional transmission systems which are highly resistant to interference such as intersymbol interference and co-channel interference. This thesis basically consists of eight sections. Following this introduction to the problems in satellite communications is a review of previous work on multi-dimensional systems, combined coding and modulation techniques, intersymbol interference, rain depolarization, and other areas of concern in this research.

Section 3 gives a detailed outline of the problems addressed in this thesis, and the steps taken in the design of the interference-resistant four-dimensional transmission systems. In Section 4, we present the methods of four-dimensional modulation and coding. The techniques involve optimal selection of four-dimensional signals from an expanded signal set, and the use of convolutional codes which maximize the minimum free Euclidean distance between channel symbol sequences at the output of the modulator. The idea of four-dimensionally coded modulation is also introduced. Asymptotic coding gains are evaluated.

Section 5 describes the application of four-dimensional modulation and coding methods on the design of a transmission system for channels with intersymbol interference. Asymptotic coding gains in the presence of intersymbol interference are evaluated, and the performance of the system is compared to that of existing optimal two-dimensional systems.

In Section 6, the design of a four-dimensional frequency-reuse transmission system is presented. The robustness of the system performance in the presence of both co-channel and intersymbol interference is studied.

The performance of the coded four-dimensional QPSK systems is simulated on the computer, using some modified portions of the Channel Modeling Program ("CHAMP") developed at COMSAT Laboratories. The results are presented in Section 7. We also examine the system performance in satellite channels subject to various nonlinearities by similar computer simulations.

The last section provides a discussion of, and conclusion from, the results obtained in this research. Suggestions are made for future research.

2. LITERATURE SURVEY

The studies of communication in the presence of noise date back to as early as the 1900's. In the 1940's Shannon showed that information could be transmitted over a noisy channel at a positive rate, limited by its channel capacity, with an arbitrarily low probability of error at the receiver [8],[9]. Since then, there have been extensive studies and considerable interests in various transmission schemes which exhibit such behavior [10]-[12].

The classical theories of detection, estimation and modulation have been extensively studied by Schwartz, Helstrom, Wozencraft, Jacobs, Van Trees and many others [13]-[16]. In a paper published in 1962, Arthurs and Dym analyzed and compared in detail three basic data transmission systems, namely phase-shift-keying (PSK), amplitude-shift-keying (ASK) and frequency-shift-keying (FSK) [17]. Various types of modulation have been studied and compared by Weaver [18]. More recently, Spilker, Viterbi, Omura and Proakis have made invaluable contributions in the area of digital communications [19]-[21].

Previous theories did not pay much attention to the economics of bandwidth utility. Amoroso has given a summary of the bandwidths of several modulation schemes under different definitions of bandwidths [22]. Due to the increasing demand for spectral resources, spectrally efficient modulation techniques have received considerable attention. Two modulation techniques which retain low spectral sidelobe levels while allowing efficient detection performance are minimum-shift-keying (MSK) and offset quaternary phase-shift keying (OQPSK). These two systems have been analyzed and compared by Gronemeyer and McBride [23].

Although spectral efficiency is a major concern in the design of communication systems, signal design for improved probability of error has not been given less attention. The fundamentals of optimal signal design can be found in a book written by Weber [24]. Cahn, Campopiano, Glazer, Lucky, Hancock, Salz, Sheehan, Paris, Simon and Smith have studied combined amplitude and phase modulation schemes, [25]-[29] whereas Foschini, Gitlin, Weinstein, Kernighan and Lin have worked on the optimization of two-dimensional signal constellations in the presence of Gaussian noise and phase jitters [30],[31].

The tradeoff between bandwidth and signal power is well known. Prabhu evaluated the performance of some modulation systems that trade bandwidth for power [32]. In satellite communications, the use of forward error correction (FEC) coding to trade off bandwidth for power has been a very common approach, since satellite repeaters are often more power limited than bandwidth limited. However, as available frequency bands become more and more congested, bandwidth efficiency will be an important criterion in the design of coding systems as well. Multilevel and polyphase signaling may be employed to increase coding gain or improve error performance without expanding bandwidth. Ungerboeck has a very good example of coding with multilevel and polyphase signaling [33]. Earlier in 1965, Zetterberg published a paper on a class of codes for polyphase signals in a band-limited Gaussian channel [34].

Coding is a very extensively studied topic, [35]-[38]. There are two types of commonly used codes, namely block codes and convolutional codes. It has been recognized that convolutional codes generally outperform block codes of the same order of complexity [39],[40]. The Viterbi decoding algorithm [41],[42] which is an optimal maximum likelihood decoding

technique, has been shown to be particularly suitable for satellite channels by Heller and Jacobs [43]. Foremost, among the recent work on convolutional coding theory is that of Forney, which includes a three-part series devoted to algebraic structure, maximum likelihood decoding, and sequential decoding, respectively [44]-[47].

The real satellite channels are never free from interference and noise. In the design of transmission systems for satellite communications, it is difficult to combat interference because its characteristics are usually nonlinear or have not been fully understood. More often than not, the channels are subject to well more than one type of interference. Stavroulakis has put together and edited a volume of papers on interference analysis of communication systems [48]. While most of the papers are devoted to the analysis of one type of interference, Fang and Shimbo presented a unified analysis of a class of digital systems in additive noise and interference [49]. Benedetto, Biglieri and Castellani have studied the combined effects of intersymbol, interchannel, and co-channel interference in M-ary CPSK systems [50]. Due to the complexity of multiple interference, it is only practical to identify the largest interferer and compensate for its undesirable effects. A widely used alternative to interference compensation is to transmit signals with sufficiently large minimum Euclidean distances between them in order to ensure satisfactory performance.

Multiple reuse of frequencies to conserve spectrum is not a very new approach. However, it is subject to many limitations which are yet to be overcome. The primary limitation is co-channel interference resulting in cross-talk between the frequency-reuse channels [51]. There have been extensive studies on co-channel interference in dual-polarized frequency-reuse

systems due to depolarization [52]-[56]. Mathematical models of the nature of rain depolarization have been developed by Oguchi and Chu [57],[58]. Depolarization measurements have been carried out by DiFonzo, Trachtman, Semplak, Tseng, Cheng and many others [59]-[61]. Oguchi has a summary and a discussion of the results obtained by many of them. Orthogonality restoring or adaptive polarization control systems have been designed by many researchers such as Chu, Kreutel, DiFonzo, Trachtman, Williams and Lee [62]-[73].

Intersymbol interference arises in pulse-modulation systems when signals in successive time dimensions are not perfectly orthogonal [74]. Appropriate baseband pulse shaping and use of sampling rates that satisfy the Nyquist's criterion can, in principle, eliminate intersymbol interference. Tufts gave a fairly thorough discussion on the Nyquist's problem in one of his papers [75]. Gerst and Diamond proposed a method of eliminating intersymbol interference by input pulse shaping [76]. In practice, interference is often unavoidable because of non-linear channel filtering and system timing errors [77]. Sometimes, intersymbol interference is introduced deliberately for the purpose of spectral shaping in certain modulation schemes for bandlimited channels. Bershad and Vena proposed a method of eliminating the effects of intersymbol interference with a state space approach [78]. The effects of intersymbol interference on pulse-modulated signals, and associated error probabilities, have been studied in considerable detail in recent literature [79]. Optimum demodulation for channels with intersymbol interference has been studied extensively by Forney [80], who showed that the Viterbi algorithm can be used to optimally demodulate signals in channels that suffer from intersymbol interference. Vermeulen and Hellman considered using a reduced state Viterbi algorithm to

combat intersymbol interference [81]. They showed that the method is asymptotically optimal for large signal-to-noise ratios. On the other hand, Viterbi and Omura suggested using an extended state Viterbi decoder for the maximum likelihood demodulation of convolutionally coded data transmitted over an AWGN channel with intersymbol interference of finite memory [20].

Conventional design of coding systems involves selection of binary codes which maximize the minimum Hamming distance between codewords. The codewords are then input to a modulator. It has been realized that the above approach does not necessarily optimize the performance of the overall system. The mid-seventies saw a revolution in the concepts of optimal coding and modulation. Combined coding and modulation techniques were introduced, initially for the design of communication systems for fading or dispersive channels. Chase, Bello, Pieper, Proakis, Reed, and Wolf are among those who have studied the above novel approach and demonstrated its promises in future communication systems [82]-[84]. The joint optimization of encoder and modulator can be viewed as a search for optimal signal-space codes. A bandwidth-efficient cl ss of signal-space codes has been proposed by Anderson and Taylor [85]. Ungerboeck presented a power-efficient coding and modulation technique with multilevel/phase signals [33]. Convolutionally encoded bits are mapped onto an expanded set of channel signals by set partitioning. The system is optimized with the criterion of maximizing the free Euclidean distance between channel signal sequences.

There have been significant advances in the area of multi-dimensional and multi-user channels since the early sixties. A very comprehensive survey of multi-way channels in information theory has been done by Van Der Meulen [86]. He gave a summary of the results obtained by many information theorists

during the period between 1961 and 1976. The multi-dimensional and multi-user channels which have been studied include the broadcast channels [87],[88], the multiple-access channels [89]-[92], and other channels with various degree of partial cooperation among the users [93]-[95]. The channel capacity regions of the systems have been derived and used as a basis for comparison. It can be deduced from Ahlswede's and Sato's papers that for a multiuser communication channel, the channel capacity region expands with increasing user-cooperation until it reaches its upper bound when the users fully cooperate with each other [96]-[98].

Single-user multi-dimensional systems have often been considered in two dimensions, such as QAM and PSK. Higher dimensional systems which have received considerable attention are various forms of diversity systems. Welti and Lee have studied some four-dimensional transmission systems which are different from orldinary diversity systems [99]. They showed that the performance of the four-dimensional systems in general exceeds that of two independent two-dimensional systems. Welti has, in particular, proposed a novel four-dimensionally coded QAM [100],[101]. Welti's results provided the motivation for the author to study four-dimensionally coded PSK, which are presented in subsequent sections of this thesis.

Much work has been done in the area of communication in the presence of noise and interference. A brief survey such as the above can hardly cover every aspect of the area. Nevertheless, it does point out the collection of previous work which provided the technical foundation and motivation for the studies reported in this thesis.

3. DESCRIPTION OF THE PROBLEM

Let us first look at multiple dimensional channels from an abstract point of view. We will consider four-dimensional channels in particular since they are our major concern here. Generalizing the following discussion to higher dimensions is straightforward. After the effect of interference on four-dimensional channels has been discussed, design procedures for an interference-resistant four-dimensional communication system will be presented briefly.

3.1 FOUR-DIMENSIONAL CHANNELS

There are many types of four-dimensional channels, which include four-user channels without cooperation (Figure 3-1), multiple-access channels (Figure 3-2), broadcast channels (Figure 3-3) and four-user channels with full cooperation (Figure 3-4). A discrete memoryless four-dimensional channel is completely characterized by its joint transition probabilities, $p(\underline{y}|\underline{x})$, where $\underline{x}$ and $\underline{y}$ are four-dimensional vectors representing the discrete inputs and outputs of the channel, respectively. The four-dimensional channel can be represented by the block diagram shown in Figure 3-5.

The capacity regions of multiple-access, broadcast and multi-user channels have been studied by Ahlswede, Cover, Sato and many other information theorists [86]-[98]. The general conclusion from their results is that the capacity region of a multi-dimensional system increases with user cooperation, when there is no perfect orthogonality among the component channels.

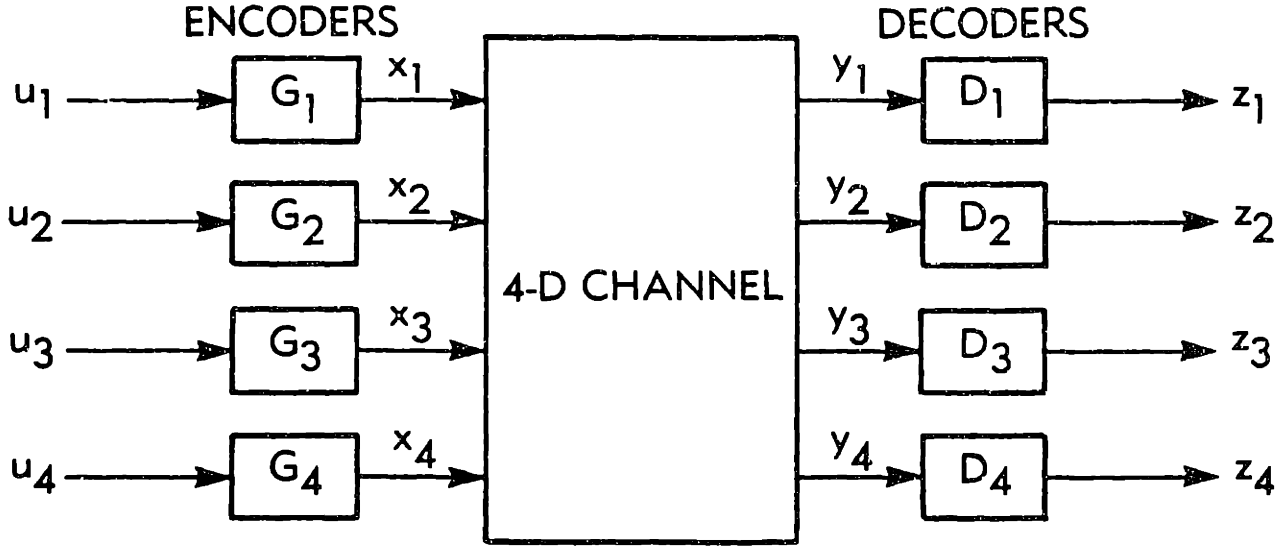

Figure 3-1. Channels Without Cooperation

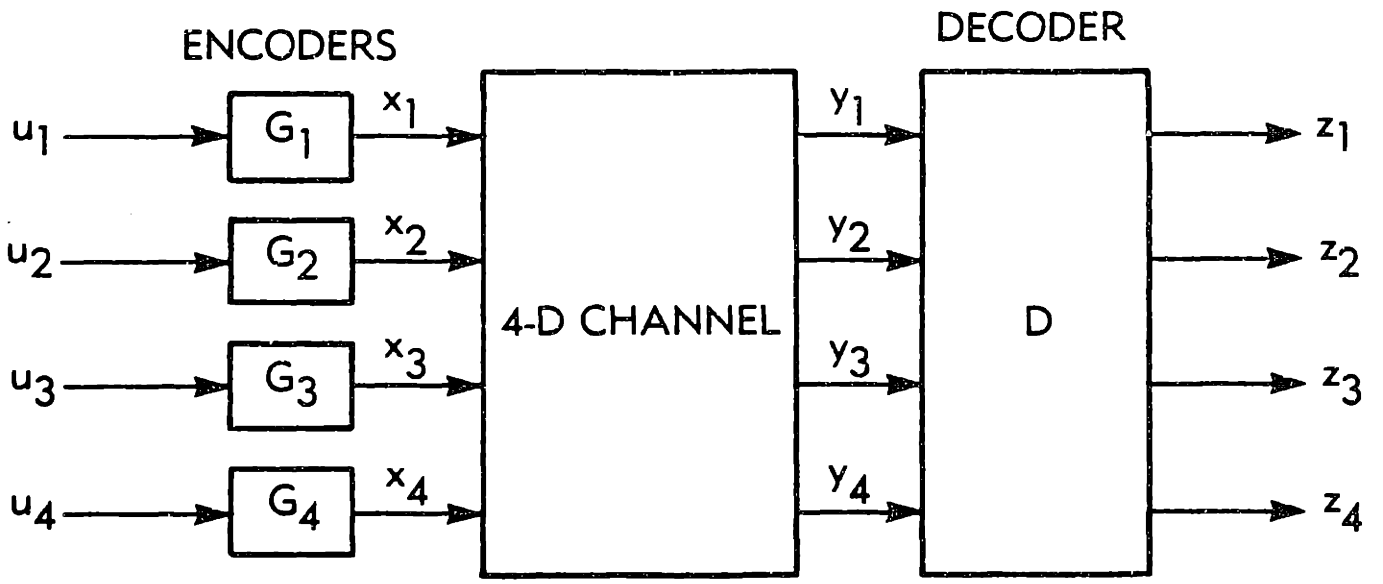

Figure 3-2. Multiple Access Channels

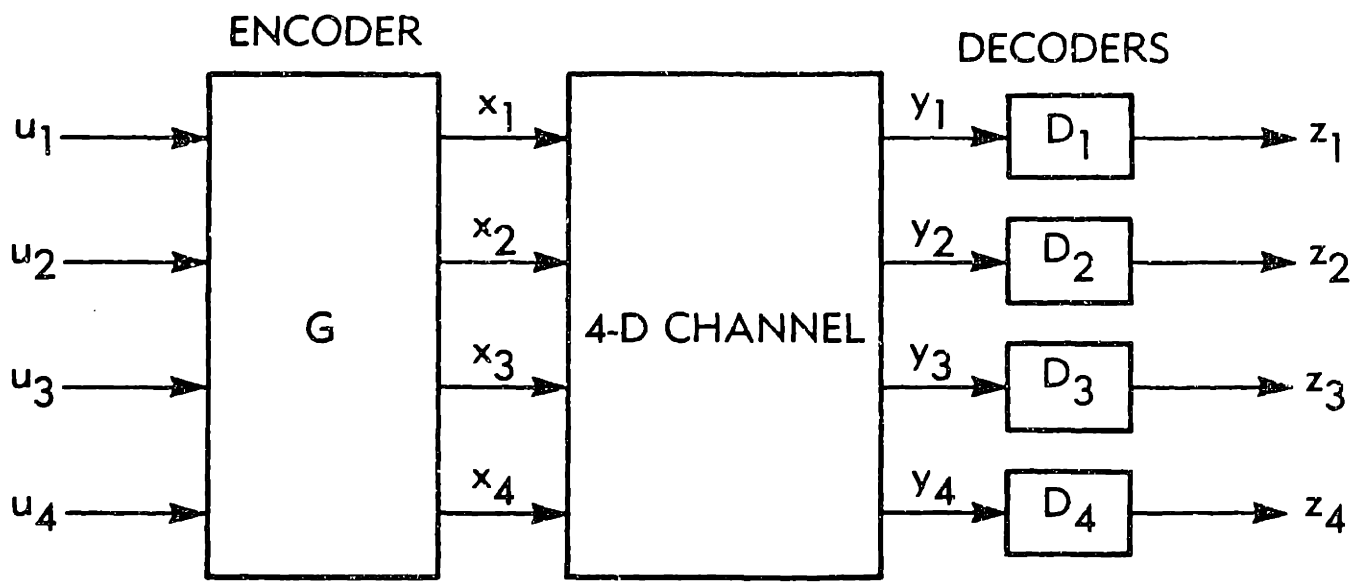

Figure 3-3. Broadcast Channels

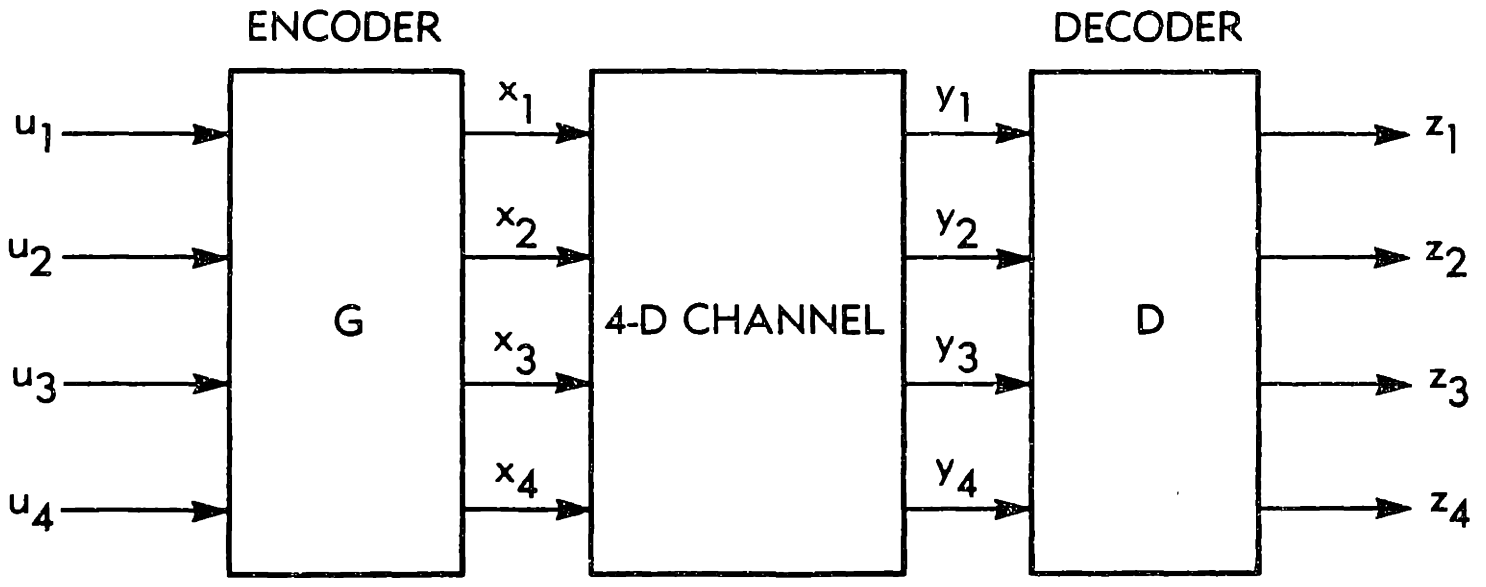

Figure 3-4. Channels With Full Cooperation

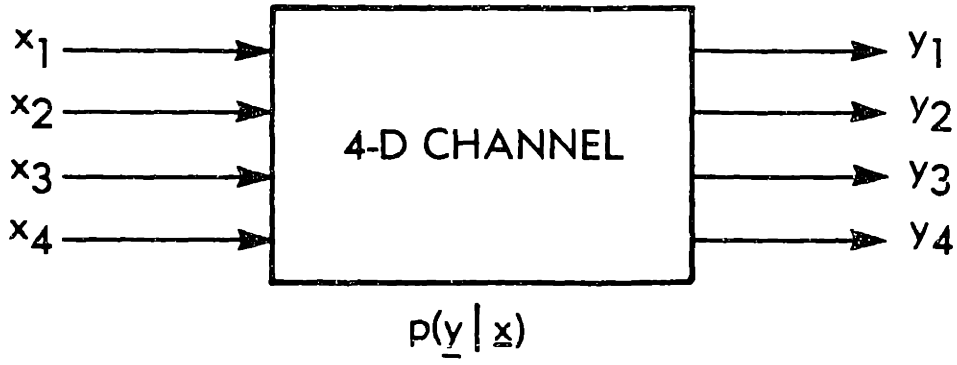

Figure 3-5. 4-D Channel Block Diagram

We will examine a less general but common class of four-dimensional discrete channels. The input/output matrix representation is given below.

$$\begin{bmatrix} y_1 \\ y_2 \\ y_3 \\ y_4 \end{bmatrix} = \begin{bmatrix} a_{11} & a_{12} & a_{13} & a_{14} \\ a_{21} & a_{22} & a_{23} & a_{24} \\ a_{31} & a_{32} & a_{33} & a_{34} \\ a_{41} & a_{42} & a_{43} & a_{44} \end{bmatrix} \begin{bmatrix} x_1 \\ x_2 \\ x_3 \\ x_4 \end{bmatrix} + \begin{bmatrix} n_1 \\ n_2 \\ n_3 \\ n_4 \end{bmatrix} \qquad (3\text{-}1)$$

where $\{a_{ij}\}$ is assumed to be a set of known interference coefficients, and n_1, n_2, n_3, and n_4 are independent AWGN. In simpler notations, the above expression can be written as follows.

$$\underline{y} = A\,\underline{x} + \underline{n} \qquad (3\text{-}2)$$

The joint transition probability is given by

$$p(\underline{y}|\underline{x}) = p(\underline{n} = \underline{y} - A\underline{x}) = \prod_{k=1}^{4} P(n_k = y_k - \sum_{j=1}^{4} a_{kj}x_j) \qquad (3\text{-}3)$$

Channels which are subject to various kinds of known cross-channel interference can be sufficiently characterized by the above joint transition probability.

A four-dimensional channel can be conveniently modeled as two two-dimensional channels, each with separately modulated in-phase and quadrature components. Figure 3-6 depicts this channel configuration.

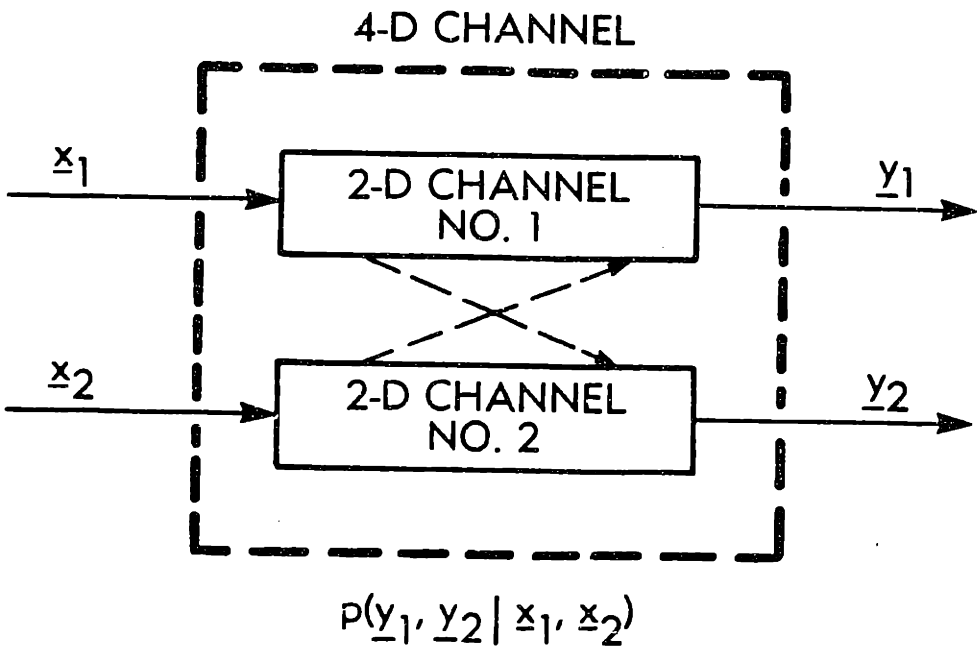

Figure 3-6. 4-D Channel Configuration

Let the matrix, A be partitioned into four two-by-two matrices.

$$A = \begin{bmatrix} A_{11} & A_{12} \\ A_{21} & A_{22} \end{bmatrix} \tag{3-4}$$

A_{11} and A_{22} are each the matrix pertaining to interference within the respective two-dimensional system. A_{12} and A_{21} account for the cross-channel interference. Traditionally, the two-dimensional systems are designed separately, and the cross-channel interference is ignored. In the research reported in this thesis, we specifically assume that A_{12} and A_{21} are non-zero matrices, which serve to describe the satellite channels more realistically.

The above model of a four-dimensional discrete channel applies equally well to continuous channels, since continuous signals can easily be represented by vectors by choosing an appropriate basis.

3.2 PROBLEM STATEMENT AND DESIGN PROCEDURES

As discussed, it is possible to improve the overall performance of two two-dimensional communication systems with interference by treating them as one four-dimensional system and including sufficient cooperation between them. It is our objective, in this study, to design a four-dimensional system whose performance is better than its corresponding independent two-dimensional systems, especially in the presence of interference that destroys channel orthogonality. The performance of the four-dimensional system in the presence of noise and interference

will be evaluated and compared to that of the two-dimensional systems.

Since the additive noise is assumed to be AWGN, the system performance depends on the Euclidean distance between signals. It is a common practice to maximize the Euclidean distance in the design of the systems. If the cross-channel interference is known or has some linear properties that can be exploited mathematically, the system performance can be improved somewhat by employing appropriate interference cancellation devices. However, more often than not, the above approach introduces correlation among the noise components, resulting in colored noise. It therefore will complicate the design. In this study, the author has taken the approach of maximizing the Euclidean distance in the presence of interference.

We are interested in two types of dimensions, namely dimensions in time and dimensions in space or polarization. In the time-dimensional system, the four-dimensional signals consist of pairs of consecutive pulses, each of which has both in-phase and quadrature components. In the space or polarization-dimensional system, the four-dimensional signals consist of pairs of pulses which are transmitted over two frequency-reuse channels that are not necessarily orthogonal in time.

In the next chapter, we will describe some simple four-dimensional modulation systems which consist of two two-dimensional systems. Attention is restricted to phase-shift-keying because it is not sensitive to non-linear amplification, which is common in satellite transmission systems. A sub-optimal coding scheme for the above systems will be discussed. The coding scheme proposed in this study consists of two parts. The first part involves coded modulation, which closely resembles joint block coding and modulation. The second part is

convolutional coding. Ideally, both parts should be optimized together. Unfortunately, this would involve complicated mathematical optimization techniques. Hence, we resort to optimizing the two parts separately. Using a combined coding and modulation approach, we manipulate the code in the signal space and try to maximize the free Euclidean distance between channel symbol sequences.

In the design of our coded four-dimensional PSK Systems, Ungerboeck's method of set-partitioning is used for the assignment of channel signals to binary codewords such that the minimum Euclidean distance between channel signals is maximized. The above method of signal assignment also enables the derivation of a simple but tight lower-bound for the Euclidean distance between the four-dimensional signals.

We have chosen to use convolutional coding because of its superior performance in satellite communications compared to many other coding schemes of equivalent complexity. In a study like this, it is important to obtain deep insights into the structure as well as the performance of the proposed systems. Using complicated convolutional codes with long constraint lengths does not necessarily provide better insights than codes with short constraint lengths. Hence, the author has chosen to employ simple codes selected according to several basic rules given by Ungerboeck.* The lower bounds for Euclidean distances between channel signals, obtained with the aid of set-partitioning, can be used in code searching by exhaustive computation. Nonetheless, in this 6 to 7 months of study, there was not enough time for the author to carry out a computer search for

*Ungerboeck claimed that small memory codes obtained according to his rules are optimum, and it could be confirmed easily by hand-search [33]. Using Ungerboeck's rules, Wilson, et al. have obtained some good rate 3/4 16-PSK phase codes [102].

codes with large constraint lengths. Lower bounds for free Euclidean distances are derived and used to evaluate the asymptotic performance of the codes.

The application of our coding scheme for four-dimensional QPSK is demonstrated in two separate sections. In Section 5, a nominally time-orthogonal four-dimensional system with intersymbol interference is considered. Lower bounds for free Euclidean distances in the presence of intersymbol interference are derived. Free Euclidean distances for the few simple codes selected are obtained by exhaustive searching. In Section 6, the coding scheme for four-dimensional QPSK is applied on a frequency-reuse system with co-channel interference. Lower bounds for free Euclidean distances in the presence of co-channel and intersymbol interference are derived.

Apart from evaluating the four-dimensional systems in terms of their asymptotic performance, their coding gains at moderate signal-to-noise ratios are also examined by computer simulation. The deterioration in performance due to co-channel interference, intersymbol interference, and other satellite channel non-linearities is also simulated. The Channel Modeling Program ("CHAMP") was used for the simulation.*

*A description of CHAMP can be found in References [103] and [104].

4. FOUR-DIMENSIONAL MODULATION AND CODING

In this section, we present the design of a four-dimensional transmission system with cooperative encoding and joint decoding. Phase-shift-keying systems are chosen because they are not very sensitive to non-linear amplification which abounds in most satellite channels [105],[106].

Let's consider the system block diagram shown in Figure 4-1. We are interested in the channel coding for the system. The four-dimensional joint coding and modulation scheme consists of basically three parts, namely:

a. Signal design for four-dimensionally coded modulation;
b. Four-dimensional channel signal assignment;
c. Selection of forward error correction (FEC) codes.

The inputs to the encoder are assumed to be two symmetrical, binary and memoryless message sequences. The encoder outputs are mapped onto the four-dimensional channel signals by the signal mapper, which plays the role of another encoder. In this respect, the above coding scheme is actually some kind of concatenated coding. The received signals are demodulated before they are fed into the decoder, which jointly decodes the message sequences. If convolutional codes are used, the decoder is a Viterbi maximum likelihood decoder. The four-dimensional signals are represented by number pairs, such as (a, b), whose components represent the corresponding two-dimensional signals.

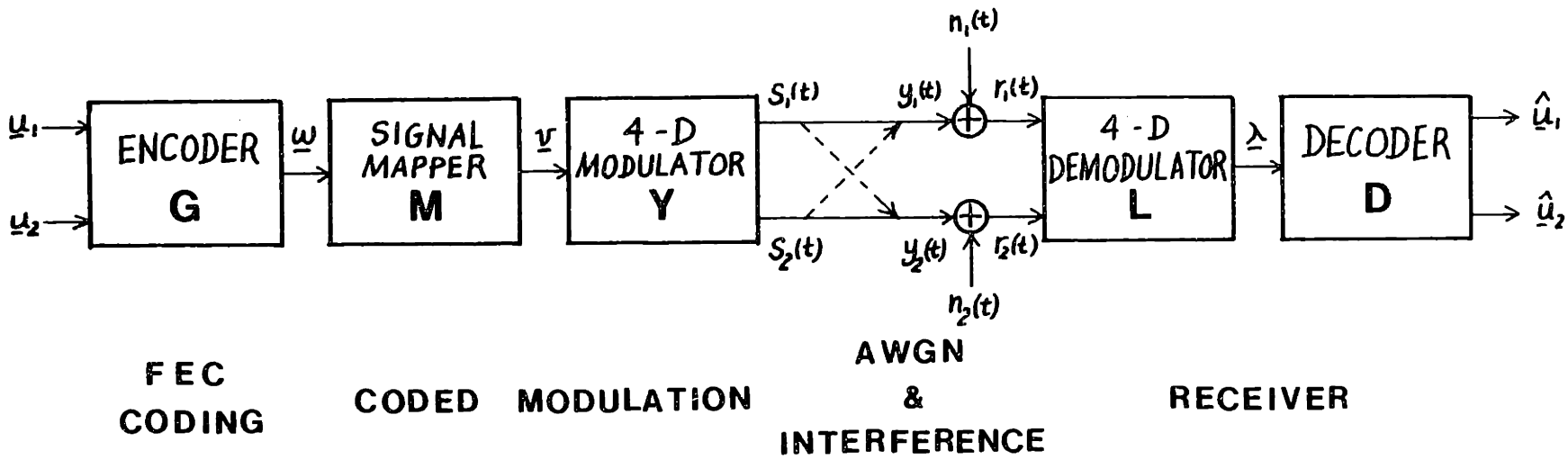

Figure 4-1. Four-Dimensional Transmission System

4.1 FOUR-DIMENSIONAL MODULATION

A four-dimensional modulator outputs pairs of two-dimensional signals during every unit of time. The pair of two-dimensional signals can be orthogonal in time, or orthogonal in space or polarization. It is assumed that the signal constellations of the two-dimensional components are identical. Thus, it suffices to specify the four-dimensional signals by a two-dimensional signal constellation together with the corresponding set of number pairs.

Consider four-dimensional QPSK as an example. The signal constellation is shown in Figure 4-2. There are altogether 16 possible four-dimensional signals, represented by(0,0),(0,1),(0,2),(0,3),(1,0),(1,1),(1,2),(1,3),(2,0),(2,1),(2,2),(2,3),(3,0),(3,1),(3,2),(3,3).

4.2 CODED MODULATION AND SIGNAL DESIGN

In an ordinary modulation, an M-ary input sequence is mapped onto an M-ary channel signal. The input sequence to the modulator is usually the output of an encoder. In coded modulation, an M-ary sequence is mapped onto an N-ary channel signal, such that N > M. Ordinary modulation and coded modulation are compared in Figure 4-3.

It is assumed in this section that the signal-space code-base is a standard n-PSK. The subset of M channel signals are selected such that the minimum Euclidean distance, denoted by d_{min}, is maximized. For two-dimensional PSK, maximization of the minimum Euclidean distance results in choosing the signals such that they are evenly distributed around a circle. Specifically,

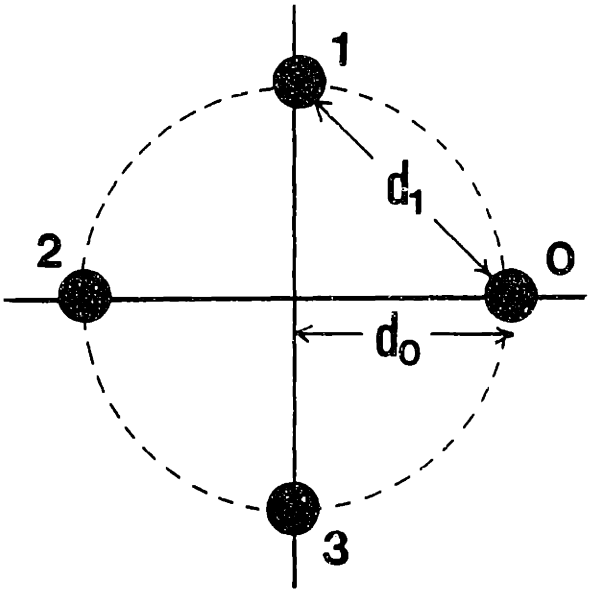

Figure 4-2. QPSK Signal Constellation

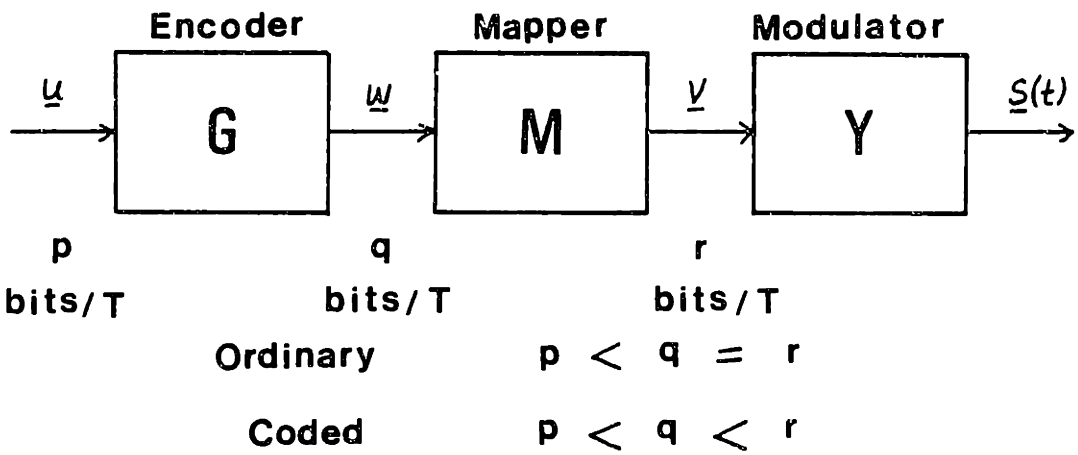

Figure 4-3. Ordinary Modulation and Coded Modulation

to choose an optimal subset of $M = 2^q$ signals from a code-base of $N = 2^r$ PSK signals, where q and r are both integers and $q < r$, the following method can be used.

Figure 4-4 shows a two-dimensional PSK constellation with $n = 2^r$ signals, distributed evenly around a circle of radius, d_0. The signals are labeled from 0 to n-1 in a counter-clockwise manner. Let d_k be the distance of the k^{th} signal from the signal labeled 0. Then, d_k is given by;

$$d_k^2 = 2\, d_0^2 \left(1 - \cos \frac{2\pi k}{n}\right) \qquad (4\text{-}1)$$

The minimum subset distance is given by

$$\Delta_0^2 = d_1^2 = 2d_0^2 \left(1 - \cos \frac{2\pi}{n}\right) \qquad (4\text{-}2)$$

Observe that every signal has two nearest neighbors. And, separating each signal from its neighbors will result in two optimal subsets, with a minimum subset distance given by

$$\Delta_1^2 = d_2^2 = 2d_0^2 \left(1 - \cos \frac{4\pi}{n}\right) \qquad (4\text{-}3)$$

The signals can be successively partitioned in the same manner, yielding optimal subsets with minimum subset distance, Δ_k, after the k^{th} partitioning, where

$$\Delta_k^2 = 2d_0^2 \left(1 - \cos 2^{k+1} \frac{\pi}{n}\right) \qquad (4\text{-}4)$$

Each optimal subset then has 2^{r-k} signals. Hence, to obtain an optimal subset with 2^q signals, the original n-PSK signals have

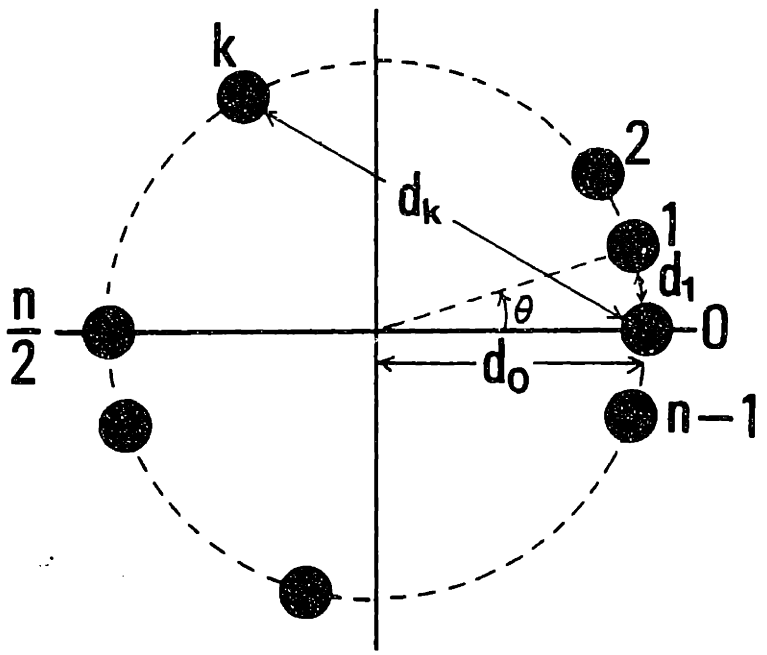

Figure 4-4. n-PSK Signal Constellation

to be partitioned (r-q) times. The above method is best illustrated by an example, say, 8-PSK with r = 3. The various stages are shown in Figure 4-5. The minimum squared subset distances for various q are listed below.

$$q = 3 \quad ; \quad \Delta_0^2 = 0.586\ d_0^2$$

$$q = 2 \quad ; \quad \Delta_1^2 = 2.000\ d_0^2$$

$$q = 1 \quad ; \quad \Delta_2^2 = 4.000\ d_0^2 \qquad (4\text{-}5)$$

The above method of signal design can be applied on the selection of four-dimensional PSK signals as well. Details are discussed in the Subsection 4.2.1.

4.2.1 SIGNAL DESIGN FOR FOUR-DIMENSIONALLY CODED PHASE-SHIFT-KEYING

It is assumed that the four-dimensional PSK signal consists of a pair of two-dimensional PSK signals with identical signal constellations. Our objective is to select a subset of $M = 2^q$ four-dimensional signals from a four-dimensional n-PSK signal set, such that the minimum subset distance is maximized. The code-base in the signal space has $N = 2^r = n^2$ signals. Each signal is represented by a number pair, (a, b). The two-dimensional components, a and b, are represented on the constellation shown in Figure 4-4.

Let's consider a typical signal, say (3, 4). We can visualize, on a two-dimensional picture shown in Figure 4-6, the signal (3, 4) being surrounded by its neighbors. It has four

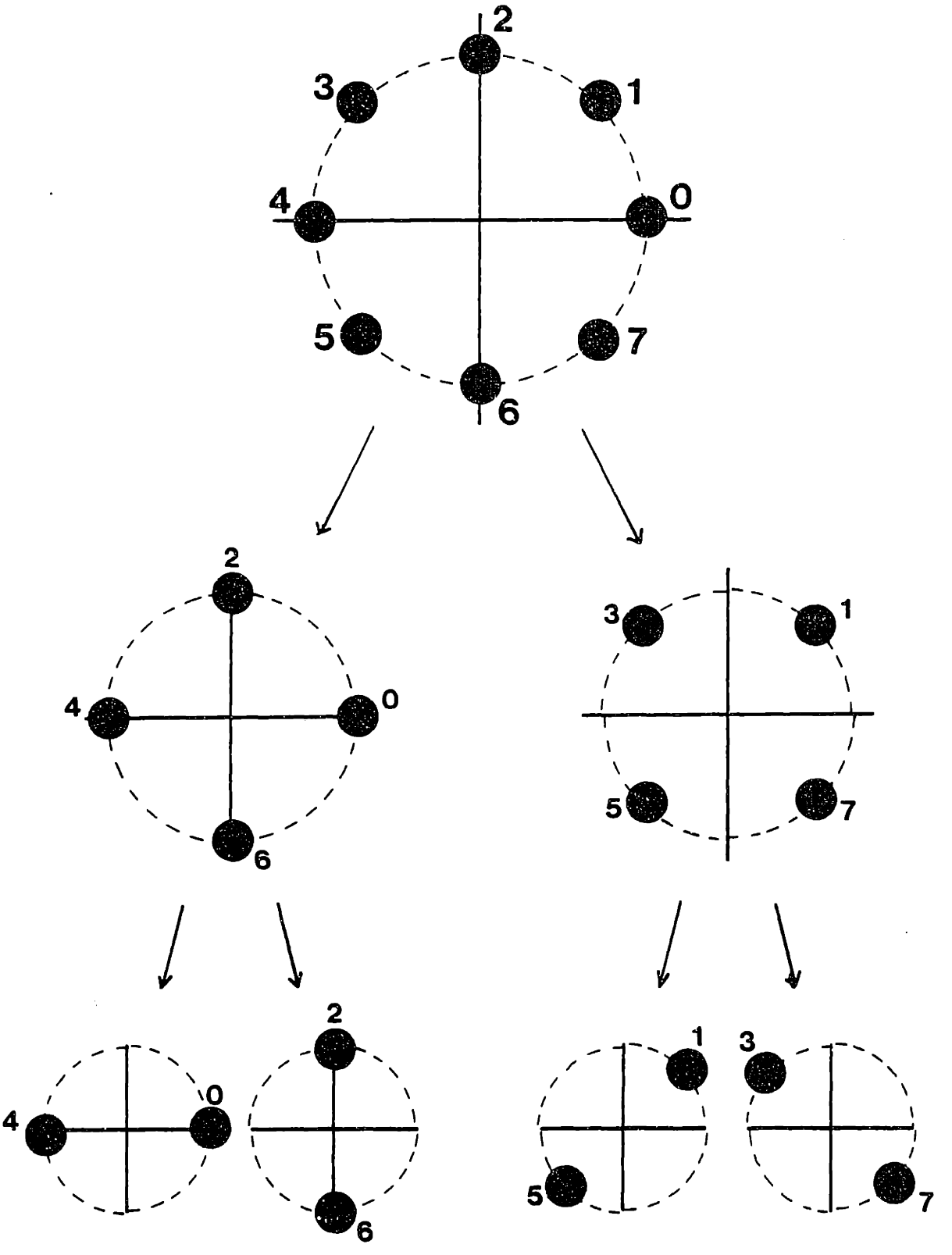

Figure 4-5. Optimal Partitioning of 8-PSK

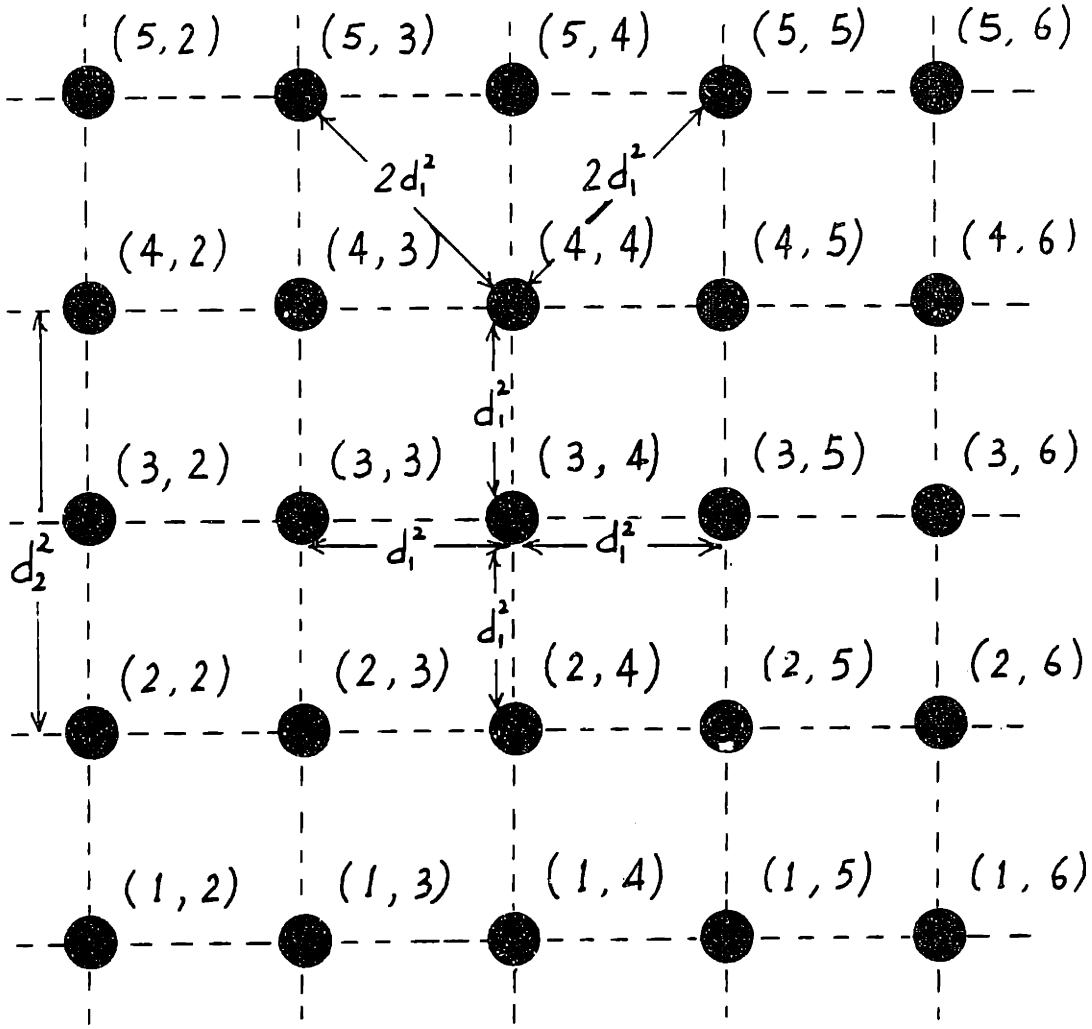

Figure 4-6. 2-D Representation of A 4-D PSK Signal and Its Neighbors

nearest neighbors, namely (3, 5), (4, 4), (3, 3) and (2, 4), which are at a squared distance of d_1^2 away from it. The next four nearest neighbors are at a squared distance of $2d_1^2$ away from (3, 4). Even further away at a squared distance of $d_2^2 \geq 2d_1^2$, there are another four neighbors. To obtain subsets with maximum minimum distance, the signals are successively partitioned such that every signal is separated from its four nearest neighbors. After the k^{th} partitioning, we obtain subsets with 2^{r-k} signals each, and minimum subset distance, Δ_k, given by the following expressions.

$$\Delta_k^2 = \begin{cases} d_x^2 \ ; \ x = 2^{k/2} \text{ for } k \text{ even} \\ 2d_x^2; \ x = 2^{(k-1)/2} \text{ for } k \text{ odd} \end{cases} \qquad (4\text{-}6)$$

It is easy to verify that $\Delta_k^2 \geq \Delta_j^2$ if $k > j \geq 0$. If a signal set with $M = 2^q$ signals is desired, the original four-dimensional signal set has to be partitioned (r-q) times. It is due to the highly symmetrical structure of the four-dimensional PSK constellation that we can partition the signals in the manner discussed above to sort out the desired signal subset. For most other constellations, more sophisticated algorithms are necessary. Notice that the above signal design technique assumes signal sets whose number of signals is an integral power of two. For practical reasons, this is not an unreasonable assumption.

We now consider four-dimensional QPSK as an example. The two-dimensional representation of the signals is shown in Figure 4-7. There are altogether N = 16 four-dimensional signals. We have n = 4 and r = 4. The minimum squared subset distances for various q are listed below.

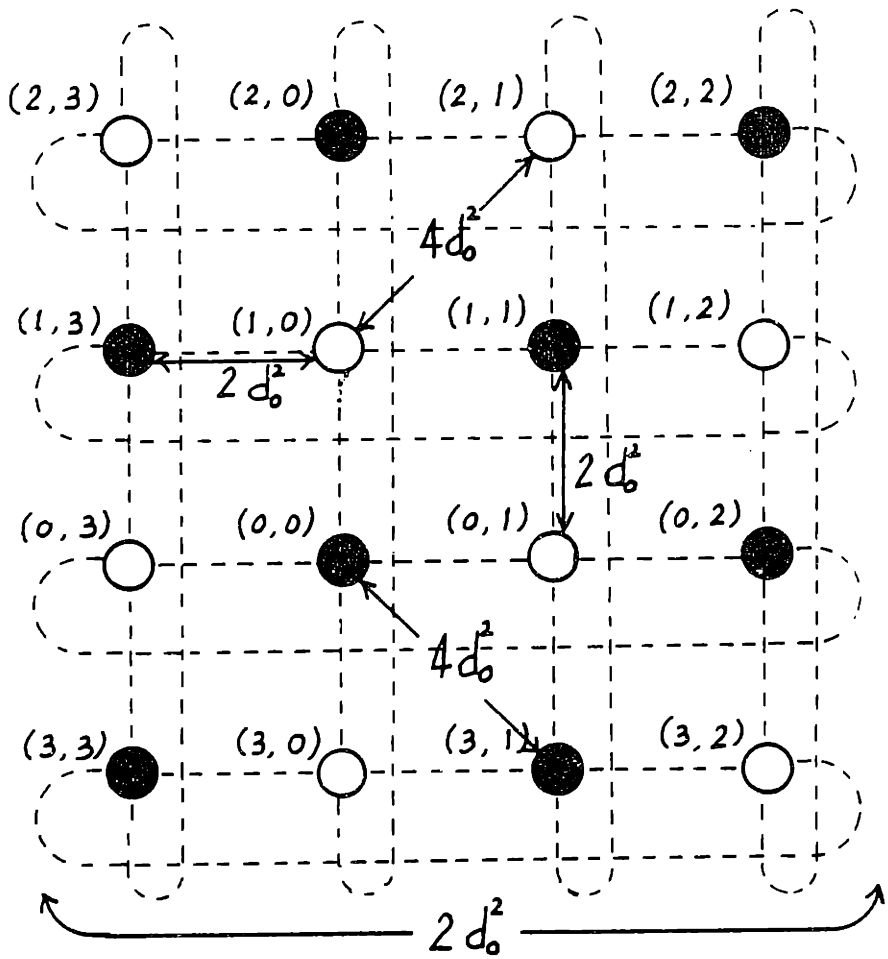

Figure 4-7. 2-D Representation of 4-D QPSK Signals

$$q = 4 \quad ; \quad \Delta_0^2 = d_1^2 = 2d_0^2$$

$$q = 3 \quad ; \quad \Delta_1^2 = 2d_1^2 = 4d_0^2$$

$$q = 2 \quad ; \quad \Delta_2^2 = d_2^2 = 4d_0^2$$

$$q = 1 \quad ; \quad \Delta_3^2 = 2d_2^2 = 8d_0^2 \qquad (4\text{-}7)$$

It is confirmed that $\Delta_k^2 \geq \Delta_j^2$ for all $k > j \geq 0$. Suppose $q = 3$, and $M = 2q = 8$. The above signal design gives rise to two optimal subsets with a minimum squared subset distance of $4d_0^2$. The two subsets are:

Subset A:

$\{(0,1), (2,3), (0,3), (2,1), (1,2), (3,0), (1,0), (3,2)\}$

Subset B:

$\{(0,0), (2,2), (0,2), (2,0), (1,1), (3,3), (1,3), (3,1)\}$.

It can be easily verified that any other collection of eight signals from the four-dimensional QPSK constellation will yield a minimum squared subset distance of $2d_0^2$.

It is worth pointing out that the above signal space codes can be generated by a rate 3/4 block coding followed by the usual one-to-one mapping of binary numbers onto the four-dimensional signals.

Let us look more closely at subset B. Notice that each of the four-dimensional signals consists of two two-dimensional components which are not independent of each other. They are either both odd-numbered signals or both even-numbered signals.

This particular four-dimensionally coded QPSK is similar to one of the four-dimensionally coded QAM proposed by Welti [100],[101].

The presence of cross-channel interference, such as intersymbol interference, and cross-polarization, can degrade the minimum Euclidean distance to a significant extent. The degradation depends on the amount of interference as well as the choice of signal subsets. The method of signal design described above does not guarantee optimality in the presence of interference.

4.3 CHANNEL SIGNAL ASSIGNMENT FOR FOUR-DIMENSIONALLY CODED PSK AND BOUND ON SQUARED DISTANCES

Given the set of four-dimensional signals, $\{(a_i, b_i); i = 1, 2 \ldots M\}$, there are many ways of assigning binary numbers to each of them. A very common assignment is the Gray Code mapping. Unfortunately, Gray Code mapping does not monotonically translate large Hamming distances into large Euclidean distances. Hence, with Gray Code mapping, it is very difficult to design encoders which achieve maximum free Euclidean distance.

Ungerboeck has proposed a very useful technique of assigning binary codewords to channel signals [33]. His approach is based on a mapping rule, called "Mapping by Set Partitioning." The mapping involves successive partitioning of a channel signal set into subsets with increasing minimum distances $\Delta_0 < \Delta_1 < \Delta_2 \ldots$ between the signals of these subsets. The concept of set partitioning has earlier been illustrated in Figure 4-5 for 8-PSK for a different purpose. The result of Ungerboeck's mapping by set partitioning is best summarized on a tree diagram, shown in Figure 4-8. The minimum subset distances are given below.

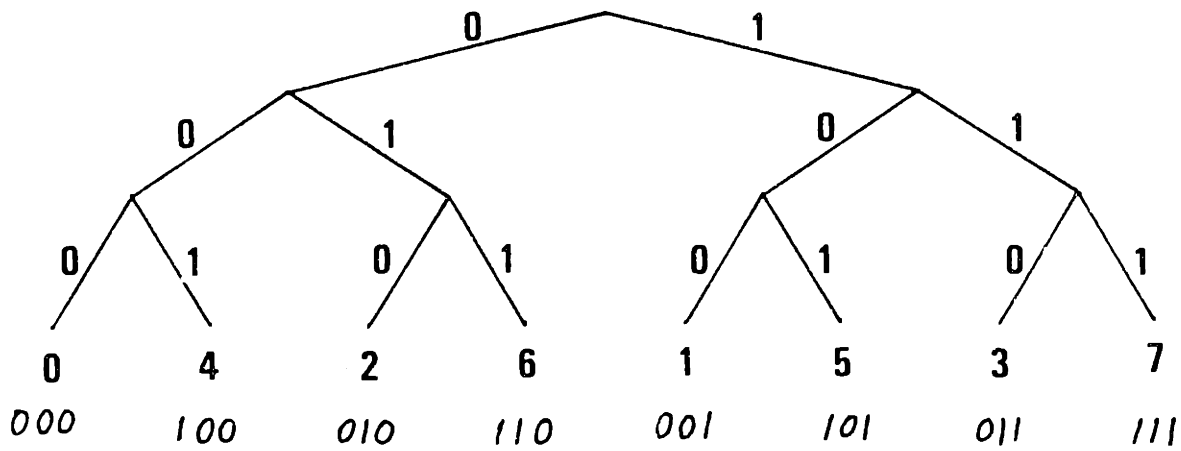

Figure 4-8. Ungerboeck's Set Partitioning of 8-PSK

$$\Delta_0 = d_1 = 0.765\ d_0$$

$$\Delta_1 = d_2 = 1.414\ d_0$$

$$\Delta_2 = d_3 = 2.000\ d_0 \qquad (4\text{-}8)$$

The above method of channel signal assignment gives rise to a very important property of the set of error vectors corresponding to the binary sums of all pairs of binary code-words. Let $\underline{\varepsilon}_k$ be an arbitrary error vector, and $q(\underline{\varepsilon}_k)$ be the number of trailing zeros in $\underline{\varepsilon}_k$. One can easily see that the Euclidean distance corresponding to $\underline{\varepsilon}_k$ is always greater than or equal to $\Delta_{q(\underline{\varepsilon}_k)}$. It is very useful to have a free distance bound which depends only on the error sequences because the bound can be used to search for good trellis or convolutional codes.

Ungerboeck's method of mapping by set partitioning can also be applied on the channel signal assignment for four-dimensionally coded PSK. Let $M(\underline{w})$ be the mapping of the code-word, $\underline{w}$, onto a four-dimensional channel signal. Then, the signals, represented by a number pair is given below:

$$(a,b) = M(\underline{w}) \qquad (4\text{-}9)$$

The squared Euclidean distance between $(a,b) = M(\underline{w})$ and $(a',b') = M(\underline{w}')$ is given by:

$$D\{(a',b'),(a,b)\} = D\{M(\underline{w}'), M(\underline{w})\} = D\{M(\underline{w} \oplus \underline{\varepsilon}), M(\underline{w})\} \qquad (4\text{-}10)$$

where $\underline{\varepsilon}$, defined by $\underline{w}' = \underline{w} \oplus \underline{\varepsilon}$ is the error vector.

In general, $D\{M(\underline{w} \oplus \underline{\varepsilon}), M(\underline{w})\}$ depends on both the error vector, and the codeword $\underline{w}$. Using Ungerboeck's method, with only slight modification, we will derive a simple lower bound on the squared Euclidean distance for a given error vector. The bound depends only on the error vector. Let the bound be $D_b(\underline{\varepsilon})$. Then we have

$$D\{M(\underline{w} \oplus \underline{\varepsilon}), M(\underline{w})\} \geq D_b(\underline{\varepsilon}) \qquad (4\text{-}11)$$

To facilitate further discussion on channel signal assignment for four-dimensionally coded PSK, we will describe a four-dimensional rotational transformation and its properties in Subsections 4.3.1 and 4.3.2, respectively.

4.3.1 FOUR-DIMENSIONAL ROTATIONAL TRANSFORMATION

Transformation of four-dimensional signals can be represented by pairs of transformations on the two-dimensional component signals. Let's define a four-dimensional rotational transformation as follows:

$$T(a,b) \triangleq \{R_a(\Delta\theta_a), R_b(\Delta\theta_b)\} \qquad (4\text{-}12)$$

where $R_a(\Delta\theta_a)$, and $R_b(\Delta\theta_b)$ are the signals resulting from rotational transformations of the two-dimensional signals, a and b by $\Delta\theta_a$ and $\Delta\theta_b$ respectively. Note that for an n-PSK, the rotational transformations, $R_a(\Delta\theta_a)$ and $R_b(\Delta\theta_b)$, are both modulo n. Figure 4-9 shows the transformation of (a,b) into (a',b') = T(a,b). Note that the transformation is discrete, and the angles of

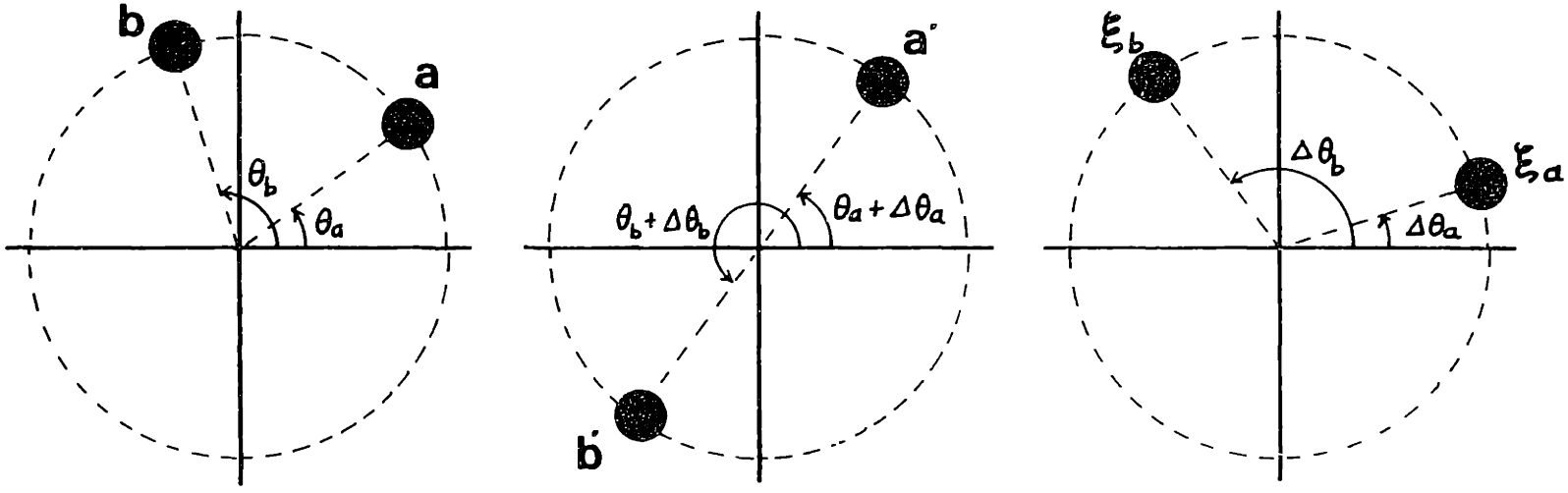

Figure 4-9. Four-Dimensional Rotational Transformation

rotation are all integral multiples of the minimum phase difference, $\theta = 2\pi/n$. In addition, it is assumed that $0 \leq |\Delta\theta| \leq \pi$.

Since the errors in a PSK system are directly related to the rotational transformations, the Euclidean distance between any pair of four-dimensional signals depends only on the phase differences between the corresponding two-dimensional component signals. Hence

$$\begin{aligned} D[(a', b'),(a, b)] &= D\{[R_a(\Delta\theta_a), R_b(\Delta\theta_b)], (a, b)\} \\ &= D\{R_a(\Delta\theta_a), a\} + D\{R_b(\Delta\theta_b), b\} \\ &= D\{R_o(\Delta\theta a), 0\} + D\{R_o(\Delta\theta_b), 0\} \\ &= D\{[R_o(\Delta\theta_a), R_o(\Delta\theta_b)], (0, 0)\} \\ &= D\{(\xi_a, \xi_b), (0, 0)\} \end{aligned} \qquad (4\text{-}13)$$

where

$$\begin{aligned} \Delta\theta_a &= \theta_a' - \theta_a \\ \Delta\theta_b &= \theta_b' - \theta_b \\ \xi_a &\triangleq R_o(\Delta\theta_a) \\ \xi_b &\triangleq R_o(\Delta\theta_b) \end{aligned}$$

Channel signal assignment gives rise to a "tree". Consider any two sub-trees emanating from two intermediate nodes at the same level, as shown in Figure 4-10.

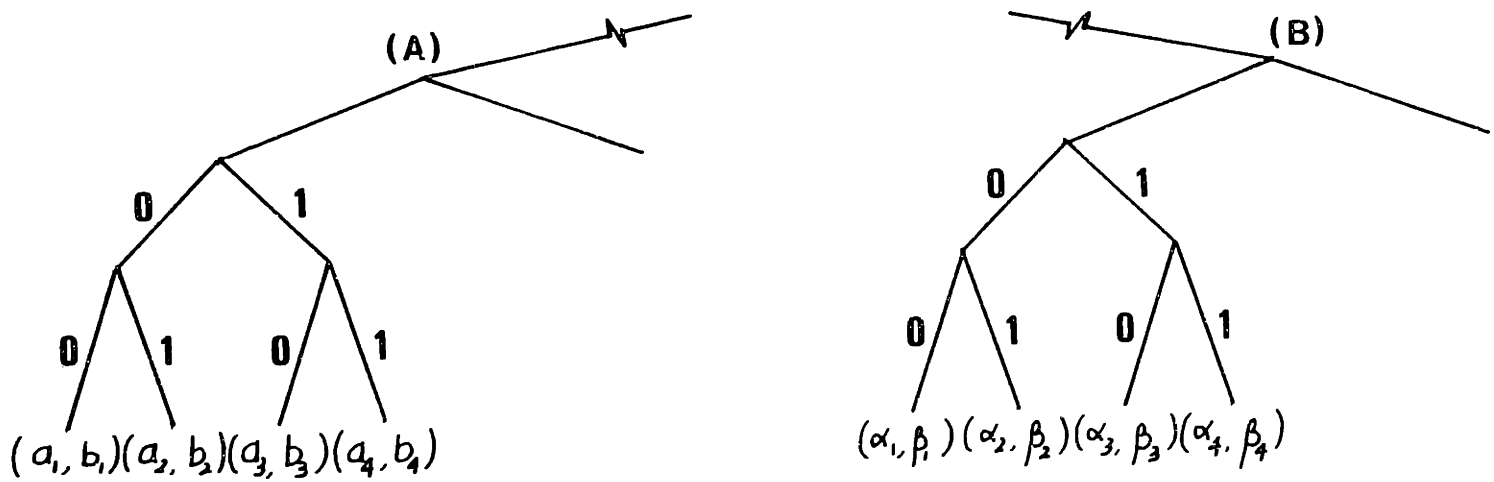

Figure 4-10. Sub-Trees At the Same Level

Theorem

If every corresponding pair of (α_i, β_i) in B and (a_i, b_i) in A are related by the same four-dimensional transformation T, i.e.,

$$(\alpha_i, \beta_i) = \{R_{ai}(\Delta\theta_a), R_{bi}(\Delta\theta_b)\} \text{ for all } i \qquad (4\text{-}14)$$

then sub-tree A and sub-tree B are said to be "equivalent" in the sense that they both have the same distance properties.

Proof

$$\begin{aligned} D\{(\alpha', \beta'), (\alpha, \beta)\} &= D\{[R_a'(\Delta\theta_a), R_b,(\Delta\theta_b)], \\ &\qquad [R_a(\Delta\theta_a), R_b(\Delta\theta_b)]\} \\ &= D\{R_a'(\Delta\theta_a), R_a(\Delta\theta_a)\} \\ &\quad + D\{R_b'(\Delta\theta_b), R_b(\Delta\theta_b)\} \\ &= D\{a', a\} + D\{b', b\} \\ &= D\{(a', b'), (a, b)\} \qquad (4\text{-}15) \end{aligned}$$

Therefore, for every pair of (a',b') and (a,b), there is a corresponding pair of (α', β') and (α, β), such that

$$D\{(a', b'), (a,b)\} = D\{(\alpha', \beta'), (\alpha, \beta)\} \qquad (4\text{-}16)$$

4.3.2 PROPERTIES OF FOUR-DIMENSIONAL ROTATIONAL TRANSFORMATION

a. A four-dimensional rotational transformation, T, moves a four-dimensional signal point by the same Euclidean distance as its inverse, T^{-1}.

$$D[T(a, b), (a, b)] = D[T^{-1}(a, b), (a, b)] \qquad (4\text{-}17)$$

b. The transformation is commutative.

$$T_1T_2(a, b) = T_2T_1(a, b) \qquad (4\text{-}18)$$

It also follows that if a transformation consists of a series of other transformations, the order in which they are taken is not important. For example,

$$T_1T_2T_3(a, b) = T_3T_2T_1(a, b) = T_1T_3T_2(a, b) \ . \ . \ ., \text{ etc.}$$

The above properties lead to the following result. Given a set of k distinct transformations, and their inverses,

$$\{T_1^{\pm 1}, T_2^{\pm 1}, T_3^{\pm 1}, \quad . \ . \ . \ . \ . \ ., T_k^{\pm 1}\}$$

there are at most $f = 2^{k-j}$ different transformations which are made up of k successive transformations selected from the set without repeating any one or its corresponding inverse. j denotes the number of the components that are the same as their respective inverses. It also follows from property (a) that the f different transformations correspond to at most f/2 different distances, D[T(a, b), (a, b)], for $f > 1$.

4.3.3 LOWER BOUNDS ON SQUARED EUCLIDEAN DISTANCES

If in the process of assigning channel signals to the input sequences, care is taken to arrange the signals such that every pair of sub-trees, emanating from intermediate nodes of the same level, are equivalent in the sense described earlier, then a tight lower bound for the squared Euclidean distance between the four-dimensional signals can be obtained easily. The bound is denoted by $D_b(\underline{\varepsilon})$, and is given by (4-11).

The key property is that one can write $M(\underline{w} \oplus \underline{\varepsilon})$ in the form

$$\prod_{j=1,\varepsilon_j=1}^{q} \left\{T_j^{\pm 1} M(\underline{w})\right\} \qquad (4\text{-}19)$$

where T_j is the transformation associated with an error in the j^{th} bit.

The derivation of the bounds is best illustrated by an example. The channel signal assignment using set-partitioning for a four-dimensionally coded 8-PSK is summarized in the tree diagram shown in Figure 4-11. There are $M = n^2/2 = 32$ coded four-dimensional signals, and 512 Euclidean distances to be determined. Fortunately, most of them can be found easily because all the sub-trees emanating from the same level are equivalent. As defined, T_1, T_2, T_3, T_4 and T_5 are the transformations that correspond to the vectors, (00001), (00010), (00100), (01000) and (10000), respectively. Thus,

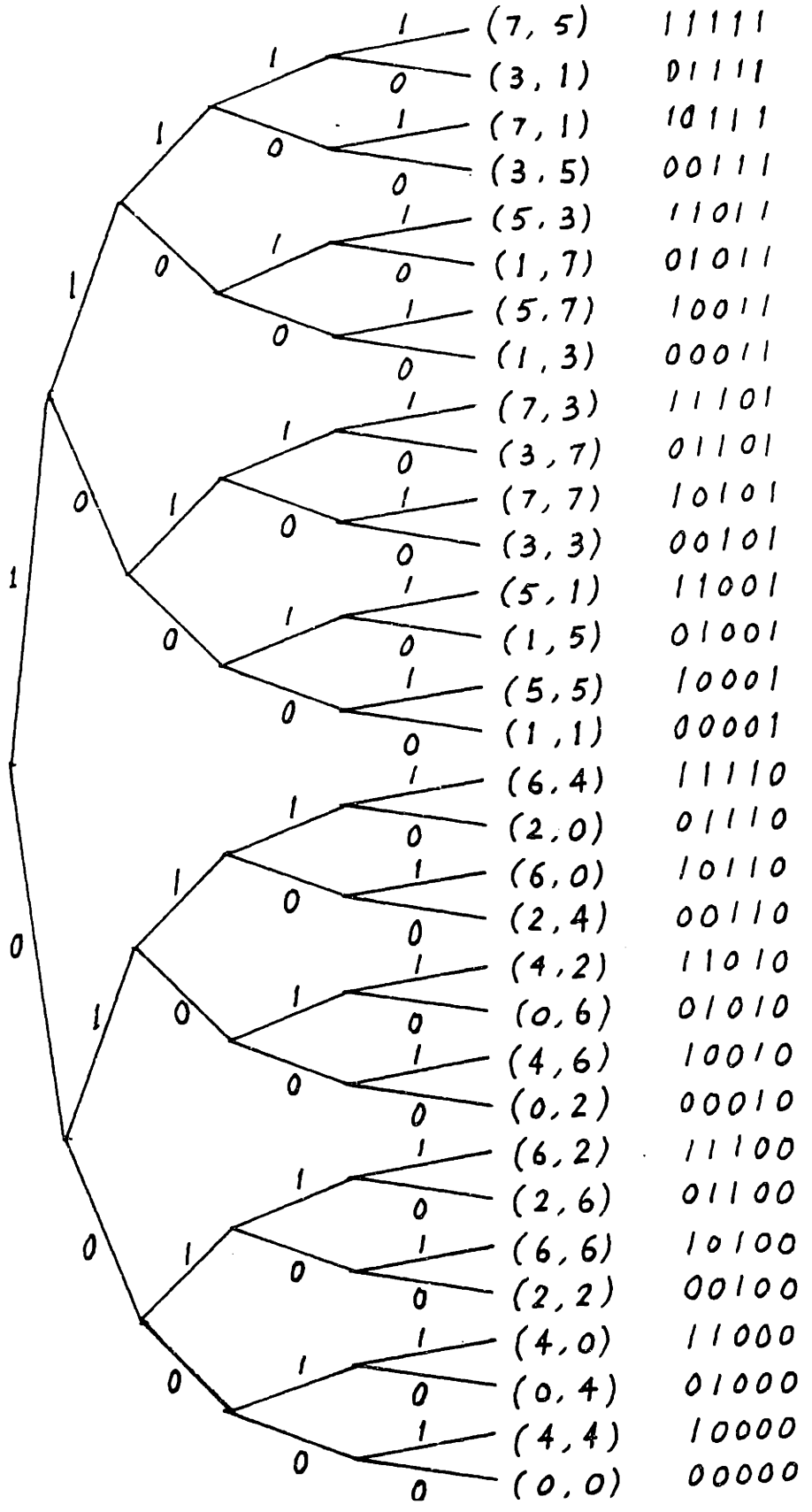

Figure 4-11. Channel Signal Assignment for 4-D Coded 8-PSK

$$T_1(0,0) = (1,1) \quad ; \quad T_1^{-1}(0,0) = (7,7)$$

$$T_2(0,0) = (0,2) \quad ; \quad T_2^{-1}(0,0) = (0,6)$$

$$T_3(0,0) = (2,2) \quad ; \quad T_3^{-1}(0,0) = (6,6)$$

$$T_4(0,0) = (0,4) \quad ; \quad T_4^{-1}(0,0) = (0,4)$$

$$T_5(0,0) = (4,4) \quad ; \quad T_5^{-1}(0,0) = (4,4) \qquad (4\text{-}20)$$

Note that $T_4^{-1} = T_4$ and $T_5^{-1} = T_5$. Other vectors correspond to various combinations of $T_1^{\pm 1}$; $T_2^{\pm 1}$; $T_3^{\pm 1}$; T_4 and T_5.

For example, consider $\underline{\varepsilon}$ = (10110), which corresponds to various combinations of $T_2^{\pm 1}$, $T_3^{\pm 1}$ and T_5. In this case, k = 3, j = 1 and f = 4. The set of f = 4 different transformations are given below.

$$\{T_2^{\pm 1} T_3^{\pm 1} T_5\} = \{T_2 T_3 T_5,\ T_2 T_3^{-1} T_5,\ T_2^{-1} T_3 T_5,\ T_2^{-1} T_3^{-1} T_5\}$$

Since $T_2T_3T_5$ and $T_2T_3^{-1}T_5$ are inverses of $T_2^{-1}T_3^{-1}T_5$ and $T_2^{-1}T_3T_5$, respectively, the above set can further be reduced to f/2 = 2 transformations that give rise to different distances. One of the reduced set is thus,

$$\{T_2 T_3 T_5,\ T_2 T_3^{-1} T_5\}$$

Whichever gives the smaller Euclidean distance will then serve as the lower bound. Since

$$T_2T_3T_5\ (0,0) = (6,0) \text{ and } T_2T_3^{-1}T_5\ (0,0) = (2,4),$$

thus,

$$D_b(10110) = D[(6,0),(0,0)] = 2\ d_0^2$$

Similarly, $D_b(\underline{\varepsilon})$ for any $\underline{\varepsilon}$ can be found. Let

$$\begin{aligned} D_0 &= 2\, d_1^2 = 1.172\, d_0^2 \\ D_1 &= 2\, d_0^2 = 2.000\, d_0^2 \\ D_2 &= 4\, d_0^2 = 4.000\, d_0^2 \\ D_3 &= 6\, d_0^2 = 6.000\, d_0^2 \\ D_4 &= 2\, d_3^2 = 6.828\, d_0^2 \\ D_5 &= 8\, d_0^2 = 8.000\, d_0^2 \end{aligned} \tag{4-21}$$

The lower bounds for the squared Euclidean distances are tabulated in Figure 4-12. In Figure 4-13, the bounds derived in this section are compared to those derived by Ungerboeck. It is obvious that the former are much tighter than the latter.

4.4 FEC CODING FOR FOUR-DIMENSIONALLY CODED PSK

Four-dimensionally coded modulation maps every q-bit binary word onto a four-dimensional channel signal chosen from an expanded N-ary signal set, such that $N > 2^q$. The subset of coded signals are selected such that the minimum Euclidean distance between the signals is maximized. This mapping with redundancy provides some coding gain. Further coding gains can be achieved by conventional FEC coding, such as block coding and convolutional coding.

Ordinarily, block codes are chosen to maximize the minimum Hamming distance between codewords at the encoder output. They do not necessarily maximize the minimum Euclidean distance between channel signals, which dominates the probability of error. The system can be improved by jointly designing the

No.	$\underline{\varepsilon}$	$T^{\underline{\varepsilon}}$	$D_b(\underline{\varepsilon})$
0	0 0 0 0 0	Identity	0
1	0 0 0 0 1	T_5	D_0
2	0 0 0 1 0	T_4	D_1
3	0 0 0 1 1	$T_4 T_5^{\pm 1}$	D_0
4	0 0 1 0 0	T_3	D_2
5	0 0 1 0 1	$T_3 T_5^{\pm 1}$	D_0
6	0 0 1 1 0	$T_3 T_4^{\pm 1}$	D_1
7	0 0 1 1 1	$T_3 T_4 T_5^{\pm 1}$, $T_3^{\pm 1} T_4^{\mp 1} T_5$	D_0
8	0 1 0 0 0	T_2	D_2
9	0 1 0 0 1	$T_2 T_5$	D_2
10	0 1 0 1 0	$T_2 T_4$	D_1
11	0 1 0 1 1	$T_2 T_4^{\pm 1} T_5$	D_0
12	0 1 1 0 0	$T_2 T_3$	D_2
13	0 1 1 0 1	$T_2 T_3^{\pm 1} T_5$	D_2
14	0 1 1 1 0	$T_2 T_3^{\pm 1} T_4$	D_1
15	0 1 1 1 1	$T_2 T_3 T_4^{\pm 1} T_5$, $T_2^{\pm 1} T_3^{\mp 1} T_4 T_5$	D_1
16	1 0 0 0 0	T_1	D_5
17	1 0 0 0 1	$T_1 T_5$	D_4
18	1 0 0 1 0	$T_1 T_4$	D_3
19	1 0 0 1 1	$T_1 T_4^{\pm 1} T_5$	D_2
20	1 0 1 0 0	$T_1 T_3$	D_2
21	1 0 1 0 1	$T_1 T_3^{\pm 1} T_5$	D_0
22	1 0 1 1 0	$T_1 T_3^{\pm 1} T_4$	D_1
23	1 0 1 1 1	$T_1 T_3 T_4^{\pm 1} T_5$, $T_1^{\pm 1} T_3^{\mp 1} T_4 T_5$	D_0
24	1 1 0 0 0	$T_1 T_2$	D_2
25	1 1 0 0 1	$T_1 T_2 T_5$	D_2
26	1 1 0 1 0	$T_1 T_2 T_4$	D_3
27	1 1 0 1 1	$T_1 T_2 T_4^{\pm 1} T_5$	D_2
28	1 1 1 0 0	$T_1 T_2 T_3$	D_2
29	1 1 1 0 1	$T_1 T_2 T_3^{\pm 1} T_5$	D_2
30	1 1 1 1 0	$T_1 T_2 T_3^{\pm 1} T_4$	D_1
31	1 1 1 1 1	$T_1 T_2 T_3^{\pm 1} T_4 T_5$, $T_1^{\pm 1} T_2^{\mp 1} T_3 T_4 T_5$	D_0

Figure 4-12. Lower Bounds on Squared Euclidean Distances

No.	$\underline{\varepsilon}$	$D_b(\underline{\varepsilon})/d_0^2$	$\Delta^2 q(\underline{\varepsilon})/d_0^2$
0	0 0 0 0 0	0	0
1	0 0 0 0 1	1.172	1.172
2	0 0 0 1 0	2	2
3	0 0 0 1 1	1.172	1.172
4	0 0 1 0 0	4	4
5	0 0 1 0 1	1.172	1.172
6	0 0 1 1 0	2	2
7	0 0 1 1 1	1.172	1.172
8	0 1 0 0 0	4	4
9	0 1 0 0 1	4	1.172
10	0 1 0 1 0	2	2
11	0 1 0 1 1	1.172	1.172
12	0 1 1 0 0	4	4
13	0 1 1 0 1	4	1.172
14	0 1 1 1 0	2	2
15	0 1 1 1 1	2	1.172
16	1 0 0 0 0	8	8
17	1 0 0 0 1	6.828	1.172
18	1 0 0 1 0	6	2
19	1 0 0 1 1	4	1.172
20	1 0 1 0 0	4	4
21	1 0 1 0 1	1.172	1.172
22	1 0 1 1 0	2	2
23	1 0 1 1 1	1.172	1.172
24	1 1 0 0 0	4	4
25	1 1 0 0 1	4	1.172
26	1 1 0 1 0	6	2
27	1 1 0 1 1	4	1.172
28	1 1 1 0 0	4	4
29	1 1 1 0 1	4	1.172
30	1 1 1 1 0	2	2
31	1 1 1 1 1	1.172	1.172

Figure 4-13. Comparison Between $D_b(\underline{\varepsilon})$ and Ungerboeck's Bounds

encoder and the signal mapper so that the minimum Euclidean distance is maximized.

Suppose block coding is used and the scheme is represented by

$$\underline{w}_k = G(\underline{u}_k)$$

and

$$(a_k, b_k) = M(\underline{w}_k) = M[G(\underline{u}_k)]$$

where the subscript k indicates the k^{th} block of the sequence involved. Since G is a one-to-one mapping, $M[G(\underline{u}_k)]$ is just equivalent to a different signal mapping of $\underline{u}_k$ onto the same set of channel signals. Thus, $(a_k, b_k) = M'(\underline{u}_k)$.

Hence, combined block coding and coded modulation is equivalent to another coded modulation with a smaller subset of coded signals. For obvious reasons, we do not further pursue the use of block coding in this study.

4.4.1 CONVOLUTIONAL CODING FOR FOUR-DIMENSIONALLY CODED n-PSK

Figure 4-14 shows the block diagram of the above coding scheme. For mathematical simplicity, we consider the number of phases, n, as an integral power of two. Thus, $n = 2^m$, where m is an integer greater than or equal to 2. (a_k, b_k) represents one of $M = 2^q$ four-dimensional n-PSK signals, chosen from a set of $N = n^2 = 2^{2m}$ possible signals. Suppose that we want to add one bit of redundancy through the signal mapper, and another bit through a convolutional encoder. Then, we have $M = 2^{2m-1} = N/2$,

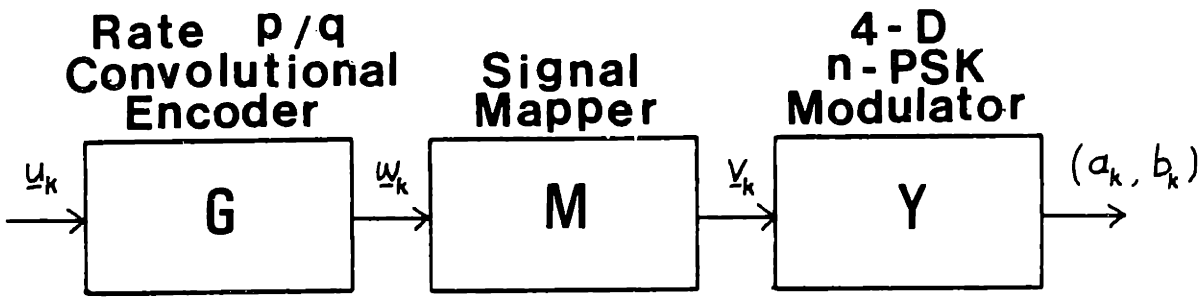

Figure 4-14. 4-D Coded n-PSK With Convolutional Coding

and the rate of the encoder is $p/q = (2m-2)/(2m-1)$ for $m > 1$. The technique of signal selection, as discussed in previous sections, can be used to obtain the M signals.

With the above configuration, the overall signaling rate is $(2m-2)/2m = (m-1)/m$. Since $2^P = 2^{2m-2} = (2^{m-1})^2 = (n/2)^2$, the corresponding uncoded system, which transmits information at the same rate, will require an n/2 - PSK modulator. Thus, in subsequent discussions, our coded four-dimensional n-PSK system will be compared with a pair of uncoded two-dimensional n/2 - PSK systems.

4.4.2 SELECTION OF CONVOLUTIONAL CODES FOR FOUR-DIMENSIONALLY CODED QPSK

The heuristic design of convolutional codes for four-dimensionally coded QPSK will be discussed in some details. First of all, recall that using an appropriate coded modulation scheme, we can derive lower bounds for the squared Euclidean distances, which are functions of the error vectors only. The scheme we have chosen is summarized in the tree diagram shown in Figure 4-15. With this channel signal assignment, it can be verified easily that the minimum squared Euclidean distance between channel signals is $4\ d_0^2$. And, the lower bounds are satisfied with equality for all error vectors. Let

$$D(\underline{\varepsilon}_k) = D\ [M(\underline{w}_k \oplus \underline{\varepsilon}_k), M(\underline{w}_k)]$$

Then,

$$D(\underline{\varepsilon}_k) = \begin{cases} 0 & ; \quad \text{if } \underline{\varepsilon}_k = (000) \\ 8\ d_0^2 & ; \quad \text{if } \underline{\varepsilon}_k = (100) \\ 4\ d_0^2 & ; \quad \text{otherwise.} \end{cases} \qquad (4\text{-}22)$$

$\underline{w}_k$ is the k^{th} input to the channel signal mapper, and $\underline{\varepsilon}_k$ is the error vector corresponding to the k^{th} input vector. M(*) is the signal mapping operation.

In the following section, we will borrow Ungerboeck's rules for the heuristic selection of convolutional codes. With only slight modification, the rules are restated as follows.

a. All four-dimensional signals should occur with equal frequency, and with a fair amount of regularity and symmetry;

b. Transitions originating from the same state receive signals either from subset B0 or B1;

c. Transitions joining in the same state receive signals either from subset B0 or B1;

d. Parallel transitions receive signals either from subset C0 or C1 or C2 or C3.

The subset labels are defined in Figure 4-15.

It has not been proved that the above rules always give rise to optimal codes. However, Ungerboeck claims that for small numbers of trellis states, the codes obtained according to the above rules are optimum and this can be confirmed by an exhaustive hand-search.

Simple rate 2/3 convolutional codes for up to 8 trellis states have been selected, and the minimum free distances have

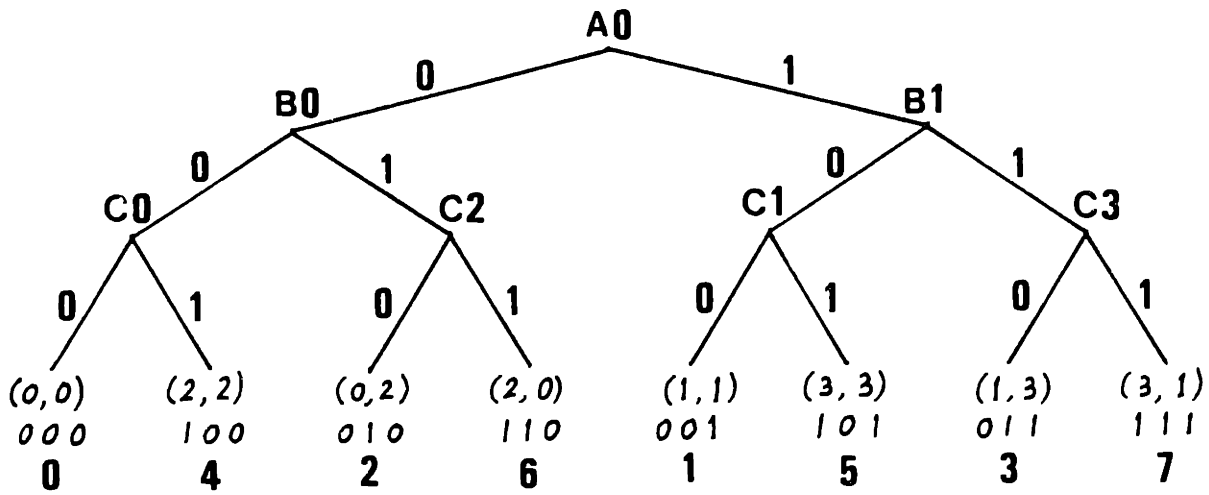

Figure 4-15. Channel Signal Assignment for 4-D Coded QPSK (n = 4, M = 8)

been determined by exhaustive examination of the trellis paths. The trellis structures for 2, 4 and 8 states, and their corresponding shift-register realizations are shown in Figures 4-16, 4-17 and 4-18, respectively.

4.5 ASYMPTOTIC PERFORMANCE OF CODED FOUR-DIMENSIONAL QPSK

The asymptotic performance of the system is dictated by the minimum Euclidean distance between channel signals. For coding schemes with memory, such as convolutional coding, the minimum free Euclidean distance is a fairly good measure of the system performance for high signal-to-noise ratios.

In this section, we will evaluate the asymptotic performance of the coded four-dimensional system in the absence of interference, and compare it with the performance of some two-dimensional systems. Comparison will be made with respect to both time-orthogonality and space- or polarization-orthogonality. It is assumed that the signals of the two-dimensional systems are encoded independently, and transmitted separately over two different two-dimensional channels. If we accept the minimum distance between channel signals as a criterion for performance measures, then their overall performance is limited by the minimum distance between channel signals in either one of the two-dimensional channels. On the other hand, the performance of the four-dimensional system is limited by the minimum distance between the four-dimensional channel signals. Since all pairs of two-dimensional systems constitute one form of four-dimensional systems, it can be expected that there exist four-dimensional systems which can do no worse than the independent two-dimensional systems.

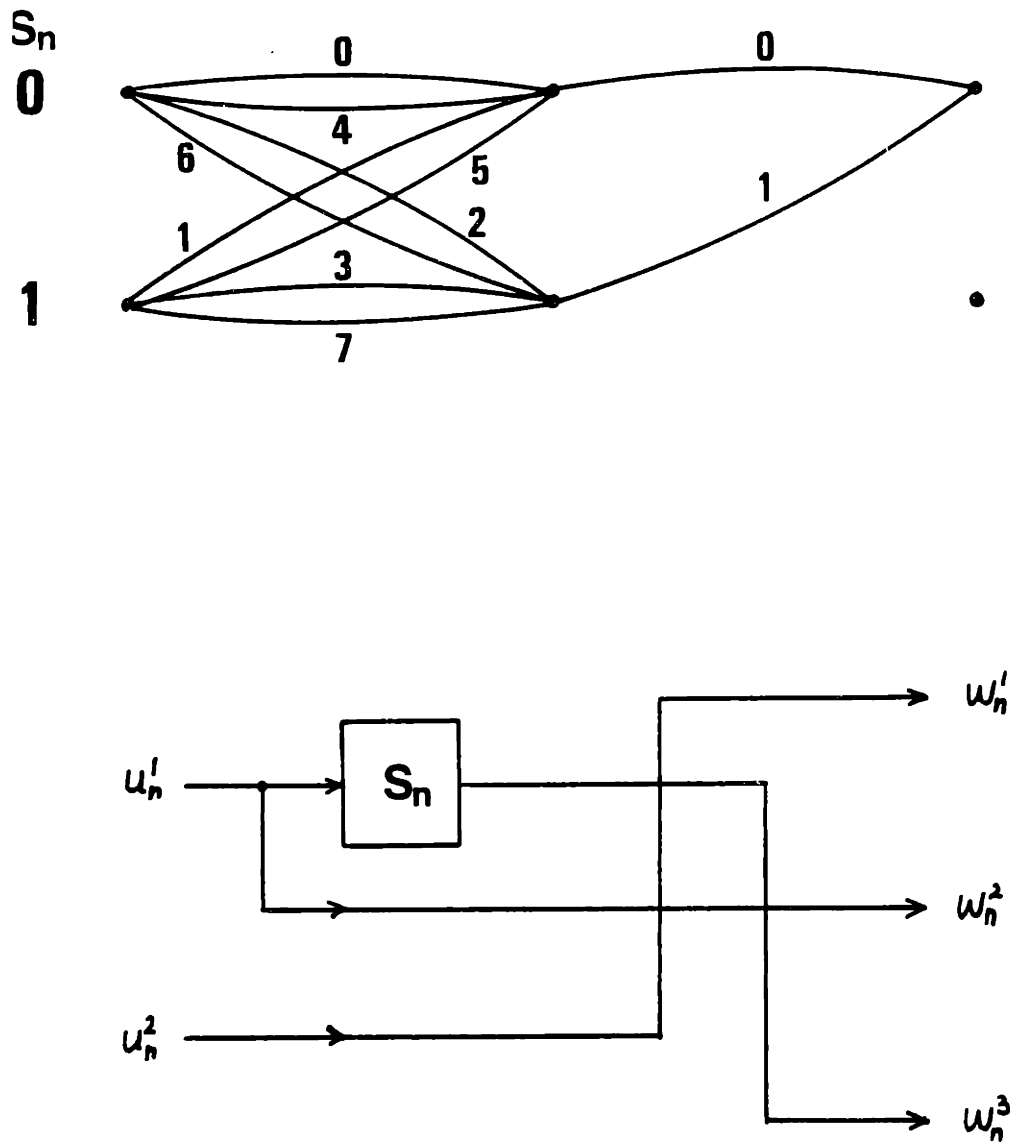

Figure 4-16. Trellis Structure with 2 States and Shift-Register Realization

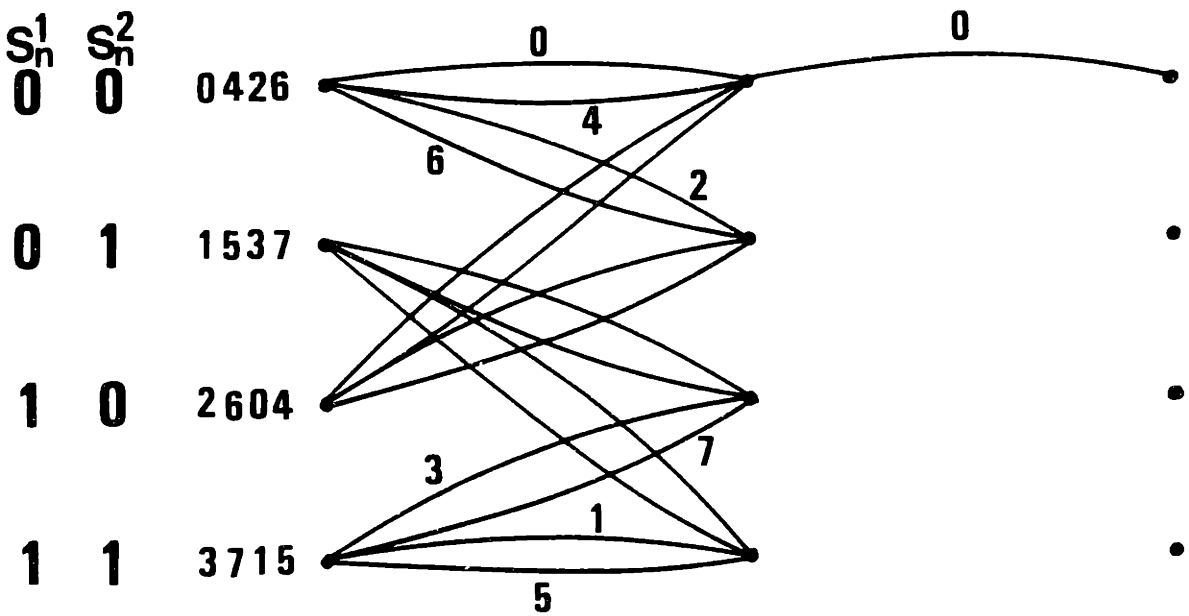

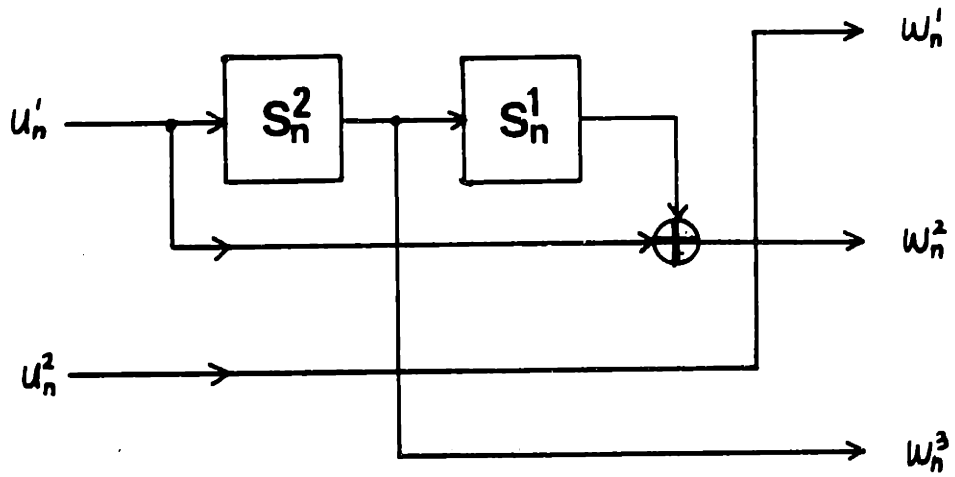

Figure 4-17. Trellis Structure with 4 States and Shift-Register Realization

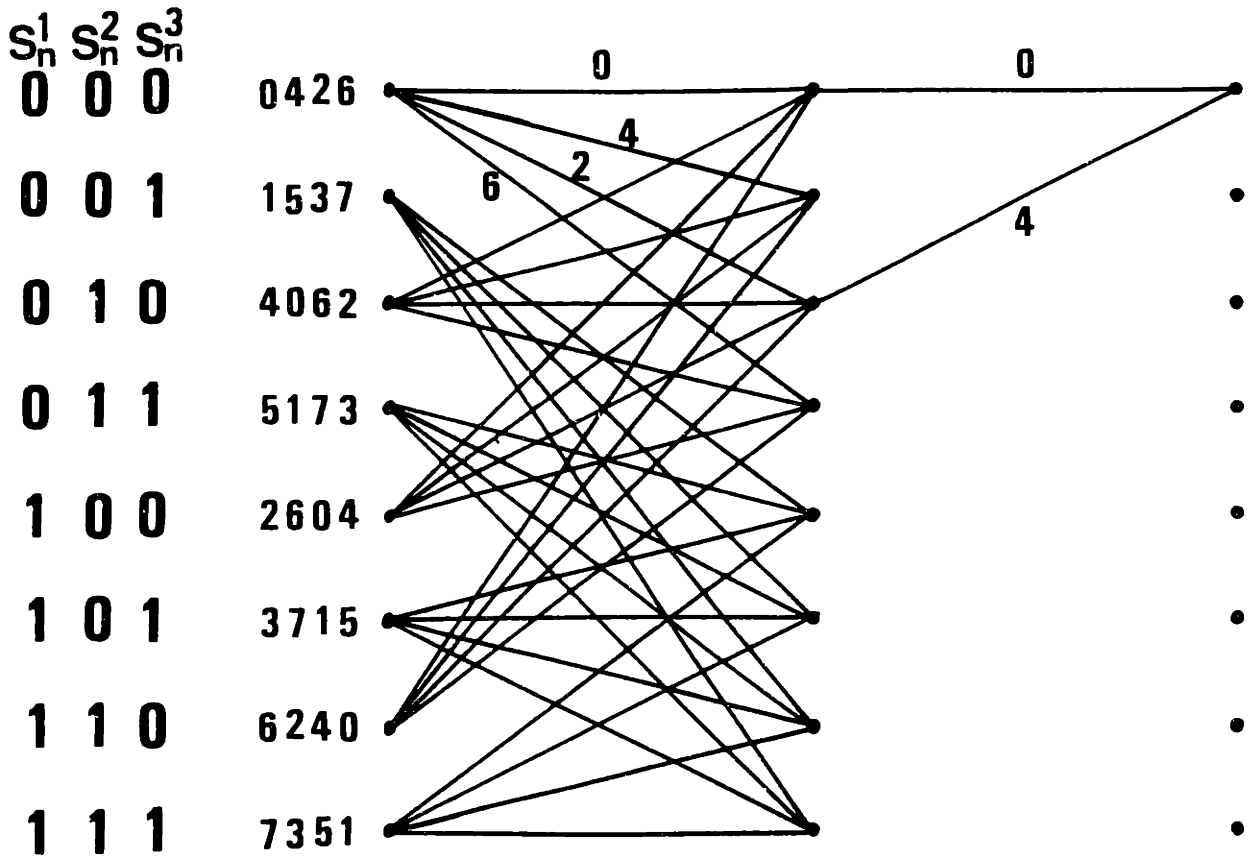

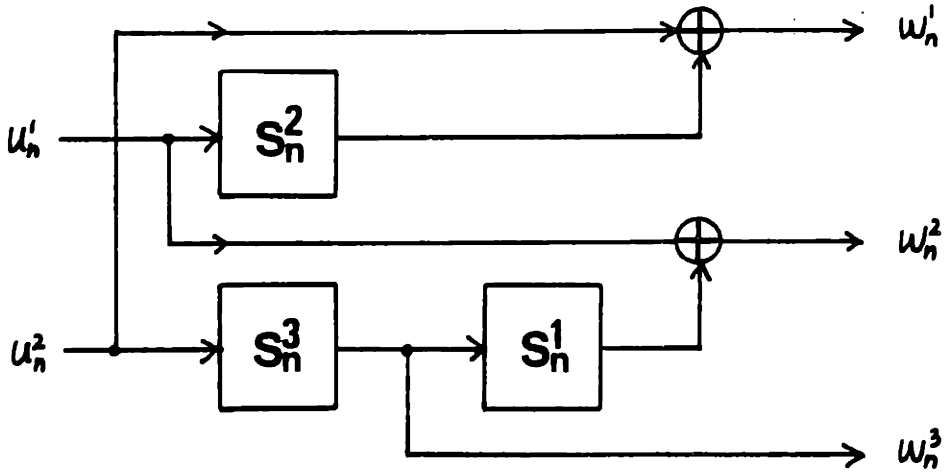

Figure 4-18. Trellis Structure with 8 States and Shift-Register Realization

The minimum squared free distances of the coded four-dimensional system have been found to be $8d_0^2$, $8d_0^2$, and $12d_0^2$ for 2, 4 and 8 trellis states respectively. In the absence of interference, the performance of the four-dimensional system with time-orthogonal two-dimensional components is the same as that with space- or polarization-orthogonal two-dimensional components.

4.5.1 CODING GAIN OF CODED 4-D n-PSK WITH RESPECT TO UNCODED 2-D n/2-PSK

The coding gain of the four-dimensionally coded n-PSK with rate (2m-2)/(2m-1) convolutional coding is now examined with respect to a pair of uncoded two-dimensional n/2-PSK where $n = 2^m$. We have considered each pair of signal pulses tc be one unit so that the two-dimensional systems can be treated as a four-dimensional system for the sake of comparison. Using two two-dimensional modulators and receivers, the space- or polarization-orthogonal signaling requires only half as much bandwidth as the time-orthogonal signaling, but the latter uses only one two-dimensional modulator and receiver.

The minimum Euclidean distance, between channel signals of the uncoded two-dimensional n/2-PSK system is given by

$$d_{min}^2 = 2d_0^2 \left[1 - \cos\left(4\pi/n\right)\right] \qquad (4\text{-}23)$$

Suppose the free Euclidean distance ensured by the overall four-dimensional coding scheme is d_f. Then the overall asymptotic coding gain is given by

$$G = 10 \log \left(d_f^2/d_{min}^2\right) = 20 \log \left(d_f/d_{min}\right)$$

Therefore,

$$G = 10 \log \left\{ \frac{d_f^2/d_0^2}{2(1 - \cos 4\pi/n)} \right\} \; ; \; n \geq 4 \qquad (4\text{-}24)$$

The coding gains for n = 4, 6, 8, 12 and 16 are plotted against d_f^2/d_0^2, and the graph is shown in Figure 4-19.

4.5.2 CODING GAIN OF CODED 4-D QPSK WITH RESPECT TO CODED 2-D QPSK

This section examines the coding gain of the four-dimensionally coded QPSK with rate 2/3 (m = 2) convolutional coding, derived in Subsection 4.5.1 with respect to a two-dimensional QPSK with rate 1/2 convolutional coding. Note that the overall coding rate of the four-dimensional system is actually 1/2, because the coded modulation has a rate of 3/4. In this respect, the comparison is fair.

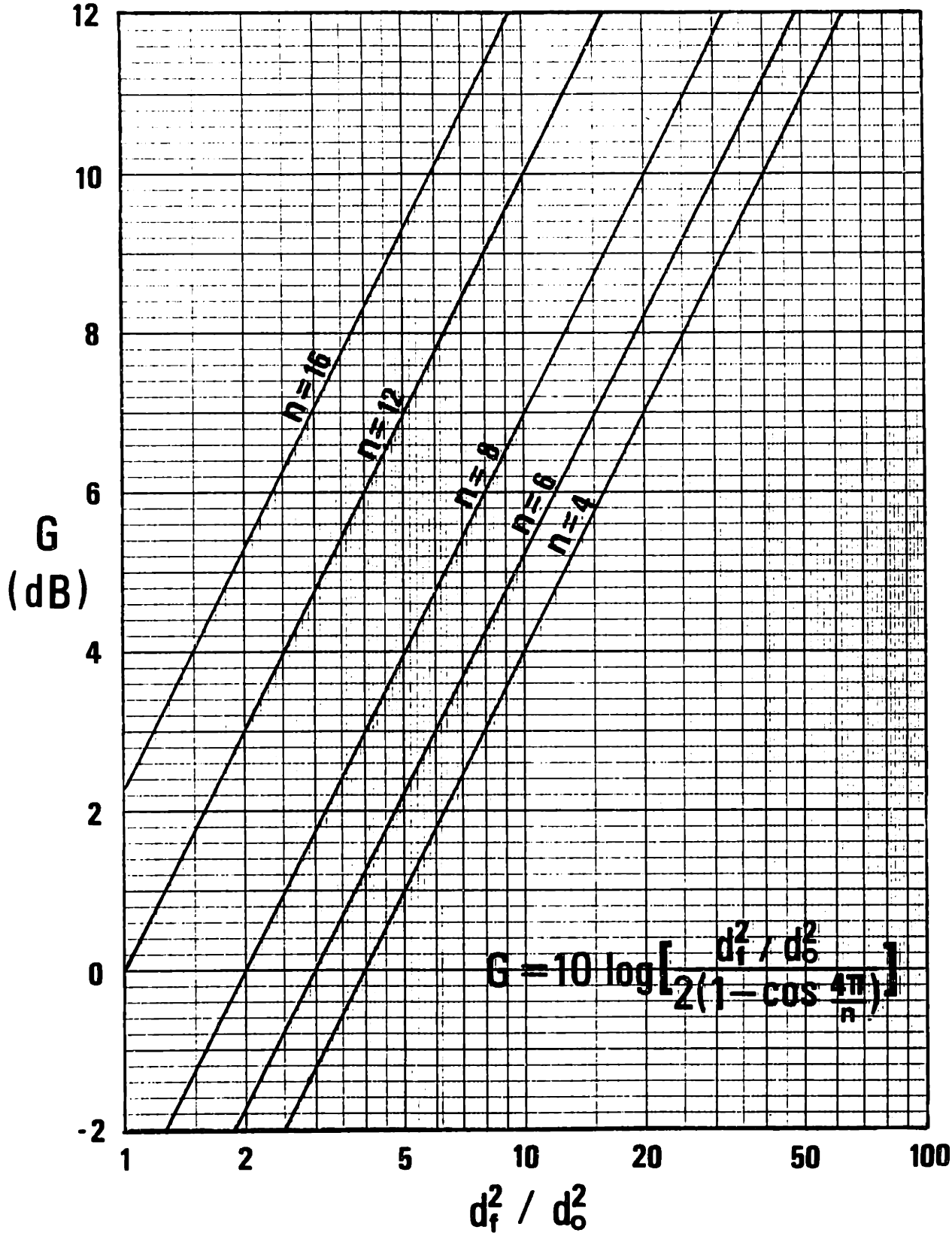

Figure 4-19. Coding Gain of Coded 4-D n-PSK With Respect to Uncoded 2-D n/2-PSK

The codes for the two-dimensional system are selected according to Ungerboeck's rules. The trellis structures for 2, 4 and 8 states are depicted in Figure 4-20. Their corresponding minimum squared free distances are 6 d_0^2, 10 d_0^2 and 12 d_0^2, respectively.

It appears that the four-dimensional system is not always better than the two-dimensional systems. The two-dimensional system with two memory registers provides a larger free distance than the four-dimensional system with the same number of memory registers. However, it will be shown in Section 5 that the coded four-dimensional systems are more robust in the presence of severe intersymbol interference than the above coded two-dimensional systems.

4.5.3 COMPARISON WITH FOUR-DIMENSIONAL REPETITION SYSTEMS

Repetitive transmission techniques can be applied to a four-dimensional system. Consider a repetitive 8-PSK system as an example. The signal assignment resulting from set partitioning are shown in Figure 4-21. The minimum squared subset distances are

$$\tilde{\Delta}_0^2 = 2\, d_1^2 = 1.172\, d_0^2$$

$$\tilde{\Delta}_1^2 = 4\, d_0^2$$

$$\tilde{\Delta}_2^2 = 8\, d_0^2 \qquad (4\text{-}25)$$

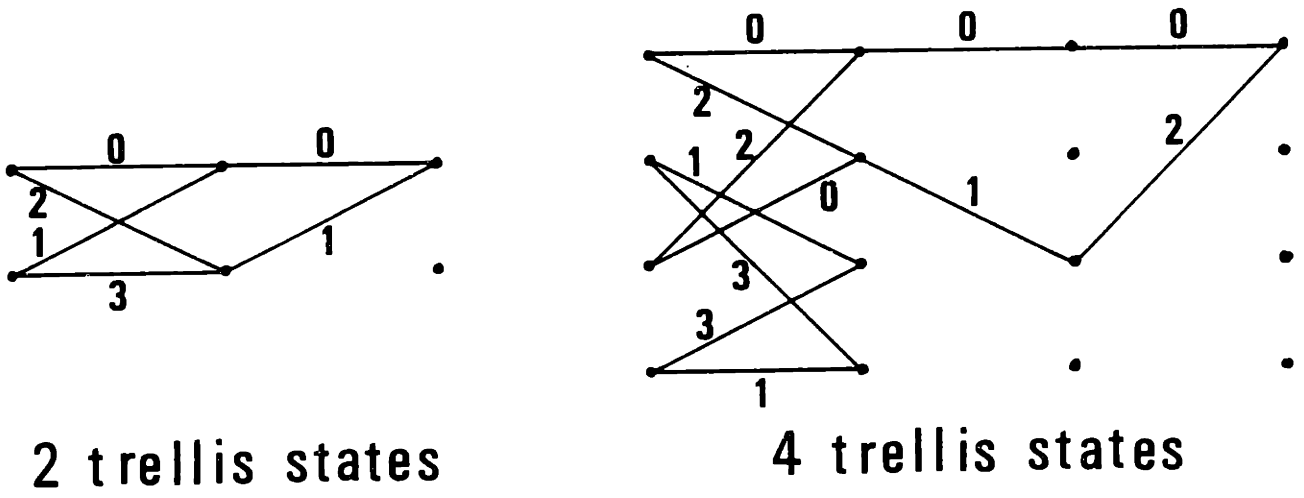

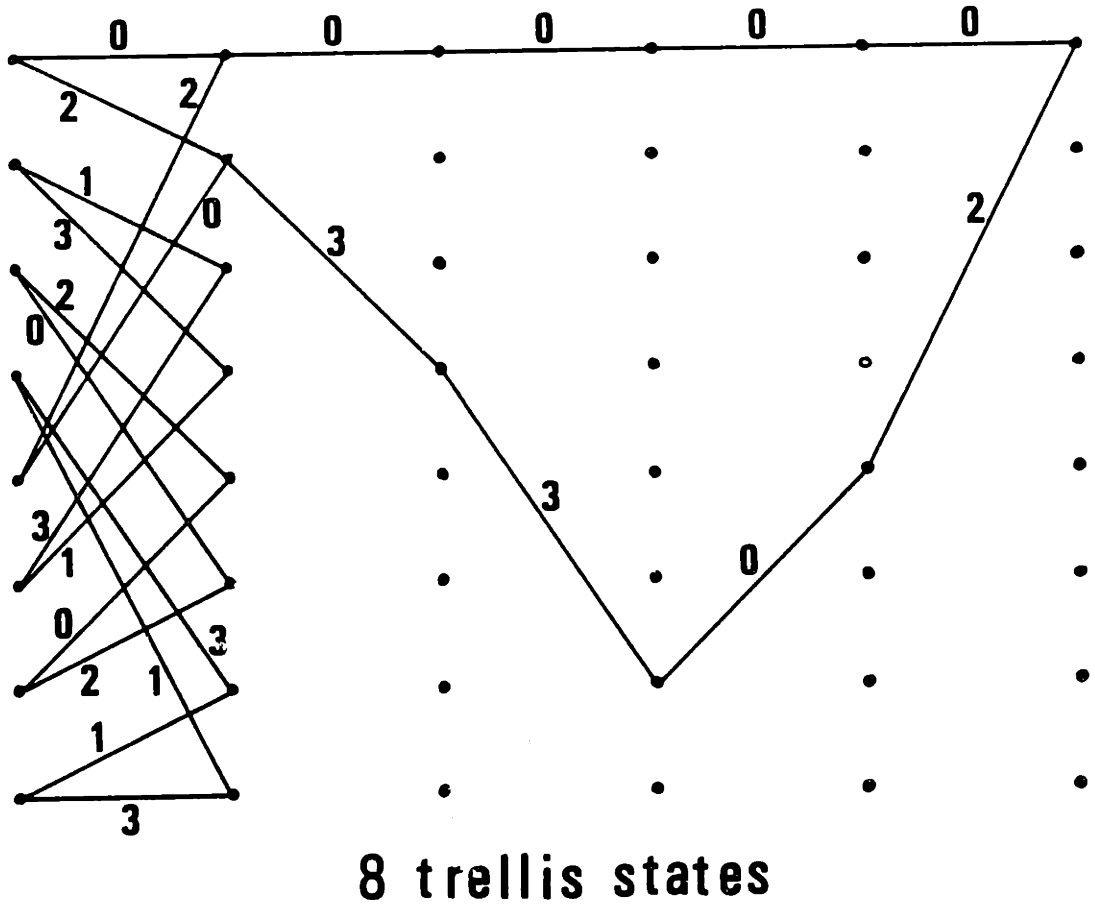

Figure 4-20. Trellis Structures for Coded 2-D QPSK

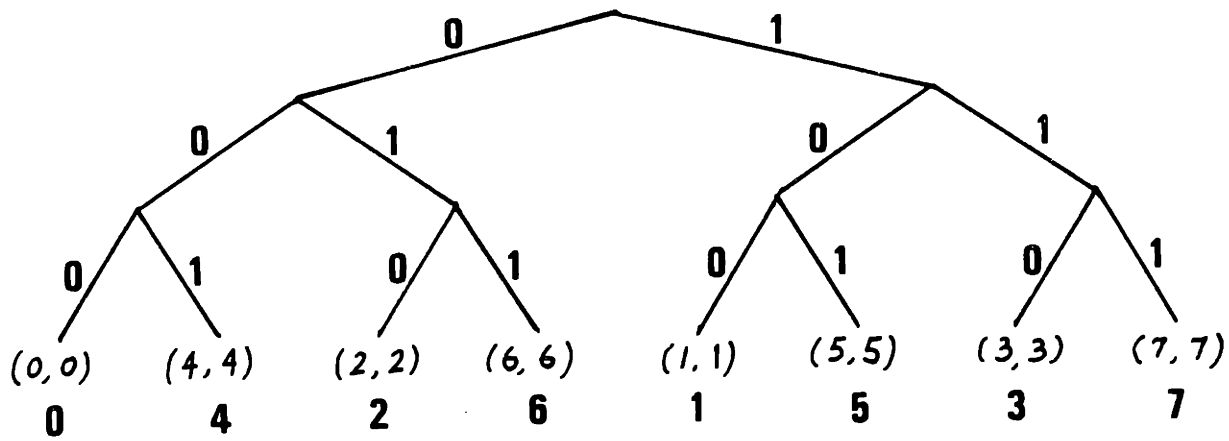

Figure 4-21. Channel Signal Assignment for Repetitive 8-PSK System

Recall that the minimum squared subset distances for the four-dimensionally coded QPSK are

$$\Delta_0^2 = 4\ d_0^2$$
$$\Delta_1^2 = 4\ d_0^2$$
$$\Delta_2^2 = 8\ d_0^2 \qquad (4\text{-}26)$$

It is thus clear that $\tilde{\Delta}_k^2 \leq \Delta_k^2$ for $k = 0,1,2$.

Theorem

Suppose $\tilde{\Delta}_k^2$ and Δ_k^2 are tight minimum squared subset distances of two different channel signal assignments, such that $\tilde{\Delta}_k^2 \leq \Delta_k^2$ for all k. Then, for the same encoder complexity, the free Euclidean distance, d_f^2 of the latter system is at least as large as the free Euclidean distance $\tilde{d}_f^2$ of the former system.

Proof

Consider a path corresponding to $d_f^2 = \alpha_0\Delta_0^2 + \alpha_1\Delta_1^2 + \ldots$ in the second system, where α_0, α_1, . . ., etc., are positive integers. An upper bound on the squared free distance, $\tilde{d}_f^2$, in the first system is $\alpha_0\tilde{\Delta}_0^2 + \alpha_1\tilde{\Delta}_1^2 + \ldots$, which is less than or equal to d_f^2 by hypothesis. Hence $\tilde{d}_f^2 \leq d_f^2$.

For the comparison we are looking at, $\tilde{\Delta}_k^2 \leq \Delta_k^2$ for $k = 0, 1, 2$. Hence, the free Euclidean distance for the coded four-dimensional QPSK with convolutional coding is always larger than or equal to that for the repetition system with equivalent encoder complexity. The squared free distances for the repetition system for various numbers of trellis states are listed below for comparison.

2 trellis states $\quad d_f^2 = \tilde{\Delta}_0^2 + \tilde{\Delta}_1^2 = 5.172\ d_0^2$

4 trellis states $\quad d_f^2 = \tilde{\Delta}_2^2 = 8.000\ d_0^2$

8 trellis states $\quad d_f^2 = \tilde{\Delta}_0^2 + 2\tilde{\Delta}_1^2 = 9.172\ d_0^2$ (4-27)

5. CODING FOR CHANNELS WITH INTERSYMBOL INTERFERENCE

5.1 DESCRIPTION OF THE SYSTEM

In this section, we will demonstrate the application of the 4-dimensional coding and modulation approach on the design of systems subject to intersymbol interference. The ordinary 2-dimensional channel is viewed as a 4-dimensional channel by considering the successive signal pulses in pairs.

A convolutionally encoded sequence, $\underline{w}$, is mapped onto the channel signal sequence, $\underline{S}$, by using the signal mapper, as described in the previous chapter. Each signal vector, $\underline{S}_k$, has an in-phase component, A_k, and a quadrature component, B_k. The modulator is assumed to be a PSK modulator. The transmitted signal, $y(t)$, is given by

$$y(t) = \sum_k \left[A_k \sqrt{2}\, h(t - kT) \cos \omega_c t + B_k \sqrt{2}\, h(t - kT) \sin \omega_c t \right] \qquad (5\text{-}1)$$

where

$$A_k = \sqrt{E} \cos \theta_k$$
$$B_k = - \sqrt{E} \sin \theta_k. \qquad (5\text{-}2)$$

and θ_k is the phase of the kth signal. $E = E_s/2$ denotes the energy of each of the two-dimensional PSK signals.

It is convenient to express the transmitted signal in terms of its odd and even time components.

$$y(t) = \sum_k \Big\{ A_k^o \sqrt{2}\, h[t - (2k-1)T] \cos \omega_c t + B_k^o \sqrt{2}\, h[t - (2k-1)T] \sin \omega_c t + A_k^e \sqrt{2}\, h(t - 2kT) \cdot \cos \omega_c t + B_k^e \sqrt{2}\, h(t - 2kT) \sin \omega_c t \Big\} \qquad (5\text{-}3)$$

where the superscripts, "o" and "e", stand for "odd" and "even", respectively.

It is assumed that the linear impulse response, h(t), which characterizes the modulator/channel filter, does not introduce crosstalk between orthogonal signal components. The channel noise, n(t), is an additive white Gaussian noise (AWGN), with a two-sided power spectral density of $N_o/2$. The received waveform is then given by

$$r(t) = y(t, \underline{u}) + n(t) \qquad (5\text{-}4)$$

The received signal is demodulated to yield log likelihood functions, $\{\lambda_k\}$, which are then input into the decoder. The Viterbi decoder, which is a maximum likelihood decoder, will be used [40],[41],[42].

5.2 DERIVATION OF LIKELIHOOD FUNCTION

The maximum likelihood decision rule decides that $\underline{u}^*$ was transmitted if and only if

$$||r(t) - y(t, \underline{u}^*)||^2 = \min_{\underline{u}} ||r(t) - y(t, u)||^2 \qquad (5\text{-}5)$$

Equivalently,

$$\Lambda[r(t), \underline{u}^*] = \max_{\underline{u}} \{\Lambda[r(t), \underline{u}]\} \qquad (5\text{-}6)$$

where

$$\Lambda[r(t), u] \triangleq \frac{2}{N_o} \int r(t)\, y(t, \underline{u})\, dt - \frac{1}{N_o} \int |y(t, \underline{u})|^2\, dt \qquad (5\text{-}7)$$

$$\int r(t)\, y(t, \underline{u})\, dt = \sum_k \{A_k^o \int \sqrt{2}\, r(t)\, h[t - (2k-1)\, T] \cdot \cos \omega_c t\, dt + B_k^o \int \sqrt{2}\, r(t)\, h[t - (2k-1)\, T] \cdot \sin \omega_c t\, dt + A_k^e \int \sqrt{2}\, r(t)\, h(t - 2kT) \cdot \cos \omega_c t\, dt + B_k^e \int \sqrt{2}\, r(t)\, h(t - 2kT) \cdot \sin \omega_c t\, dt\}$$

or

$$\int r(t)\, y(t, \underline{u})\, dt = \sum_k \{A_k^o r_{2k-1}^c + B_k^o r_{2k-1}^s + A_k^e r_{2k}^c + B_k^e r_{2k}^s\} \qquad (5\text{-}8)$$

where

$$r_k^c \triangleq \int \sqrt{2}\, r(t)\, h(t - kT) \cos \omega_c t \, dt$$
$$r_k^s \triangleq \int \sqrt{2}\, r(t)\, h(t - kT) \sin \omega_c t \, dt \qquad (5\text{-}9)$$

Let's define

$$h_{k-\ell} \triangleq \int h(t - kT)\, h(t - \ell T)\, dt = h_{\ell-k} \qquad (5\text{-}10)$$

and assume that h(t) has a Fourier transform whose bandwidth is much smaller than the carrier frequency. Then,

$$\int |y(t, \underline{u})|^2 \, dt = \sum_k \sum_j \{[A_k^o A_j^o + B_k^o B_j^o + A_k^e A_j^e + B_k^e B_j^e] \cdot h_{2(k-j)} + [A_k^o A_j^e + B_k^o B_j^e]\, h_{2(k-j)-1} + [A_k^e A_j^o + B_k^e B_j^o]\, h_{2(k-j)+1}\} \qquad (5\text{-}11)$$

Hence, the likelihood function is given by

$$\Lambda[\underline{r}, \underline{u}] = \sum_k \{\frac{2}{N_o} [A_k^o r_{2k-1}^c + B_k^o r_{2k-1}^s + A_k^e r_{2k}^c + B_k^e r_{2k}^s] - \frac{1}{N_o} \sum_j [(A_k^o A_j^o + B_k^o B_j^o + A_k^e A_j^e + B_k^e B_j^e)\, h_{2(k-j)} + (A_k^o A_j^e + B_k^o B_j^e)\, h_{2(k-j)-1} + (A_k^e A_j^o + B_k^e B_j^o)\, h_{2(k-j)+1}]\} \qquad (5\text{-}12)$$

And it can be expressed in the following form.

$$\Lambda(\underline{r}, \underline{u}) = \sum_{k} \lambda_k \tag{5-13}$$

where

$$\begin{aligned}\lambda_k \triangleq \frac{1}{N_o} \{ & 2(A_k^o r_{2k-1}^c + B_k^o r_{2k-1}^s + A_k^e r_{2k}^c + B_k^e r_{2k}^s) \\ & - \sum_{j} [(A_k^o A_j^o + B_k^o B_j^o + A_k^e A_j^e + B_k^e B_j^e) h_{2(k-j)} \\ & + (A_k^o A_j^e + B_k^o B_j^e) h_{2(k-j)-1} \\ & + (A_k^e A_j^o + B_k^e B_j^o) h_{2(k-j)+1}]\}\end{aligned} \tag{5-14}$$

For the satellite channel we are considering, $h_i << h_o$ for non-zero i. It is then reasonable to assume that $h_i/h_o \approx 0$ for $i > 1$. The likelihood function can then be simplified and broken down into two parts, namely $\Lambda_0(r(t), \underline{u})$ and $\Lambda_1(\underline{u})$.

$$\begin{aligned}\Lambda_0(r(t), \underline{u}) \triangleq \sum_{k} \{ & \frac{2}{N_o} (A_k^o r_{2k-1}^c + B_k^o r_{2k-1}^s + A_k^e r_{2k}^c + B_k^e r_{2k}^s) \\ & - \frac{h_o}{N_o} [(A_k^o)^2 + (B_k^o)^2 + (A_k^e)^2 + (B_k^e)^2]\}\end{aligned} \tag{5-15}$$

is the likelihood function when there is no intersymbol interference, and

$$\Lambda_1(\underline{u}) \triangleq \sum_k \frac{h_1}{N_o}\Big\{\big[2A_k^oA_k^e + 2B_k^oB_k^e + A_k^oA_{k-1}^e + B_k^oB_{k-1}^e$$

$$+ A_k^eA_{k+1}^o + B_k^eB_{k+1}^o\big]\Big\} \qquad (5\text{-}16)$$

is the correction term due to intersymbol interference.

$$\Lambda(r(t), \underline{u}) = \Lambda_0(r(t), \underline{u}) - \Lambda_1(\underline{u}) \qquad (5\text{-}17)$$

The maximization of $\Lambda(r(t), \underline{u})$ over all possible $\underline{u}$ can be efficiently performed with an extended state Viterbi algorithm [19],[107].

5.3 EUCLIDEAN DISTANCE BETWEEN CHANNEL SYMBOL SEQUENCES AND BOUND ON SQUARED DISTANCES IN THE PRESENCE OF INTERSYMBOL INTERFERENCE

The probability of error is a common measure of the performance of communications systems. In general, the probability of error depends on the Euclidean distances between signals, and is particularly dictated by the minimum distance.

In this section, we determine the Euclidean distance between channel symbol sequences. Later, we will derive a lower bound on the minimum squared free distance, which will be used to evaluate the asymptotic performance of our coded four-dimensional systems in the presence of intersymbol interference.

The transmitted signal can be expressed as a sum of its in-phase and quadrature components. Thus,

$$y(t) = y^i(t) + y^q(t) \qquad (5\text{-}18)$$

where

$$y^i(t) = \sum_k \sqrt{2} \{A_k^o h[t - (2k - 1) T] + A_k^e h(t - 2kT)\} \cos \omega_c t \quad (5\text{-}19)$$

$$y^q(t) = \sum_k \sqrt{2} \{B_k^o h[t - (2k - 1) T] + B_k^e h(t - 2kT)\} \sin \omega_c t \quad (5\text{-}20)$$

Let's denote the operation of the modulation by Y(*). Suppose $y(t) = Y(\underline{S})$ and $\tilde{y}(t) = Y(\underline{\tilde{S}})$. Then the squared Euclidean distance between the two signals is given by

$$\begin{aligned} D[\underline{S}, \underline{\tilde{S}}] &= ||y(t) - \tilde{y}(t)||^2 \\ &= ||y^i(t) - \tilde{y}^i(t)||^2 + ||y^q(t) - \tilde{y}^q(t)||^2 \end{aligned} \quad (5\text{-}21)$$

Thus,

$$D[\underline{S}, \underline{\tilde{S}}] = D^i[\underline{S}, \underline{\tilde{S}}] + D^q[\underline{S}, \underline{\tilde{S}}] \quad (5\text{-}22)$$

where

$$D^i[\underline{S}, \underline{\tilde{S}}] \triangleq ||y^i(t) - \tilde{y}^i(t)||^2 \quad (5\text{-}23)$$

and

$$D^q[\underline{S}, \tilde{\underline{S}}] \triangleq ||y^q(t) - \tilde{y}^q(t)||^2 \qquad (5\text{-}24)$$

Let

$$\Delta\underline{S}_k \triangleq \underline{S}_k - \tilde{\underline{S}}_k = [(A_k - \tilde{A}_k), (B_k - \tilde{B}_k)] = (\Delta A_k, \Delta B_k) \qquad (5\text{-}25)$$

And assume that $h_i/h_o \approx 0$ for $i > 1$.

$$D^i(\underline{S}, \tilde{\underline{S}}) = \sum_k \{h_0[(\Delta A_k^o)^2 + (\Delta A_k^e)^2] + h_1[2\Delta A_k^o \Delta A_k^e + \Delta A_k^o \Delta A_{k-1}^e + \Delta A_k^e \Delta A_{k+1}^o]\} \qquad (5\text{-}26)$$

$$D^q(\underline{S}, \tilde{\underline{S}}) = \sum_k \{h_0[(\Delta B_k^o)^2 + (\Delta B_k^e)^2] + h_1[2\Delta B_k^o \Delta B_k^e + \Delta B_k^o \Delta B_{k-1}^e + \Delta B_k^e \Delta B_{k+1}^o]\} \qquad (5\text{-}27)$$

Therefore, the squared Euclidean distance between $\underline{S}$ and $\tilde{\underline{S}}$ is as follows:

$$D(\underline{S}, \tilde{\underline{S}}) = \sum_k \{h_0[(\Delta A_k^o)^2 + (\Delta A_k^e)^2 + (\Delta B_k^o)^2 + (\Delta B_k^e)^2] + h_1[2\Delta A_k^o \Delta A_k^e + 2\Delta B_k^o \Delta B_k^e + \Delta A_k^o \Delta A_{k-1}^e + \Delta B_k^o \Delta B_{k-1}^e + \Delta A_k^e \Delta A_{k+1}^o + \Delta B_k^e \Delta B_{k+1}^o]\} \qquad (5\text{-}28)$$

Equivalently,

$$D(\underline{S}, \underline{\tilde{S}}) = \sum_k \{h_0[(\Delta A_k^o)^2 + (\Delta A_k^e)^2 + (\Delta B_k^o)^2 + (\Delta B_k^e)^2]$$

$$+ 2h_1[\Delta A_k^o \Delta A_k^e + \Delta B_k^o \Delta B_k^e + \Delta A_k^o \Delta A_{k-1}^e + \Delta B_k^o \Delta B_{k-1}^e]\} \quad (5\text{-}29)$$

where the summation is over all k for which at least one of the coefficients of h_0 and h_1 is nonzero.

For phase-shift keying,

$$\Delta A_k = \sqrt{E}\,(\cos\,\theta_k - \cos\,\tilde{\theta}_k)$$
$$\Delta B_k = -\sqrt{E}\,(\sin\,\theta_k - \sin\,\tilde{\theta}_k) \quad (5\text{-}30)$$

It can be easily shown that

$$[(\Delta A_k^o)^2 + (\Delta A_k^e)^2 + (\Delta B_k^o)^2 + (\Delta B_k^e)^2]$$
$$= E[4 - 2\cos\,(\theta_k^o - \tilde{\theta}_k^o) - 2\cos\,(\theta_k^e - \tilde{\theta}_k^e)] \quad (5\text{-}31)$$

$$(\Delta A_k^o \Delta A_k^e + \Delta B_k^o \Delta B_k^e) = E[\cos\,(\theta_k^o - \theta_k^e) + \cos\,(\tilde{\theta}_k^o - \tilde{\theta}_k^e)$$
$$- \cos\,(\tilde{\theta}_k^o - \theta_k^e) - \cos\,(\theta_k^o - \tilde{\theta}_k^e)] \quad (5\text{-}32)$$

and

$$(\Delta A_k^o \Delta A_{k-1}^e + \Delta B_k^o \Delta B_{k-1}^e) = E[\cos(\theta_k^o - \theta_{k-1}^e) + \cos(\tilde{\theta}_k^o - \tilde{\theta}_{k-1}^e) - \cos(\theta_k^o - \tilde{\theta}_{k-1}^e) - \cos(\tilde{\theta}_k^o - \theta_{k-1}^e)] \quad (5\text{-}33)$$

Hence,

$$D(\underline{S}, \tilde{\underline{S}}) = 2E \sum_k \{h_0[2 - \cos(\theta_k^o - \tilde{\theta}_k^o) - \cos(\theta_k^e - \tilde{\theta}_k^e)] + h_1[\cos(\theta_k^o - \theta_k^e) + \cos(\tilde{\theta}_k^o - \tilde{\theta}_k^e) - \cos(\tilde{\theta}_k^o - \theta_k^e) - \cos(\theta_k^o - \tilde{\theta}_k^e) + \cos(\theta_k^o - \theta_{k-1}^e) + \cos(\tilde{\theta}_k^o - \tilde{\theta}_{k-1}^e) - \cos(\theta_k^o - \tilde{\theta}_{k-1}^e) - \cos(\tilde{\theta}_k^o - \theta_{k-1}^e)]\} \quad (5\text{-}34)$$

In Section 4, we have derived a lower bound on the squared Euclidean distances between channel signals in the absence of intersymbol interference. The bound depends only on the error vectors.

$$D[M(\underline{w}_k \oplus \underline{\varepsilon}_k), M(\underline{w}_k)] \geq D_b(\underline{\varepsilon}_k) \quad (5\text{-}35)$$

Without much confusion, the corresponding bound on the squared Euclidean distances between channel symbol sequences will be written as

$$D[M(\underline{w} \oplus \underline{\varepsilon}),\ M(\underline{w})] \geq \sum_{k} D_b(\underline{\varepsilon}_k) \tag{5-36}$$

where $\underline{w}$ and $\underline{\varepsilon}$ are sequences of $\underline{w}_k$ and $\underline{\varepsilon}_k$, respectively.

Using results just derived, we will proceed to derive a similar lower bound on the squared Euclidean distances, which depends only on the error sequence and the intersymbol interference parameters. The squared Euclidean distance between two channel symbol sequences, $\underline{S}$ and $\tilde{\underline{S}}$, can be written as follows:

$$\frac{D(\underline{S},\ \tilde{\underline{S}})}{2E} = h_0 A_0(\underline{S},\ \tilde{\underline{S}}) + h_1 A_1(\underline{S},\ \tilde{\underline{S}}) \tag{5-37}$$

Since the first intersymbol interference parameter, h_1, can be positive or negative, the squared Euclidean distance is upper and lower bounded as follows:

$$\frac{D(\underline{S},\ \tilde{\underline{S}})}{2E} \leq h_0 A_0(\underline{S},\ \tilde{\underline{S}}) + |h_1|\ A_1(\underline{S},\ \tilde{\underline{S}}) \tag{5-38}$$

$$\frac{D(\underline{S},\ \tilde{\underline{S}})}{2E} \geq h_0 A_0(\underline{S},\ \tilde{\underline{S}}) - |h_1|\ A_1(\underline{S},\ \tilde{\underline{S}}) \tag{5-39}$$

In the absence of intersymbol interference,

$$D(\underline{S},\ \tilde{\underline{S}}) = 2Eh_0 A_0(\underline{S},\ \tilde{\underline{S}}) \triangleq D_o(\underline{S},\ \tilde{\underline{S}}) \tag{5-40}$$

where

$$A_0(\underline{S}, \tilde{\underline{S}}) \triangleq \sum_k \left[2 - \cos\left(\theta_k^o - \tilde{\theta}_k^o\right) - \cos\left(\theta_k^e - \tilde{\theta}_k^e\right)\right] \quad (5\text{-}41)$$

Suppose $M(\underline{w})$ corresponds to $\underline{S}$, and $M(\tilde{\underline{w}}) = M(\underline{w} + \underline{\varepsilon})$ corresponds to $\tilde{\underline{S}}$, then

$$D_o(\underline{S}, \tilde{\underline{S}}) \equiv D[M(\underline{w}), M(\tilde{\underline{w}})] \geq h_o \sum_k D_b(\underline{\varepsilon}_k) \quad (5\text{-}42)$$

The term which accounts for the effect of intersymbol interference on the squared distances is

$$D_1(\underline{S}, \tilde{\underline{S}}) = 2Eh_1A_1(\underline{S}, \tilde{\underline{S}}) \quad (5\text{-}43)$$

where

$$\begin{aligned} A_1(\underline{S}, \tilde{\underline{S}}) \triangleq \sum_k \Big[&\cos\left(\theta_k^o - \theta_k^e\right) + \cos\left(\tilde{\theta}_k^o - \tilde{\theta}_k^e\right) \\ &- \cos\left(\tilde{\theta}_k^o - \theta_k^e\right) - \cos\left(\theta_k^o - \tilde{\theta}_k^e\right) \\ &+ \cos\left(\theta_k^o - \theta_{k-1}^e\right) + \cos\left(\tilde{\theta}_k^o - \tilde{\theta}_{k-1}^e\right) \\ &- \cos\left(\theta_k^o - \tilde{\theta}_{k-1}^e\right) - \cos\left(\tilde{\theta}_k^o - \theta_{k-1}^e\right)\Big] \end{aligned} \quad (5\text{-}44)$$

Suppose a lower bound can be found for $D_1(\underline{S}, \tilde{\underline{S}})$, and it depends only on the error sequence and h_1. Then we can write

$$D_1(\underline{S}, \tilde{\underline{S}}) \geq - |h_1| \sum_k D_b' (\underline{\varepsilon}_k, \underline{\varepsilon}_{k-1}) \qquad (5\text{-}45)$$

For convenience, we shall use e_k in place of $\underline{\varepsilon}_k$, where e_k is the octal representation of the binary vector $\underline{\varepsilon}_k$. Thus,

$$D(\underline{S}, \tilde{\underline{S}}) \geq h_o \sum_k D_b(e_k) - |h_1| \sum_k D_b' (e_k, e_{k-1}) \qquad (5\text{-}46)$$

The squared free Euclidean distance, d_f^2, is then lower bounded as follows:

$$d_f^2 \geq \min_{\underline{e}} \left\{ h_o \sum_k D_b(e_k) - |h_1| \sum_k D_b' (e_k, e_{k-1}) \right\} \qquad (5\text{-}47)$$

We want to choose a coding scheme for our four-dimensional systems such that d_f^2 is maximized. The above bound, being independent of the codeword sequences, $\underline{w}$, is very useful for code searching or for evaluating the asymptotic performance of the convolutional codes used.

5.3.1 LOWER BOUND ON d_f^2 FOR FOUR-DIMENSIONAL QPSK IN THE PRESENCE OF INTERSYMBOL INTERFERENCE

Having derived a general lower bound on d_f^2, we would like to investigate the bound for four-dimensional QPSK in further detail and tighten it.

The channel signal mapping for the class of four-dimensionally coded QPSK we have chosen is shown in Figure 5-1. It has the property that $|\theta_k^o - \theta_k^e| = \pi/2$ for all k.

From previous discussion, $D_b(e_k)$ has already been determined. Equation (4-22) is repeated below, with d_0^2 replaced by E.

$$D_b(e_k) = \begin{cases} 0 & \text{if } e_k = 0 \\ 4E & \text{if } e_k = 1, 2, 3, 5, 6, \text{ or } 7 \\ 8E & \text{if } e_k = 4 \end{cases} \qquad (5\text{-}48)$$

$\sum_k D_b'(e_k, e_{k-1})$ can be derived from equation (5-44). We will do it for a special case as follows.

Four-dimensionally coded PSK enables us to have some control over $A_1(\underline{S}, \underline{\tilde{S}})$. For example, if we always choose $|\theta_k^o - \theta_k^e| = \pi/2$, and also $|\tilde{\theta}_k^o - \tilde{\theta}_k^e| = \pi/2$, then $[\cos(\theta_k^o - \theta_k^e) + \cos(\tilde{\theta}_k^o - \tilde{\theta}_k^e)] = 0$. These two cosine terms simply vanish in $A_1(\underline{S}, \underline{\tilde{S}})$ and can no longer degrade the squared Euclidean distance.

Then, we have

$$\begin{aligned} A_1(\underline{S}, \underline{\tilde{S}}) = \sum_k [&-\cos(\tilde{\theta}_k^o - \theta_k^e) - \cos(\theta_k^o - \tilde{\theta}_k^e) \\ &+ \cos(\theta_k^o - \theta_{k-1}^e) + \cos(\tilde{\theta}_k^o - \tilde{\theta}_{k-1}^e) \\ &- \cos(\theta_k^o - \tilde{\theta}_{k-1}^e) - \cos(\tilde{\theta}_k^o - \theta_{k-1}^e)] \end{aligned} \qquad (5\text{-}49)$$

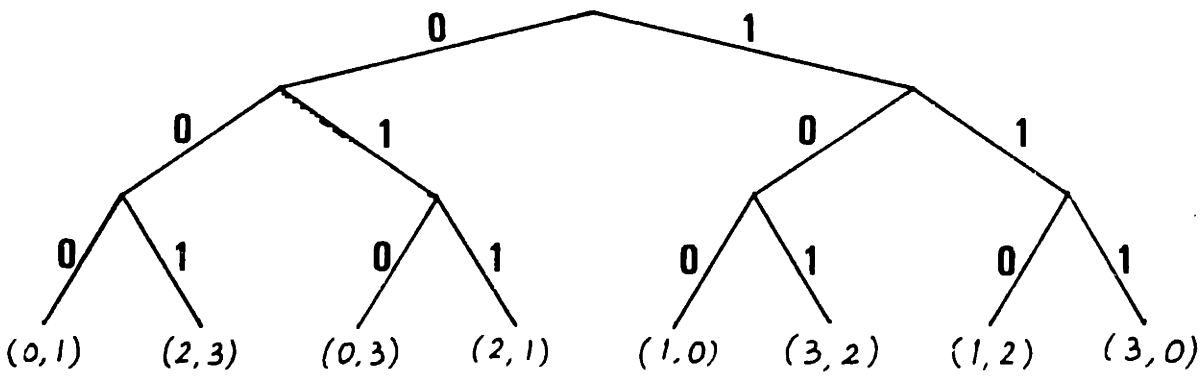

Figure 5-1. 4-D QPSK Signal Assignment With $|\theta_k^o - \theta_k^e| = \pi/2$

A trivial bound on $D_1(\underline{S}, \underline{\tilde{S}})$ is as follows:

$$D_1(\underline{S}, \underline{\tilde{S}}) = 2Eh_1A_1(\underline{S}, \underline{\tilde{S}}) \geq - |h_1| \sum_k D_b'(e_k, e_{k-1}) \quad (5\text{-}50)$$

where

$$D_b'(e_k, e_{k-1}) = 12E \quad (5\text{-}51)$$

For PSK systems with small numbers of phases, fairly tight bounds can be derived. For the four-dimensional QPSK system we are considering,

$$\cos\left(\tilde{\theta}_k^o - \theta_k^e\right) + \cos\left(\theta_k^o - \tilde{\theta}_k^e\right) = \begin{cases} 0 \text{ if } e_k = 0, 1, 2, \\ \qquad\quad 4, 5, \text{ or } 6 \\ \\ \pm 2 \text{ if } e_k = 3 \text{ or } 7 \end{cases} \quad (5\text{-}52)$$

and the various values of $[\cos(\theta_k^o - \theta_{k-1}^e) + \cos(\tilde{\theta}_k^o - \tilde{\theta}_{k-1}^e) - \cos(\theta_k^o - \tilde{\theta}_{k-1}^e) - \cos(\tilde{\theta}_k^o - \theta_{k-1}^e)]$ are listed on the table shown below.

e_k	e_{k-1}	$[\cos(\theta_k^o - \theta_{k-1}^e) + \cos(\tilde{\theta}_k^o - \tilde{\theta}_{k-1}^e) - \cos(\theta_k^o - \tilde{\theta}_{k-1}^e) - \cos(\tilde{\theta}_k^o - \theta_{k-1}^e)]$
0	any	0
2	any	0
any	0	0
any	6	0
4	2	0, ±4
4	4	0, ±4
6	2	0, ±4
6	4	0, ±4
odd	odd	0, ±2
odd	2	±2
odd	4	±2
4	odd	±2
6	odd	±2

Hence, we can choose $D_b'(e_k, e_{k-1})$ to be as follows.

$$D_b'(e_k, e_{k-1}) \triangleq W_1(e_k) + W_2(e_k, e_{k-1}) \tag{5-53}$$

where

$$W_1(e_k) \triangleq \begin{cases} 0 & \text{if } e_k = 0, 1, 2, 4, 5, \text{ or } 6 \\ 4E & \text{if } e_k = 3 \text{ or } 7 \end{cases} \tag{5-54}$$

and

$$W_2(e_k, e_{k-1}) \triangleq \begin{cases} 0 & \text{if } e_k = 0, 2, \text{ or } e_{k-1} = 0, 6 \\ 8E & \text{if } (e_k, e_{k-1}) = (4, 2), (4, 4), (6, 2), (6, 4) \\ 4E & \text{otherwise} \end{cases} \quad (5\text{-}55)$$

Thus, the squared free Euclidean distance, d_f^2, is lower bounded as follows:

$$d_f^2 \geq \min_{\underline{e}} \left\{ h_0 \sum_k D_b(e_k) - |h_1| \sum_k [W_1(e_k) + W_2(e_k, e_{k-1})] \right\} \quad (5\text{-}56)$$

We will later make use of the above bound to evaluate the asymptotic coding gains of our coded four-dimensional QPSK systems in the presence of intersymbol interference.

5.4 DERIVATION OF SQUARED EUCLIDEAN DISTANCE BOUNDS FOR TWO-DIMENSIONAL PSK IN THE PRESENCE OF INTERSYMBOL INTERFERENCE

Before we can compare the performance of our four-dimensional systems with respect to that of conventional two-dimensional PSK systems, we have to derive similar lower bounds on the squared Euclidean distance between channel signals of the two dimensional systems.

In a two-dimensional PSK system, the number of channel signals, M, corresponds directly to the number of phases. Let

$$\theta_k \triangleq \frac{2\pi}{M} a_k \; ; \; a_k \in \{0, 1, 2, \ldots, M-1\} \quad (5\text{-}57)$$

The transmitted two-dimensional signal is

$$y(t) = \sum_k \left[A_k \sqrt{2}\, h(t - kT) \cos \omega_c t + B_k \sqrt{2}\, h(t - kT) \sin \omega_c t \right] \quad (5\text{-}58)$$

where

$$A_k \triangleq \sqrt{E} \cos \theta_k \text{ and}$$

$$B_k \triangleq -\sqrt{E} \sin \theta_k. \quad (5\text{-}59)$$

The squared Euclidean distance between transmitted signals, $y(t) = Y(\underline{a})$ and $\tilde{y}(t) = Y(\tilde{\underline{a}})$ is given by

$$D(\underline{a}, \tilde{\underline{a}}) = ||y(t) - \tilde{y}(t)||^2 \quad (5\text{-}60)$$

$$D(\underline{a}, \tilde{\underline{a}}) = \sum_k \left[\Delta A_k \sqrt{2}\, h(t - kT) \cos \omega_c t + \Delta B_k \sqrt{2}\, h(t - kT) \sin \omega_c t \right] \quad (5\text{-}61)$$

where

$$\Delta A_k \triangleq A_k - \tilde{A}_k = \sqrt{E} (\cos \theta_k - \cos \tilde{\theta}_k)$$

$$\Delta B_k \triangleq B_k - \tilde{B}_k = -\sqrt{E} (\sin \theta_k - \sin \tilde{\theta}_k) \quad (5\text{-}62)$$

Again, h(t) is assumed to have the same property as described earlier. Then the squared Euclidean distance can be obtained simply from our previous results for the four-dimensional systems.

$$D(\underline{a}, \tilde{\underline{a}}) = \sum_k \sum_j \left(\Delta A_k \Delta A_j h_{k-j} + \Delta B_k \Delta B_j h_{k-j}\right)$$

$$D(\underline{a}, \tilde{\underline{a}}) = 2E \sum_k h_0[1 - \cos(\theta_k - \tilde{\theta}_k)]$$

$$+2E \sum_{\ell \geq 1} h_\ell[\cos(\theta_k - \theta_{k-\ell}) + \cos(\tilde{\theta}_k - \tilde{\theta}_{k-\ell})$$

$$- \cos(\theta_k - \tilde{\theta}_{k-\ell}) - \cos(\tilde{\theta}_k - \theta_{k-\ell})] \qquad (5\text{-}63)$$

Again, assuming $|h_i|/h_o << 1$ for $i > 1$,

$$D(\underline{a}, \tilde{\underline{a}}) = D_0(\underline{a}, \tilde{\underline{a}}) + D_1(\underline{a}, \tilde{\underline{a}}) \qquad (5\text{-}64)$$

where

$$D_0(\underline{a}, \tilde{\underline{a}}) \triangleq 2Eh_0 \sum_k [1 - \cos(\theta_k - \tilde{\theta}_k)] \qquad (5\text{-}65)$$

is the squared Euclidean distance in the absence of intersymbol interference. And

$$D_1(\underline{a}, \tilde{\underline{a}}) \triangleq 2Eh_1 \sum_k [\cos(\theta_k - \theta_{k-1}) + \cos(\tilde{\theta}_k - \tilde{\theta}_{k-1}) - \cos(\theta_k - \tilde{\theta}_{k-1}) - \cos(\tilde{\theta}_k - \theta_{k-1})] \quad (5\text{-}66)$$

represents the degradation due to intersymbol interference. Again, we will examine the squared Euclidean distance of two-dimensional QPSK in detail, and derive a tight lower bound on the squared free distance. The table below shows the relationship between the error vectors and their corresponding angular differences.

e_k	$\underline{\varepsilon}_k$	$\Delta\theta_k$
0	00	0
1	01	$\pm\pi/2$
2	10	$\pm\pi$
3	11	$\pm\pi/2$

We can easily show that

$$\begin{aligned}
&[\cos(\theta_k - \theta_{k-1}) + \cos(\tilde{\theta}_k - \tilde{\theta}_{k-1}) \\
&- \cos(\theta_k - \tilde{\theta}_{k-1}) - \cos(\tilde{\theta}_k - \theta_{k-1})] \\
&= 4\cos\left[\left(\frac{\Delta\theta_k - \Delta\theta_{k-1}}{2}\right) + (\tilde{\theta}_k - \tilde{\theta}_{k-1})\right] \\
&\cdot \sin\left(\frac{\Delta\theta_k}{2}\right) \sin\left(\frac{\Delta\theta_{k-1}}{2}\right)
\end{aligned} \quad (5\text{-}67)$$

Using the above identity, we have derived the following table.

e_k	e_{k-1}	$[\cos(\theta_k - \theta_{k-1}) + \cos(\tilde{\theta}_k - \tilde{\theta}_{k-1}) - \cos(\theta_k - \tilde{\theta}_{k-1}) - \cos(\tilde{\theta}_k - \theta_{k-1})]$
0	any	0
any	0	0
odd	odd	0, ±2
2	odd	±2
odd	2	±2
2	2	0, ±4

Using similar notations as before, we can lower bound the squared Euclidean distance as follows:

$$D(\underline{a}, \tilde{\underline{a}}) \geq h_o \sum_k D_b(e_k) - |h_1| \sum_k D_b'(e_k, e_{k-1}) \qquad (5\text{-}68)$$

where

$$D_b(e_k) = \begin{cases} 0 & \text{if } e_k = 0 \\ 2E & \text{if } e_k = 1 \text{ or } 3 \\ 4E & \text{if } e_k = 2 \end{cases} \qquad (5\text{-}69)$$

and

$$D_b'(e_k, e_{k-1}) = \begin{cases} 0 & \text{if } e_k = 0 \text{ or } e_{k-1} = 0 \\ 8E & \text{if } e_k = e_{k-1} = 2 \\ 4E & \text{otherwise} \end{cases} \qquad (5\text{-}70)$$

It is important to point out that given the same set of QPSK signals, the energy per symbol, E_s, for the four-dimensional systems is twice as much as that for the two-dimensional systems.

A tight lower bound on the squared free Euclidean distance is given as follows:

$$d_f^2 \geq \min_{\underline{e}} \left\{ h_0 \sum_k D_b(e_k) - |h_1| \sum_k D_b'(e_k, e_{k-1}) \right\} \qquad (5\text{-}71)$$

5.5 COMPARISON BETWEEN THE FOUR-DIMENSIONAL AND TWO-DIMENSIONAL SYSTEMS IN TERMS OF BOUNDS ON d_f^2

Simple trellis codes for both the four-dimensional and two-dimensional systems have been selected in Section 4. Their respective robustness in the presence of intersymbol interference will be evaluated in terms of their squared free distance bounds derived in Sections 5.3.1 and 5.4, respectively.

For simple codes with small numbers of trellis states, the squared free distances can be determined by hand. When the number of trellis states is large, it may be necessary to use a computer to determine the distances. In this section, the squared free distances, for 2, 4, and 8 trellis states, of both the two-dimensional and four-dimensional systems have been determined by hand, and compared. Figures 5-2, 5-3, and 5-4 show the minimum squared free distances as a function of the normalized intersymbol interference parameter, $|h_1|/h_0$, for both systems. We can deduce from the graphs that when the level of

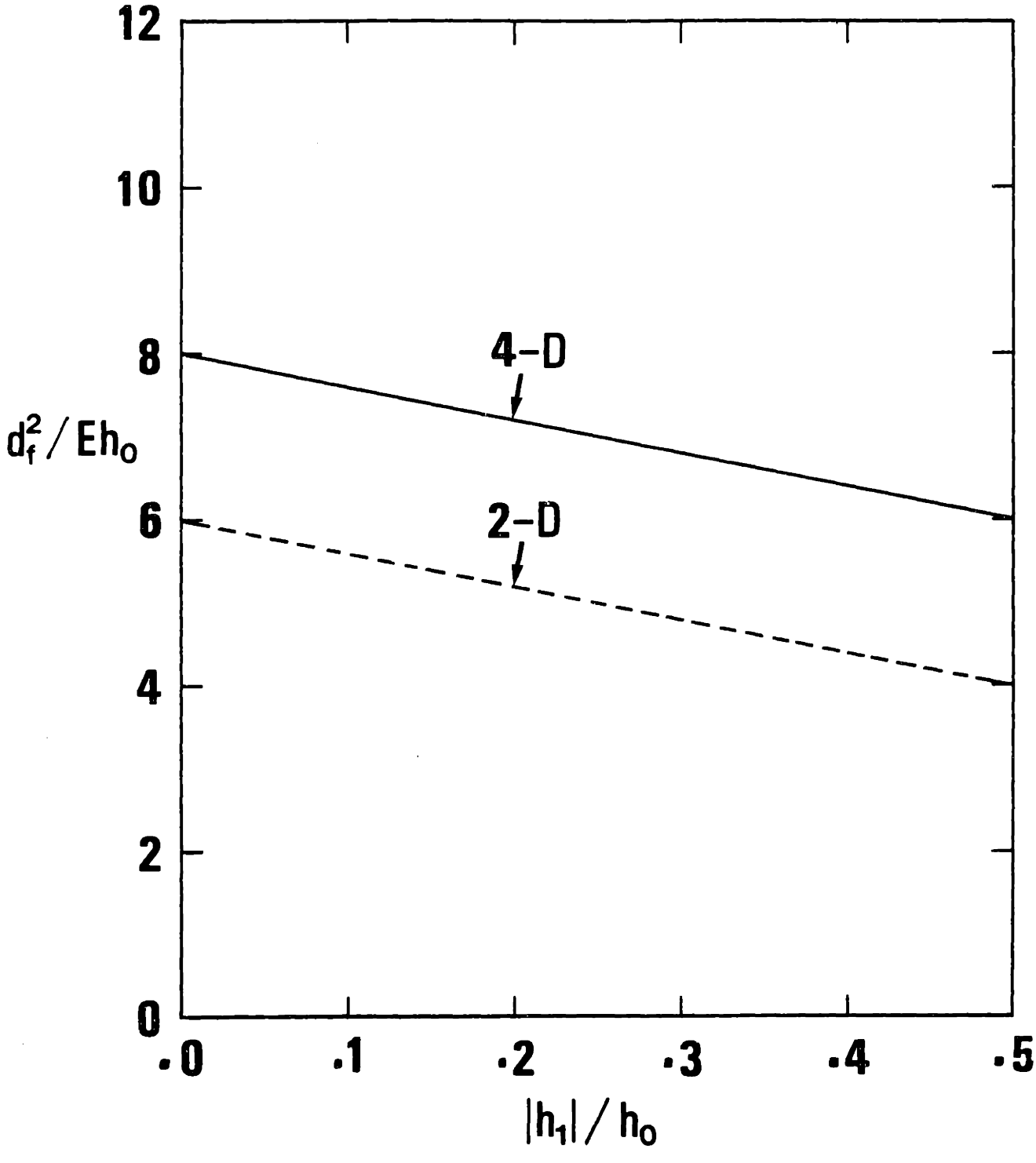

Figure 5-2. d_f^2/Eh_o vs $|h_1|/h_0$ for 2 Trellis States

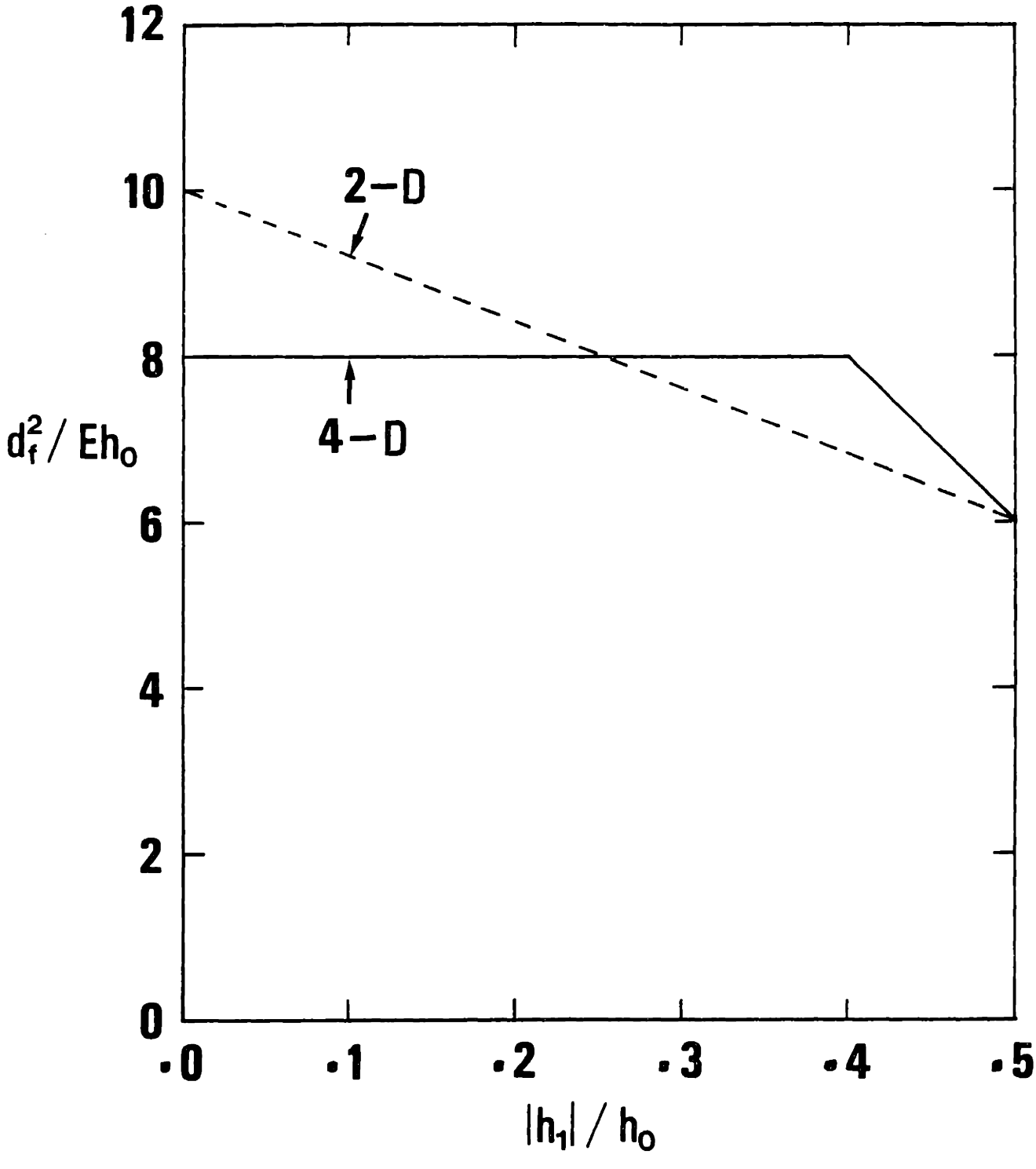

Figure 5-3. d_f^2/Eh_o vs $|h_1|/h_0$ for 4 Trellis States

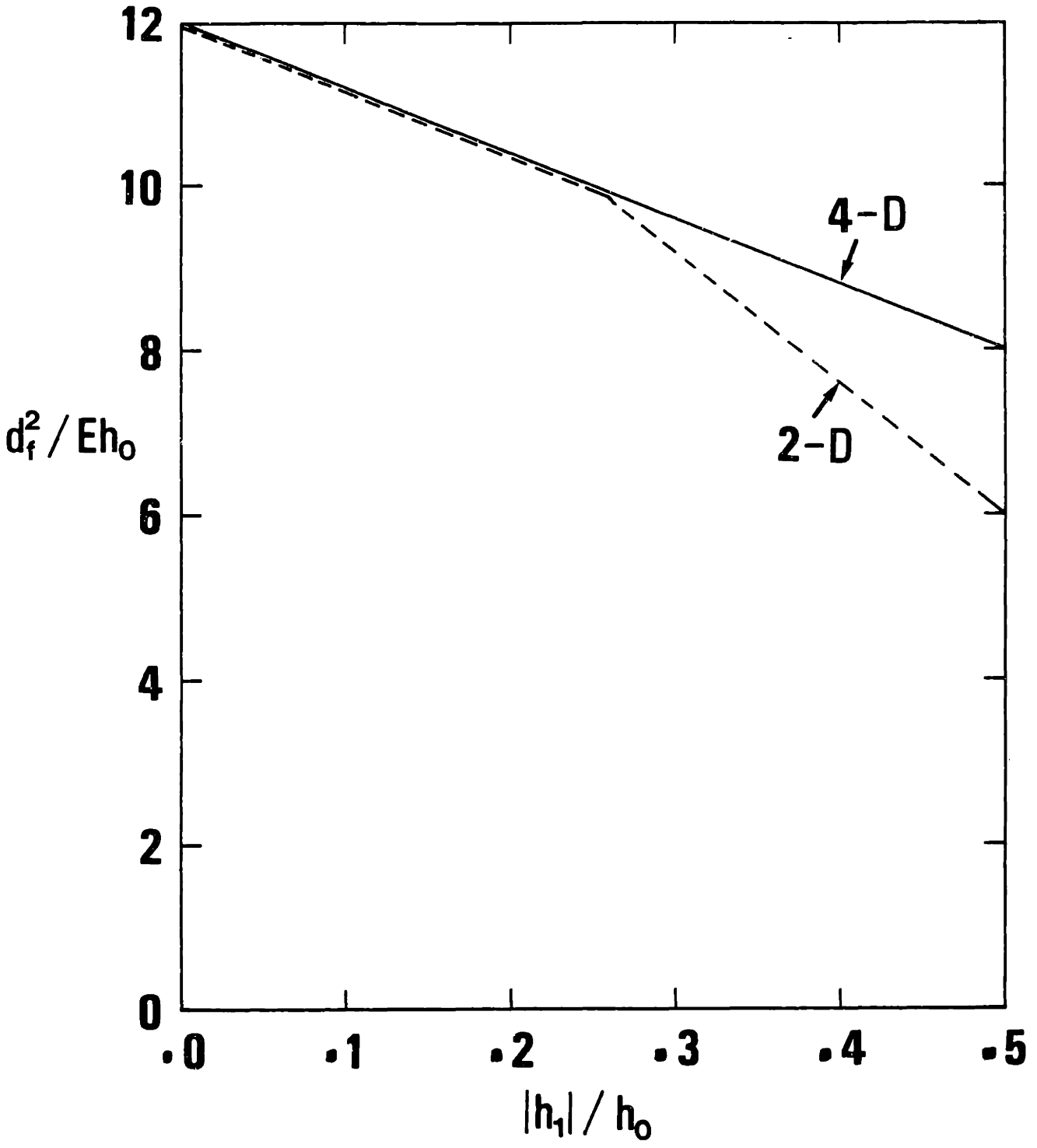

Figure 5-4. d_f^2/Eh_o vs $|h_1|/h_0$ for 8 Trellis States

intersymbol interference is high, the four-dimensional systems generally provide better protection to the signals than the corresponding two-dimensional systems.

6. CODING FOR FREQUENCY-REUSE SYSTEMS WITH CO-CHANNEL AND INTERSYMBOL INTERFERENCE

6.1 DESCRIPTION OF THE SYSTEM

Multiple reuse of frequencies contributes to an increase in the utilization of channel bandwidth. Orthogonality between frequency-reuse channels can be achieved by antenna beam isolation or by orthogonal polarization. Co-channel interference arises when adjacent antenna beams overlap, or when dual-polarized waves are depolarized by the propagation medium. Although a satisfactory level of channel discrimination can be achieved by using high quality antenna systems and adaptive cross-polarization canceling devices, it is often extremely difficult, costly, and impractical to maintain reliable performance under all weather and operational conditions. A suboptimal, but practical solution is to employ coding and modulation systems that are highly resistant to co-channel interference.

The nature of co-channel interference is usually very complicated and time-varying. In the past, the interfering signals have often been treated as additive white Gaussian noise. This assumption is, in fact, an over-simplification, especially when the number of co-channel interferers is small.

With today's technology, co-channel interference can often be measured or estimated with some confidence. Measurements can be done by periodically detecting pilot signals which are specially assigned in the transmission. Since the interference is usually quasi-static, adaptive adjustment in the measurements can be made as the interference varies slowly over time. Under normal operational conditions and fair weather, 15-20 dB

of discrimination between frequency-reuse channels is usually achievable. In addition, with advanced phase-lock techniques, reasonably good synchronization is possible. Hence, it is reasonable to assume in our model that the co-channel interference is known, carrier-to-interference ratio is moderate, and there is perfect synchronization.

Consider a pair of frequency-reuse channels. Each of the transmitted four-dimensional signals consists of two two-dimensional PSK components.

$$S_{i1}(t) = \sqrt{2E_1}\, h(t) \cos(\omega_c t + \theta_{i1})$$
$$S_{i2}(t) = \sqrt{2E_1}\, h(t) \cos(\omega_c t + \theta_{i2}) \qquad (6\text{-}1)$$

where h(t), which defines the envelope of the signal pulses, is assumed to have a narrow bandwidth compared to the carrier frequency, ω_c.

The energy of the four-dimensional signal is E_s and is given by

$$E_s = \int S_{i1}^2(t)\, dt + \int S_{i2}^2(t)\, dt = E_1 + E_2 \qquad (6\text{-}2)$$

The two two-dimensional signals interfere with each other due to imperfect isolation. Assume for the time being that there is no intersymbol interference in each of the two two-dimensional channels. In the absence of noise, the received signals in the two nominally orthogonal channels are, respectively:

$$
\begin{aligned}
y_1(t) &= \alpha_{11}\sqrt{2E_1}\,h(t)\cos(\omega_c t + \theta_1 + \beta_{11}) \\
&\quad + \alpha_{12}\sqrt{2E_2}\,h(t)\cos(\omega_c t + \theta_2 + \beta_{12}) \\
y_2(t) &= \alpha_{21}\sqrt{2E_1}\,h(t)\cos(\omega_c t + \theta_1 + \beta_{21}) \\
&\quad + \alpha_{22}\sqrt{2E_2}\,h(t)\cos(\omega_c t + \theta_2 + \beta_{22}) \\
&\qquad 0 \le t \le T
\end{aligned} \tag{6-3}
$$

where $\{\alpha\}$ and $\{\beta\}$ are the co-channel interference parameters corresponding respectively to the attenuation factors and the phase-shifts of the transmitted signals. In the presence of noise, the received signals are:

$$
\begin{aligned}
r_1(t) &= y_1(t) + n_1(t) \\
r_2(t) &= y_2(t) + n_2(t)
\end{aligned} \tag{6-4}
$$

where $n_1(t)$ and $n_2(t)$ are independent additive white Gaussian noise (AWGN), with spectral height $N_o/2$.

Without loss of generality, we will normalize the signals in the two channels by α_{11} and α_{22}, respectively. Let $\alpha_{12}/\alpha_{11} = \rho_{12}$ and $\alpha_{21}/\alpha_{22} = \rho_{21}$. Our earlier assumptions imply that $\rho_{12} << 1$ and $\rho_{21} << 1$. Assuming $\beta_{11} = \beta_{22} = 0$, we will express the received signals in the following form:

$$
\begin{aligned}
r_1(t) &= \sqrt{2E_1}\;\; h(t)\cos(\omega_c t + \theta_1) \\
&\quad + \rho_{12}\sqrt{2E_2}\,h(t)\cos(\omega_c t + \theta_2 + \delta_{12}) + n_1(t) \\
r_2(t) &= \sqrt{2E_2}\;\; h(t)\cos(\omega_c t + \theta_2) \\
&\quad + \rho_{21}\sqrt{2E_1}\,h(t)\cos(\omega_c t + \theta_1 + \delta_{21}) + n_2(t)
\end{aligned} \tag{6-5}
$$

To facilitate further discussion, we would like to introduce vector notations by using the following basis:

$$\phi_c(t) = \sqrt{2}\, h(t) \cos \omega_c t$$
$$\phi_s(t) = -\sqrt{2}\, h(t) \sin \omega_c t \qquad (6\text{-}6)$$

Then, $s_1(t)$ and $s_2(t)$ can be represented by the following vectors:

$$\underline{s}_1 = \begin{pmatrix} s_1^c \\ s_1^s \end{pmatrix} = \begin{pmatrix} \sqrt{E_1} \cos \theta_1 \\ \sqrt{E_1} \sin \theta_1 \end{pmatrix}$$
$$\underline{s}_2 = \begin{pmatrix} s_2^c \\ s_2^s \end{pmatrix} = \begin{pmatrix} \sqrt{E_2} \cos \theta_2 \\ \sqrt{E_2} \sin \theta_2 \end{pmatrix} \qquad (6\text{-}7)$$

Let $\underline{S}$ be a four-dimensional vector such that

$$\underline{S} = \begin{bmatrix} \underline{s}_1 \\ \underline{s}_2 \end{bmatrix} = \begin{bmatrix} s_1^c \\ s_1^s \\ s_2^c \\ s_2^s \end{bmatrix} \qquad (6\text{-}8)$$

Similarly, we can represent the received signals and the noise by four-dimensional vectors:

$$\underline{R} = \begin{bmatrix} r_1^c \\ r_1^s \\ r_2^c \\ r_2^s \end{bmatrix} ; \quad \underline{Y} = \begin{bmatrix} y_1^c \\ y_1^s \\ y_2^c \\ y_2^s \end{bmatrix} ; \text{ and } \underline{N} = \begin{bmatrix} n_1^c \\ n_1^s \\ n_2^c \\ n_2^s \end{bmatrix} \tag{6-9}$$

Hence, $\underline{R} = \underline{Y} + \underline{N}$. (6-10)

It is easy to show that

$$\begin{bmatrix} y_1^c \\ y_1^s \\ y_2^c \\ y_2^s \end{bmatrix} = \begin{bmatrix} 1 & 0 & \rho_{12}\cos\delta_{12} & -\rho_{12}\sin\delta_{12} \\ 0 & 1 & \rho_{12}\sin\delta_{12} & \rho_{12}\cos\delta_{12} \\ \rho_{21}\cos\delta_{21} & -\rho_{21}\sin\delta_{21} & 1 & 0 \\ \rho_{21}\sin\delta_{21} & \rho_{21}\cos\delta_{21} & 0 & 1 \end{bmatrix} \begin{bmatrix} s_1^c \\ s_1^s \\ s_2^c \\ s_2^s \end{bmatrix} \tag{6-11}$$

which can be written simply as

$$\underline{Y} = A\underline{S} \tag{6-12}$$

Let us define a two-by-two rotational matrix as follows.

$$Q(\delta) = \begin{bmatrix} \cos\delta & -\sin\delta \\ \sin\delta & \cos\delta \end{bmatrix} \tag{6-13}$$

Then, the matrix A can be expressed as a simple block matrix.

$$A = \begin{bmatrix} I_2 & \rho_{12}Q(\delta_{12}) \\ \rho_{21}\ Q(\delta_{21}) & I_2 \end{bmatrix} \tag{6-14}$$

6.2 COHERENT DETECTION OF FOUR-DIMENSIONAL SIGNALS IN FREQUENCY-REUSE SYSTEMS

We will first consider the sub-optimal detection, in which the interfering signals are assumed to be Gaussian random processes. The received signal vectors are:

$$\begin{aligned} \underline{r}_1 &= \underline{s}_1 + \rho_{12}\underline{s}_2' + \underline{n}_1 = \underline{s}_1 + \underline{n}_1' \\ \underline{r}_2 &= \underline{s}_2 + \rho_{21}\underline{s}_1' + \underline{n}_2 = \underline{s}_2 + \underline{n}_2' \end{aligned} \tag{6-15}$$

where $\underline{s}_1'$ and $\underline{s}_2'$ are the signals $\underline{s}_1$ and $\underline{s}_2$ which have been phase-shifted. $\underline{n}_1'$ and $\underline{n}_2'$ are AWGN with spectral heights $N_{01}/2$ and $N_{02}/2$, respectively, and

$$\begin{aligned} \frac{N_{01}}{2} &= \frac{N_0}{2} + \rho_{12}^2 E_2 \\ \frac{N_{02}}{2} &= \frac{N_0}{2} + \rho_{21}^2 E_1 \end{aligned} \tag{6-16}$$

The log likelihood function can be reduced to

$$\Lambda(\underline{r}_1, \underline{r}_2) = \frac{2}{N_{01}} (\underline{r}_1^T \underline{s}_1) + \frac{2}{N_{02}} (\underline{r}_2^T \underline{s}_2) \qquad (6\text{-}17)$$

Let's consider four-dimensional BPSK as an example. Assuming equally likely signals, we can show that the probability of error for the above sub-optimal receiver is given by:

$$P_r(\varepsilon) = 1 - \left[\text{erfc} \left(-\sqrt{\frac{2E_1}{N_{01}}}\right)\right] \cdot \left[\text{erfc} \left(-\sqrt{\frac{2E_2}{N_{02}}}\right)\right] \qquad (6\text{-}18)$$

where erfc(*) is defined as

$$\text{erfc}(y) \triangleq \int_y^\infty \frac{1}{\sqrt{2\pi}} \exp\left(\frac{-x^2}{2}\right) dx \qquad (6\text{-}19)$$

Specifically, if $E_1 = E_2 = E_b$, and $N_{01} = N_{02} = N_0^*$, and $\rho_{12} = \rho_{21} = \rho$, then

$$P_r(\varepsilon) = 1 - \left[\text{erfc} \left(-\sqrt{\frac{2E_b}{N_0^*}}\right)\right]^2 \qquad (6\text{-}20)$$

and

$$\frac{E_b}{N_o^*} = \frac{E_b/N_o}{1 + 2\rho^2 (E_b/N_o)} \qquad (6\text{-}21)$$

The bit error rate (BER) is at least half the symbol error rate, since each four-dimensional BPSK symbol corresponds to two bits, and the probability of double bit errors is very small. Thus,

$$\text{BER} \geq \frac{1}{2} \Pr(\varepsilon) = \frac{1}{2} \left\{ 1 - \left[\operatorname{erfc} \left(-\sqrt{\frac{2E_b}{N_o^*}} \right) \right]^2 \right\} \qquad (6\text{-}22)$$

The graph of BER versus E_b/N_o for various values of ρ is shown in Figure 6-1. Note that when there is no co-channel interference ($\rho = 0$), the BER versus E_b/N_o curve is the same as that for two-dimensional BPSK.

The optimal receiver does not assume that the interfering signals are Gaussian, but does assume that the matrix, A, is known. The log likelihood function is proportional to $||\underline{r} - A\underline{S}||^2$, which can be expanded and simplified by dropping terms which do not directly depend on the signal, $\underline{S}$. The log likelihood function can thus be reduced to the following:

$$\Lambda(\underline{r}_1, \underline{r}_2) \approx \Lambda_0(\underline{r}_1, \underline{r}_2) + \Lambda_I(\underline{r}_1, \underline{r}_2) \qquad (6\text{-}23)$$

where

$$\Lambda_0(\underline{r}_1, \underline{r}_2) \triangleq \frac{2}{N_0} (\underline{r}_1^T \underline{S}_1 + \underline{r}_2^T \underline{S}_2) \qquad (6\text{-}24)$$

is the usual likelihood function when there is no co-channel interference, and

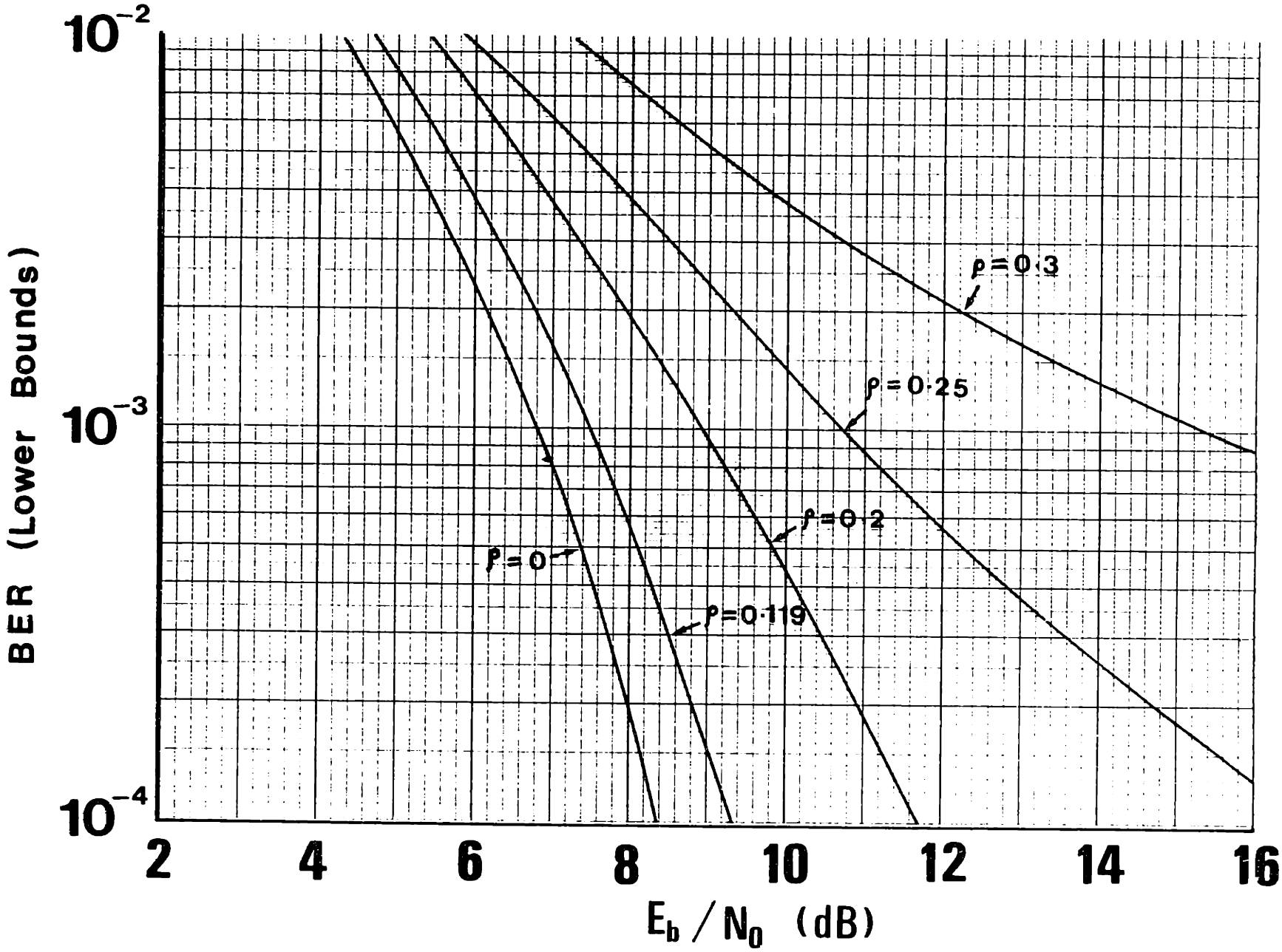

Figure 6-1. Performance of Sub-Optimal Receiver in the Presence of of Co-Channel Interference

$$\Lambda_I(\underline{r}_1, \underline{r}_2) \triangleq \frac{2}{N_o} \rho_{12}\, \underline{r}_1^T Q(\delta_{12})\, \underline{s}_2 + \rho_{21}\, \underline{r}_2^T Q(\delta_{21})\, \underline{s}_1$$

$$- \rho_{12}\, \underline{s}_1^T Q(\delta_{12})\, \underline{s}_2 - \rho_{21}\, \underline{s}_2^T Q(\delta_{21})\, \underline{s}_1$$

$$= \frac{2}{N_o} \rho_{12}\, (\underline{r}_1 - \underline{s}_1)^T Q(\delta_{12}) \underline{s}_2$$

$$+ \frac{2}{N_o} \rho_{21}\, (\underline{r}_2 - \underline{s}_2)^T Q(\delta_{21})\, \underline{s}_1 \qquad (6\text{-}25)$$

is the correction term which accounts for the co-channel interference.

6.3 RECEIVER DESIGN FOR FREQUENCY-REUSE SYSTEMS IN THE PRESENCE OF CO-CHANNEL AND INTERSYMBOL INTERFERENCE

Suppose we have applied the method of coding, developed earlier, on the design of the frequency-reuse system we are now considering. The transmitter consists of a convolutional encoder, concatenated to a four-dimensional signal mapper whose structure has been described in earlier sections. The same trellis codes obtained earlier will be used here. During each symbol period, the four-dimensional modulator outputs a pair of PSK signals, which are then transmitted through two nominally orthogonal channels employing the same frequency. It is assumed that $E_1 = E_2 = E = E_s/2$ where E_s is the energy of each of the four-dimensional symbols.

In the absence of AWGN, the received signals are:

$$y_1(t) = \sum_k \sqrt{2E} \left[\cos\left(\omega_c t + \theta_{1k}\right) h(t - kT) + \rho_{12} \cos\left(\omega_c t + \theta_{2k} + \delta_{12}\right) h(t - kT)\right]$$

and

$$y_2(t) = \sum_k \sqrt{2E} \left[\cos\left(\omega_c t + \theta_{2k}\right) h(t - kT) + \rho_{21} \cos\left(\omega_c t + \theta_{1k} + \delta_{21}\right) h(t - kT)\right] \qquad (6\text{-}26)$$

Alternatively, we can write

$$y_1(t) = \sum_k \left\{\sqrt{2E} \left[S_{1k}^c + \rho_{12} S_{2k}^c \cos \delta_{12} - \rho_{12} S_{2k}^s \sin \delta_{12}\right] \cdot h(t - kT) \cos \omega_c t - \sqrt{2E} \left[S_{1k}^s + \rho_{12} S_{2k}^s \sin \delta_{12} + \rho_{12} S_{2k}^s \cos \delta_{12}\right] \cdot h(t - kT) \sin \omega_c t\right\} \qquad (6\text{-}27)$$

and

$$y_2(t) = \sum_k \Big\{ \sqrt{2E}\,[S_{2k}^c + \rho_{21}\, S_{1k}^c \cos\,\delta_{21} - \rho_{21}\, S_{1k}^s \sin\,\delta_{21}]$$
$$\cdot\, h(t - kT)\, \cos\,\omega_c t$$
$$- \sqrt{2E}\,[S_{2k}^s + \rho_{21}\, S_{1k}^c \sin\,\delta_{21} + \rho_{21}\, S_{1k}^s \cos\,\delta_{21}]$$
$$\cdot\, h(t - kT)\, \sin\,\omega_c t \Big\} \qquad (6\text{-}28)$$

Let us define the following.

$$u_{1k}^c \triangleq [S_{1k}^c + \rho_{12}\, S_{2k}^c \cos\,\delta_{12} - \rho_{12}\, S_{2k}^s \sin\,\delta_{12}]$$
$$u_{1k}^s \triangleq [S_{1k}^s + \rho_{12}\, S_{2k}^c \sin\,\delta_{12} + \rho_{12}\, S_{2k}^s \cos\,\delta_{12}]$$
$$u_{2k}^c \triangleq [S_{2k}^c + \rho_{21}\, S_{1k}^c \cos\,\delta_{21} - \rho_{21}\, S_{1k}^s \sin\,\delta_{21}]$$
$$u_{2k}^s \triangleq [S_{2k}^s + \rho_{21}\, S_{1k}^c \sin\,\delta_{21} + \rho_{21}\, S_{1k}^s \cos\,\delta_{21}] \qquad (6\text{-}29)$$

Then the received signals in the absence of the additive white Gaussian noise are:

$$y_1(t) = \sum_k \sqrt{2E}\ \left[u_{1k}^c h(t - kT) \cos \omega_c t - u_{1k}^s h(t - kT) \sin \omega_c t\right]$$

$$y_2(t) = \sum_k \sqrt{2E}\ \left[u_{2k}^c h(t - kT) \cos \omega_c t - u_{2k}^s h(t - kT) \sin \omega_c t\right] \qquad (6\text{-}30)$$

For given interference parameters, the log likelihood function is:

$$\Lambda[\underline{r}(t)] = \frac{2}{N_o}\int_{-\infty}^{\infty} r_1(t)\ y_1(t)\ dt + \frac{2}{N_o}\int_{-\infty}^{\infty} r_2(t)\ y_2(t)\ dt - \frac{1}{N_o}\int_{-\infty}^{\infty} y_1^2(t)\ dt - \frac{1}{N_o}\int_{-\infty}^{\infty} y_2^2(t)\ dt \qquad (6\text{-}31)$$

$$\int_{-\infty}^{\infty} r_j(t) y_j(t) dt = \sum_k \left\{\sqrt{E}\ u_{jk}^c \int_{-\infty}^{\infty} \sqrt{2}\ \ r_j(t)\ h(t - kT) \cos \omega_c t\ dt - \sqrt{E}\ u_{jk}^s \int_{-\infty}^{\infty} \sqrt{2}\ r_j(t)\ h(t - kT) \sin \omega_c t\ dt\right\};$$

$$j = 1,2 \qquad (6\text{-}32)$$

Let

$$r_{jk}^{c} \triangleq \int_{-\infty}^{\infty} \sqrt{2}\, r_j(t)\, h(t - kT) \cos \omega_c t \, dt$$

$$r_{jk}^{s} \triangleq \int_{-\infty}^{\infty} \sqrt{2}\, r_j(t)\, h(t - kT) \sin \omega_c t \, dt \quad ; \quad j = 1,2 \qquad (6\text{-}33)$$

Then,

$$\int_{-\infty}^{\infty} r_j(t)\, y_j(t)\, dt = \sqrt{E} \sum_{k} \left(u_{jk}^{c} r_{jk}^{c} - u_{jk}^{s} r_{jk}^{s} \right) \qquad (6\text{-}34)$$

$$\int_{-\infty}^{\infty} y_j^2(t)\,dt = E\sum_k\sum_\ell \left\{\int_{-\infty}^{\infty} \sqrt{2}\,[u_{jk}^c h(t-kT)\cos\omega_c t - u_{jk}^s h(t-kT)\sin\omega_c t] \cdot \sqrt{2}\,[u_{j\ell}^c h(t-\ell T)\cos\omega_c t - u_{j\ell}^s h(t-\ell T)\sin\omega_c t]\right\}$$

$$j = 1,2$$

$$\int_{-\infty}^{\infty} y_j^2(t)\,dt = E\sum_k\sum_\ell [(u_{jk}^c u_{j\ell}^c + u_{jk}^s u_{j\ell}^s)\,h_{k-\ell}] \quad ;$$

$$j = 1,2 \qquad (6\text{-}35)$$

where

$$h_{k-\ell} \triangleq \int_{-\infty}^{\infty} h(t-kT)\,h(t-\ell T)\,dt = h_{\ell-k} \qquad (6\text{-}36)$$

Hence,

$$\Lambda[\underline{r}(t)] = \frac{2}{N_o}\left\{\sqrt{E}\sum_k (u_{1k}^c r_{1k}^c - u_{1k}^s r_{1k}^s + u_{2k}^c r_{2k}^c - u_{2k}^s r_{2k}^s)\right\} - \frac{1}{N_o}\left\{E\sum_k\sum_\ell [(u_{1k}^c u_{1\ell}^c + u_{1k}^s u_{1\ell}^s + u_{2k}^c u_{2\ell}^c + u_{2k}^s u_{2\ell}^s) \cdot h_{k-\ell}]\right\} \qquad (6\text{-}37)$$

Let

$$\lambda_k \triangleq \frac{2}{\sqrt{E}} \left(u_{1k}^c r_{1k}^c - u_{1k}^s r_{ik}^s + u_{2k}^c r_{2k}^c - u_{2k}^s r_{2k}^s\right)$$

$$- \sum_{\ell} \left[\left(u_{1k}^c u_{1\ell}^c + u_{1k}^s u_{1\ell}^s + u_{2k}^c u_{2\ell}^c + u_{2k}^s u_{2\ell}^s\right) h_{k-\ell}\right] \qquad (6\text{-}38)$$

Then,

$$\Lambda[\underline{r}(t)] = \frac{E}{N_o} \sum_{k} \lambda_k \qquad (6\text{-}39)$$

We have thus derived the metric for maximum likelihood detection. λ_k is a function of $\underline{r}(t)$, $\underline{\theta}_k$, ρ_{12}, ρ_{21}, δ_{12}, δ_{21}, and the intersymbol interference parameters $\{h_i\}$.

Given the received signals $\underline{r}(t)$ and the interference parameters, the maximum likelihood receiver maximizes $\Lambda[\underline{r}(t)]$ with respect to $\underline{\theta}$, the entire sequence of $(\theta_{1k}, \theta_{2k})$. The above maximization can be done by using the Viterbi Algorithm with extended states [19], [107].

6.4 EUCLIDEAN DISTANCE BETWEEN SIGNALS IN THE PRESENCE OF CO-CHANNEL INTERFERENCE AND BOUNDS ON SQUARED DISTANCES

Given the coding scheme derived in previous sections, we would like to evaluate the potential coding gains of the four-dimensional systems in the presence of co-channel interference. We will first assume that there is no intersymbol interference, and derive the squared Euclidean distance between signals.

Recall that the received signals are given by

$$\underline{R} = A\underline{S} + \underline{N} \tag{6-40}$$

The squared Euclidean distance between $\underline{S}$ and $\tilde{\underline{S}}$, in the absence of the AWGN, is given by

$$D[\underline{S}, \tilde{\underline{S}}) = ||A\underline{S} - A\tilde{\underline{S}}||^2 = ||A\Delta\underline{S}||^2 = \Delta\underline{S}^T A^T A \Delta\underline{S} \tag{6-41}$$

Let

$$B \triangleq A^T A = \begin{bmatrix} B_{11} & B_{12} \\ B_{21} & B_{22} \end{bmatrix}$$

$$B_{11} = (1 + \rho_{21}^2)\, I_2 \approx I_2 \qquad \text{for } \rho_{21} << 1$$

$$B_{22} = (1 + \rho_{12}^2)\, I_2 \approx I_2 \qquad \text{for } \rho_{12} << 1$$

$$B_{12} = \rho_{12} Q(\delta_{12}) + \rho_{21} Q^T(\delta_{21})$$

$$B_{21} = \rho_{12} Q^T(\delta_{12}) + \rho_{21} Q(\delta_{21}) = B_{12}^T \quad . \tag{6-43}$$

We can simplify B_{12} as follows.

$$B_{12} = \rho_{12} \begin{bmatrix} \cos\delta_{12} & -\sin\delta_{12} \\ \sin\delta_{12} & \cos\delta_{12} \end{bmatrix} + \rho_{21} \begin{bmatrix} \cos\delta_{21} & \sin\delta_{21} \\ -\sin\delta_{21} & \cos\delta_{21} \end{bmatrix}$$

$$= \rho_o \begin{bmatrix} \cos\phi & -\sin\phi \\ \sin\phi & \cos\phi \end{bmatrix} \tag{6-44}$$

where

$$\rho_o \cos \phi = \rho_{12} \cos \delta_{12} + \rho_{21} \cos \delta_{21}$$
$$\rho_o \sin \phi = \rho_{12} \sin \delta_{12} - \rho_{21} \sin \delta_{21} \qquad (6\text{-}45)$$

Therefore,

$$\phi = \tan^{-1} \left\{ \frac{\rho_{12} \sin \delta_{12} - \rho_{21} \sin \delta_{21}}{\rho_{12} \cos \delta_{12} + \rho_{21} \cos \delta_{21}} \right\} \qquad (6\text{-}46)$$

and

$$\rho_o = \left[\rho_{12}^2 + \rho_{21}^2 + 2\rho_{12}\rho_{21} \cos (\delta_{12} + \delta_{21})\right]^{1/2} \approx \rho_{12} + \rho_{21} \qquad (6\text{-}47)$$

Then, we have

$$B_{12} \approx \begin{bmatrix} I_2 & \rho_o Q(\phi) \\ \rho_o Q^T(\phi) & I_2 \end{bmatrix} \qquad (6\text{-}48)$$

$$D(\underline{S}, \tilde{\underline{S}}) = [\Delta \underline{S}_1^T, \Delta \underline{S}_2^T] \begin{bmatrix} (1 + \rho_{21}^2) I_2 & B_{12} \\ B_{12}^T & (1 + \rho_{12}^2) I_2 \end{bmatrix} \begin{bmatrix} \Delta \underline{S}_1 \\ \Delta \underline{S}_2 \end{bmatrix}$$

$$= (1 + \rho_{21}^2) ||\Delta \underline{S}_1||^2 + (1 + \rho_{12}^2) ||\Delta \underline{S}_2||^2$$

$$+ 2\Delta \underline{S}_1^T B_{12} \Delta \underline{S}_2 \qquad (6\text{-}49)$$

Thus, for small co-channel interference,

$$D(\underline{S}, \tilde{\underline{S}}) \approx ||\Delta\underline{S}_1||^2 + ||\Delta\underline{S}_2||^2 + 2\rho_o \Delta\underline{S}_1^T Q(\phi)\Delta\underline{S}_2$$

$$= D_o(\underline{S}, \tilde{\underline{S}}) + D_\rho(\underline{S}, \tilde{\underline{S}}) \qquad (6\text{-}50)$$

where

$$D_o(\underline{S}, \tilde{\underline{S}}) = ||\Delta\underline{S}_1||^2 + ||\Delta\underline{S}_2||^2 \qquad (6\text{-}51)$$

is the squared Euclidean distance in the absence of interference. And, $D_\rho(\underline{S}, \tilde{\underline{S}}) = 2\rho_o\Delta\underline{S}_1^T Q(\phi)\Delta\underline{S}_2$ accounts for the dependence of the squared distance on co-channel interference.

By the Schwarz inequality,

$$|\Delta\underline{S}_1^T Q(\phi)\Delta\underline{S}_2| \leq ||\Delta\underline{S}_1|| \cdot ||Q(\phi)\Delta\underline{S}_2|| = ||\Delta\underline{S}_1|| \cdot ||\Delta S_2|| \qquad (6\text{-}52)$$

Also, since

$$2||\Delta\underline{S}_1|| \cdot ||\Delta\underline{S}_2|| \leq ||\Delta\underline{S}_1||^2 + ||\Delta\underline{S}_2||^2 \qquad (6\text{-}53)$$

we have

$$|D_\rho(\underline{S}, \tilde{\underline{S}})| \leq \rho_o \left[||\Delta\underline{S}_1||^2 + ||\Delta\underline{S}_2||^2\right] \qquad (6\text{-}54)$$

Hence,

$$D(\underline{S}, \tilde{\underline{S}}) \geq (1 - \rho_o)\, D_o(\underline{S}, \tilde{\underline{S}}) \qquad (6\text{-}55)$$

From the above result, we can conclude that co-channel interference degrades the signal separation by at most $[-10 \log (1 - \rho_o)]$ dB. Since $\rho_o << 1$, the degradation is normally small.

Assuming that PSK signals are used, it is easy to show that

$$||\Delta \underline{S}_1|| \cdot ||\Delta \underline{S}_2|| = |2\sqrt{E} \sin\left(\frac{\Delta\theta_1}{2}\right)| \cdot |2\sqrt{E} \sin\left(\frac{\Delta\theta_2}{2}\right)| \quad (6\text{-}56)$$

where $\Delta\theta_1 = \theta_1 - \tilde{\theta}_1$ and $\Delta\theta_2 = \theta_2 - \tilde{\theta}_2$.

Hence, the squared Euclidean distance can be lower bounded as follows.

$$D(\underline{S}, \tilde{\underline{S}}) \geq D_o(\underline{S}, \tilde{\underline{S}}) - 8E\rho_o \left|\sin\left(\frac{\Delta\theta_1}{2}\right) \sin\left(\frac{\Delta\theta_2}{2}\right)\right| \quad (6\text{-}57)$$

6.4.1 BOUND ON d_f^2 FOR 4-D QPSK IN THE PRESENCE OF CO-CHANNEL INTERFERENCE

We now proceed to improve the bound on squared Euclidean distance for the coded four-dimensional QPSK systems studied in previous sections. As usual, we will derive a bound which does not depend on $\Delta\theta_1$ and $\Delta\theta_2$, but rather only on the error in the binary sequence at the output of the convolutional encoder.

It has already been shown in Subsection 4.4.2 that

$$D_o(\underline{S}^k, \tilde{\underline{S}}^k) = D_b(e_k) = \begin{cases} 0 & \text{if } e_k = 0 \\ 8E & \text{if } e_k = 4 \\ 4E & \text{if ek = 1, 2, 3, 5, 6, or 7} \end{cases} \quad (6\text{-}58)$$

Table 6-1 shows the relationship between error and angular differences $|\Delta\theta_{1k}|$ and $|\Delta\theta_{2k}|$.

Table 6-1. Relationship Between Error and Angular Differences, $|\Delta\theta_{1k}|$ and $|\Delta\theta_{2k}|$

e_k	$\underline{\varepsilon}_k$	$\lvert\Delta\theta_{1k}\rvert$	$\lvert\Delta\theta_{2k}\rvert$
0	000	0	0
1	001	$\pi/2$	$\pi/2$
2	010	0	π
3	011	$\pi/2$	$\pi/2$
4	100	π	π
5	101	$\pi/2$	$\pi/2$
6	110	π	0
7	111	$\pi/2$	$\pi/2$

Note: $\Delta\theta_{1k} = \theta_{1k} - \tilde{\theta}_{1k}$

$\Delta\theta_{2k} = \theta_{2k} - \tilde{\theta}_{2k}$

Hence,

$$2\left|\sin\left(\frac{\Delta\theta_{1k}}{2}\right)\sin\left(\frac{\Delta\theta_{2k}}{2}\right)\right| = \begin{cases} 0 & \text{if } e_k = 0, 2, \text{ or } 6 \\ 1 & \text{if } e_k = 1, 3, 5, \text{ or } 7 \\ 2 & \text{if } e_k = 4 \end{cases} \tag{6-59}$$

Let us define:

$$w(e_k) \triangleq \begin{cases} 0 & \text{if } e_k = 0, 2, \text{ or } 6 \\ 4E & \text{if } e_k = 1, 3, 5, \text{ or } 7 \\ 8E & \text{if } e_k = 4 \end{cases} \tag{6-60}$$

Then,

$$|D_\rho(\underline{S}^k, \underline{\tilde{S}}^k)| \leq \rho_o w(e_k) \tag{6-61}$$

And, $D(\underline{S}^k, \underline{\tilde{S}}^k)$ is lower bounded by

$$B(e_k) = \begin{cases} 0 & \text{if } e_k = 0 \\ 4E & \text{if } e_k = 2 \text{ or } 6 \\ 4E(1 - \rho_o) & \text{if } e_k = 1, 3, 5, \text{ or } 7 \\ 8E(1 - \rho_o) & \text{if } e_k = 4 \end{cases} \tag{6-62}$$

Suppose $\underline{v}$ and $\underline{\tilde{v}}$ represent the entire sequence of $\underline{S}^k$ and $\underline{\tilde{S}}^k$, respectively.

$$D(\underline{v}, \underline{\tilde{v}}) = \sum_k D(\underline{S}^k, \underline{\tilde{S}}^k) \tag{6-63}$$

Then

$$D(\underline{v}, \underline{\tilde{v}}) \geq \sum_k B(e_k) = \sum_k D_b(e_k) - \rho_o \sum_k w(e_k) \tag{6-64}$$

And, the squared free distance is bounded as follows.

$$d_f^2 \geq \min_{\underline{e}} \left\{ \sum_k D_b(e_k) - \rho_o \sum_k w(e_k) \right\} \tag{6-65}$$

6.5 EUCLIDEAN DISTANCE AND BOUND ON d_f^2 IN THE PRESENCE OF BOTH CO-CHANNEL AND INTERSYMBOL INTERFERENCE

When intersymbol interference is also present, the squared Euclidean distance is only slightly modified.

$$D(\underline{v}, \underline{\tilde{v}}) = ||y_1(t) - \tilde{y}_1(t)||^2 + ||y_2(t) - \tilde{y}_2(t)||^2 \qquad (6\text{-}66)$$

where

$$y_1(t) - \tilde{y}_1(t) = \sum_k \left[\Delta u_{1k}^c \sqrt{2E}\, h(t - kT) \cos \omega_c t + \Delta u_{1k}^s \sqrt{2E}\, h(t - kT) \sin \omega_c t\right] \qquad (6\text{-}67)$$

$$y_2(t) - \tilde{y}_2(t) = \sum_k \left[\Delta u_{2k}^c \sqrt{2E}\, h(t - kT) \cos \omega_c t + \Delta u_{2k}^s \sqrt{2E}\, h(t - kT) \sin \omega_c t\right] \qquad (6\text{-}68)$$

Thus,

$$D(\underline{v}, \underline{\tilde{v}}) = E \sum_k \sum_j \left[\Delta u_{1k}^c \Delta u_{1j}^c + \Delta u_{1k}^s \Delta u_{1j}^s + \Delta u_{2k}^c \Delta u_{2j}^c + \Delta u_{2k}^s \Delta u_{2j}^s\right] \qquad (6\text{-}69)$$

And, assuming $h_i = 0$ for $i > 1$,

$$D(\underline{v}, \tilde{\underline{v}}) \approx E \sum_k \Big\{ h_o \Big[(\Delta u_{1k}^c)^2 + (\Delta u_{1k}^s)^2 + (\Delta u_{2k}^c)^2 + (\Delta u_{2k}^s)^2 \Big] + 2h_1 \Big[\Delta u_{1k}^c \, \Delta u_{1j}^c + \Delta u_{1k}^s \, \Delta u_{1j}^s + \Delta u_{2k}^c \, \Delta u_{2j}^c + \Delta u_{2k}^s \, \Delta u_{2j}^s \Big] \Big\} \tag{6-70}$$

where

$$j = k - 1$$

Recall that when $h_1 = 0$, and $h_0 = 1$

$$D(\underline{s}^k, \tilde{\underline{s}}^k) = \Delta \underline{s}_1^T \, \Delta \underline{s}_1 + \Delta \underline{s}_2^T \, \Delta \underline{s}_2 + \Delta \underline{s}_1^T \, B_{12} \Delta \underline{s}_2 + \Delta s_2^T \, B_{12}^T \, \Delta \underline{s}_1 \tag{6-71}$$

Suppose when there is intersymbol interference,

$$D(\tilde{\underline{s}}^k, \underline{s}^k) = D_o(\tilde{\underline{s}}^k, \underline{s}^k) + D_\rho(\tilde{\underline{s}}^k, \underline{s}^k) + D_1(\underline{s}^k, \tilde{\underline{s}}^k; \underline{s}^{k-1}, \tilde{\underline{s}}^{k-1}) \tag{6-72}$$

Then, by inspection,

$$D_1(\underline{s}^k, \tilde{\underline{s}}^k; \underline{s}^j, \tilde{\underline{s}}^j) = 2h_1 \Big\{ (\Delta \underline{s}_1^k)^T (\Delta \underline{s}_1^j) + (\Delta \underline{s}_2^k)^T (\Delta \underline{s}_2^j) + (\Delta \underline{s}_1^k)^T B_{12} (\Delta \underline{s}_2^j) + (\Delta \underline{s}_2^k)^T B_{12}^T (\Delta \underline{s}_1^j) \Big\}$$

$$\text{for } j = k - 1 \tag{6-73}$$

Again, using the Schwarz inequality, we can derive a bound on $D_1(\underline{s}^k, \tilde{\underline{s}}^k; \underline{s}^j, \tilde{\underline{s}}^j)$

$$|D_1(\underline{s}^k, \tilde{\underline{s}}^k; \underline{s}^j, \tilde{\underline{s}}^j)| \leq |h_1| \left[w_1^o(e_k, e_j) + \rho_o\, w_1^\rho(e_k, e_j)\right] \quad (6\text{-}74)$$

where

$$w_1^o(e_k, e_j) \triangleq 8E \left\{ \left| \sin\left(\frac{\Delta\theta_{1k}}{2}\right) \sin\left(\frac{\Delta\theta_{1j}}{2}\right) \right| + \left| \sin\left(\frac{\Delta\theta_{2k}}{2}\right) \sin\left(\frac{\Delta\theta_{2j}}{2}\right) \right| \right\} \quad (6\text{-}75)$$

$$w_1^\rho(e_k, e_j) \triangleq 8E \left\{ \left| \sin\left(\frac{\Delta\theta_{1k}}{2}\right) \sin\left(\frac{\Delta\theta_{2j}}{2}\right) \right| + \left| \sin\left(\frac{\Delta\theta_{2k}}{2}\right) \sin\left(\frac{\Delta\theta_{1j}}{2}\right) \right| \right\} \text{ for } j = k - 1 \quad (6\text{-}76)$$

Table 6-2 shows the values of $w_1^o(e_k, e_{k-1})$ and $w_1^\rho(e_k, e_{k-1})$ for various combinations of e_k and e_{k-1}.

We thus have derived a bound on the squared Euclidean distance in the presence of both co-channel and intersymbol interference.

$$D(\underline{v}, \tilde{\underline{v}}) \geq D_o(\underline{v}, \tilde{\underline{v}}) - \rho_o \sum_k w(e_k) - |h_1| \sum_k w_1^o(e_k, e_{k-1}) - \rho_o\, |h_1| \sum_k w_1^\rho(e_k, e_{k-1}) \quad (6\text{-}77)$$

Table 6-2. $w_1^{o}(e_k, e_{k-1})$ and $w_1^{\rho}(e_k, e_{k-1})$

	w_1^{o}/E / w_1^{ρ}/E	e_{k-1} = 0	1	2	3	4	5	6	7
e_k	0	0	0	0	0	0	0	0	0
		0	0	0	0	0	0	0	0
	1	0	8	$4\sqrt{2}$	8	$8\sqrt{2}$	8	$4\sqrt{2}$	8
		0	8	$4\sqrt{2}$	8	$8\sqrt{2}$	8	$4\sqrt{2}$	8
	2	0	$4\sqrt{2}$	8*	$4\sqrt{2}$	8	$4\sqrt{2}$	0*	$4\sqrt{2}$
		0	$4\sqrt{2}$	0*	$4\sqrt{2}$	8	$4\sqrt{2}$	8*	$4\sqrt{2}$
	3	0	8	$4\sqrt{2}$	8	$8\sqrt{2}$	8	$4\sqrt{2}$	8
		0	8	$4\sqrt{2}$	8	$8\sqrt{2}$	8	$4\sqrt{2}$	8
	4	0	$8\sqrt{2}$	8	$8\sqrt{2}$	16	$8\sqrt{2}$	8	$8\sqrt{2}$
		0	$8\sqrt{2}$	8	$8\sqrt{2}$	16	$8\sqrt{2}$	8	$8\sqrt{2}$
	5	0	8	$4\sqrt{2}$	8	$8\sqrt{2}$	8	$4\sqrt{2}$	8
		0	8	$4\sqrt{2}$	8	$8\sqrt{2}$	8	$4\sqrt{2}$	8
	6	0	$4\sqrt{2}$	0*	$4\sqrt{2}$	8	$4\sqrt{2}$	8*	$4\sqrt{2}$
		0	$4\sqrt{2}$	8*	$4\sqrt{2}$	8	$4\sqrt{2}$	0*	$4\sqrt{2}$
	7	0	8	$4\sqrt{2}$	8	$8\sqrt{2}$	8	$4\sqrt{2}$	8
		0	8	$4\sqrt{2}$	8	$8\sqrt{2}$	8	$4\sqrt{2}$	8

*$w_1^{o}/E \neq w_1^{\rho}/E$.

Since $w_1^{o}(e_k, e_{k-1})$ and $w_1^{\rho}(e_k, e_{k-1})$ are pretty much the same except for a few combinations of e_k and e_{k-1}, the bound can be simplified by defining

$$w_1(e_k, e_{k-1}) = \max \left[w_1^{o}(e_k, e_{k-1}), w_1^{\rho}(e_k, e_{k-1}) \right] \qquad (6\text{-}78)$$

Minimizing the bound over the entire error sequence will then give us a bound on the squared free distance, d_f^2.

$$d_f^2 \geq \min_{\underline{e}} \sum_k D_b(e_k) - \rho_o \sum_k w(e_k)$$

$$- (1 + \rho_o)|h_1| \sum_k w_1(e_k, e_{k-1}) \qquad (6\text{-}79)$$

The above bound on the squared free distance will be evaluated in the next section for our coded four-dimensional QPSK system which consists of a rate 2/3 convolutional encoder with eight trellis states. The system performance will be simulated on a computer, and the results will be compared to the bound we have derived.

7. SYSTEM PERFORMANCE EVALUATION USING DIGITAL COMPUTER SIMULATION

7.1 INTRODUCTION

With rapid advancement in computer technology over the past few decades, the cost of computer simulation has dropped significantly with respect to that of hardware simulation. Software simulation has, therefore, become an important procedure in the design of modern communication systems. Despite inevitable limitations in the mathematical models used for simulation, the results often provide fairly accurate predictions of the actual performance of the simulated systems.

An interactive computer program, known as CHAMP, has been developed at COMSAT Laboratories for the performance evaluation of communication systems in various transmission environments, including the nonlinear satellite channels. The program consists of a large collection of subprograms, each of which is used to simulate a different module, such as signal generator, filter, nonlinear amplifier, and the like. Some of the subprograms have been modified by the author in order to simulate the coded four-dimensional QPSK systems.

7.2 PERFORMANCE OF CODED FOUR-DIMENSIONAL QPSK SYSTEMS IN THE PRESENCE OF AWGN, CO-CHANNEL AND INTERSYMBOL INTERFERENCE

The asymptotic performance of the coded four-dimensional QPSK systems has been evaluated in earlier sections. Lower bounds on the squared free distances in the absence as well

as presence of co-channel and intersymbol interference have been derived for the coded four-dimensional QPSK systems which employ rate 2/3 convolutional coding. Let us now examine the bound, derived in Section 6, more closely.

$$d_f^2 \geq \min_{\underline{e}} \left\{ \sum_k D_b(e_k) - \rho_0 \sum_k w(e_k) - \right.$$

$$\left. - (1 + \rho_0)|h_1| \sum_k w_1(e_k, e_{k-1}) \right\} \qquad (7\text{-}1)$$

The first sum, in the above expression, is the bound on the squared Euclidean distance when there is no co-channel and intersymbol interference. The second sum accounts for the degradation in the squared distance due to co-channel interference only. The last sum accounts for the further degradation when both co-channel and intersymbol interference are present.

We have chosen to simulate the system performance in the presence of a co-channel interference with 18.5 dB of carrier-to-interference ratio ($\rho_0 \approx 0.2$)*, and a controlled intersymbol interference with $h_1/h_0 = 1/6$, since the above interference levels are typical of current satellite channels. Using the above values of ρ_0 and h_1, we can evaluate the bounds for the coded four-dimensional systems. The bounds for the four-dimensional system which employs a rate 2/3 convolutional encoder with eight trellis states have been evaluated.

*From equation (6-47), $\rho_0 \approx \rho_{12} + \rho_{21} \approx 2\rho$. And, 18.5 dB of C/I ratio corresponds to $\rho \approx 0.119$.

a. AWGN only

$$d_f^2 \geq \min_{\underline{e}} \left\{ \sum_k D_b(e_k) \right\} = 12E \qquad (7\text{-}2)$$

where E is the energy of each of the two-dimensional PSK components.

b. AWGN and co-channel interference

$$d_f^2 \geq \min_{\underline{e}} \left\{ \sum_k D_b(e_k) - \rho_0 \sum_k w(e_k) \right\} = 10.4E \qquad (7\text{-}3)$$

c. AWGN, co-channel and intersymbol interference

$$d_f^2 \geq \min_{\underline{e}} \sum_k \left\{ D_b(e_k) - \rho_0 \sum_k w(e_k) - (1 + \rho_0)|h_1| \sum_k w_1(e_k, e_{k-1}) \right\} = 8.8E \qquad (7\text{-}4)$$

Hence, the co-channel interference alone degrades the performance by at most about 0.62 dB. When intersymbol interference is also present, the overall degradation asymptotically approaches about 1.35 dB.

The non-asymptotic performance of the coded four-dimensional systems, in the environment as described above, has been simulated. The block diagram for the simulation is depicted in Figure 7-1. The transmitter consists of a rate 2/3 convolutional encoder and a rate 3/4 channel signal mapper. The outputs

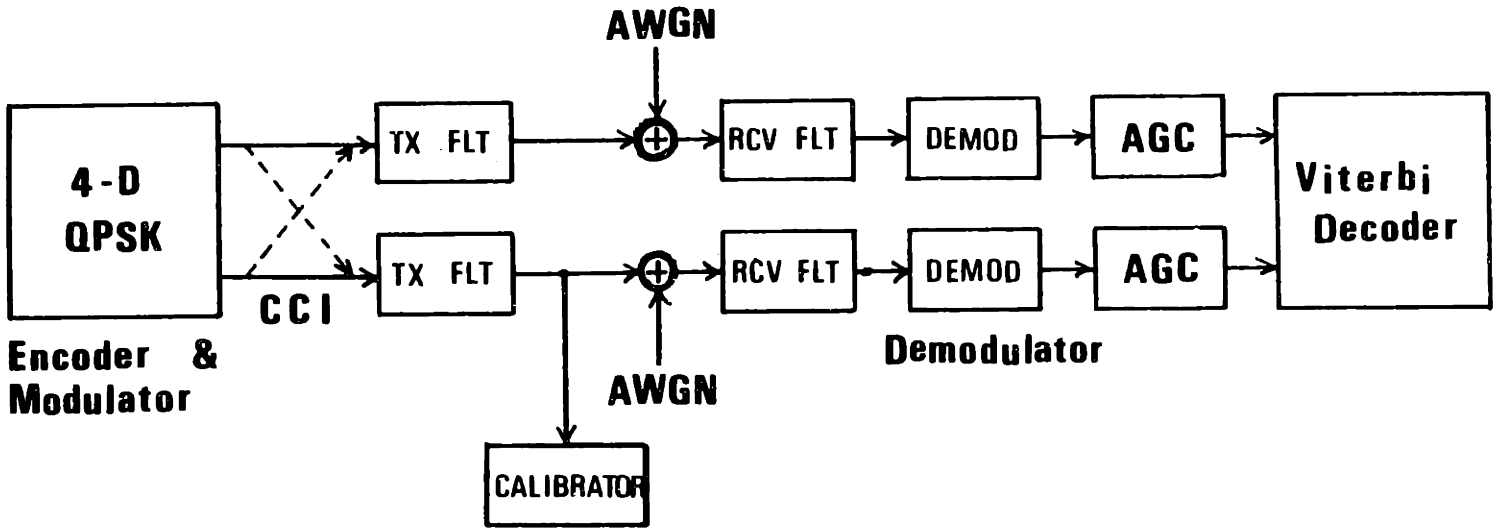

Figure 7-1. Simulation Block Diagram for 4-D Channel with AWGN, CCI, and ISI

of the transmitter are two sequences of complex impulses. The transmit and receive filters have an impulse response which is a raised cosine. Controlled intersymbol interference with $h_1/h_0 = 1/6$ is achieved by spreading the raised cosine pulses so that there is a 50 percent overlapping between adjacent pulses. The demodulator performs synchronization and phase recovery, and samples the RF signals to recover the baseband signals. The automatic gain control normalizes the baseband signals to unity to facilitate soft decisions by the decoder, which is a maximum likelihood Viterbi decoder. A 5-bit quantization has been used, and the decoder has a path memory length of 80. No extended state has been used in the decoder, so that any coding gain achieved is attributed to the coding scheme introduced in this study. The signal calibrator measures the energy of the signals, and provides a reference for the level of the additive white Gaussian noise.

For the sake of comparison, the non-asymptotic performance of the uncoded two-dimensional BPSK systems in the same environment has also been simulated. The block diagram for the simulation is shown in Figure 7-2.

The results of the above simulations are summarized on the graphs of bit error rate versus E_b/N_o, as shown in Figures 7-3 and 7-4.

7.3 PERFORMANCE OF CODED FOUR-DIMENSIONAL QPSK SYSTEMS IN NONLINEAR SATELLITE CHANNELS

The performance of the coded four-dimensional QPSK systems in the nonlinear INTELSAT V channel has been simulated. Assuming that the systems will be used for time-division multiple access transmission, we have also calibrated the signals in

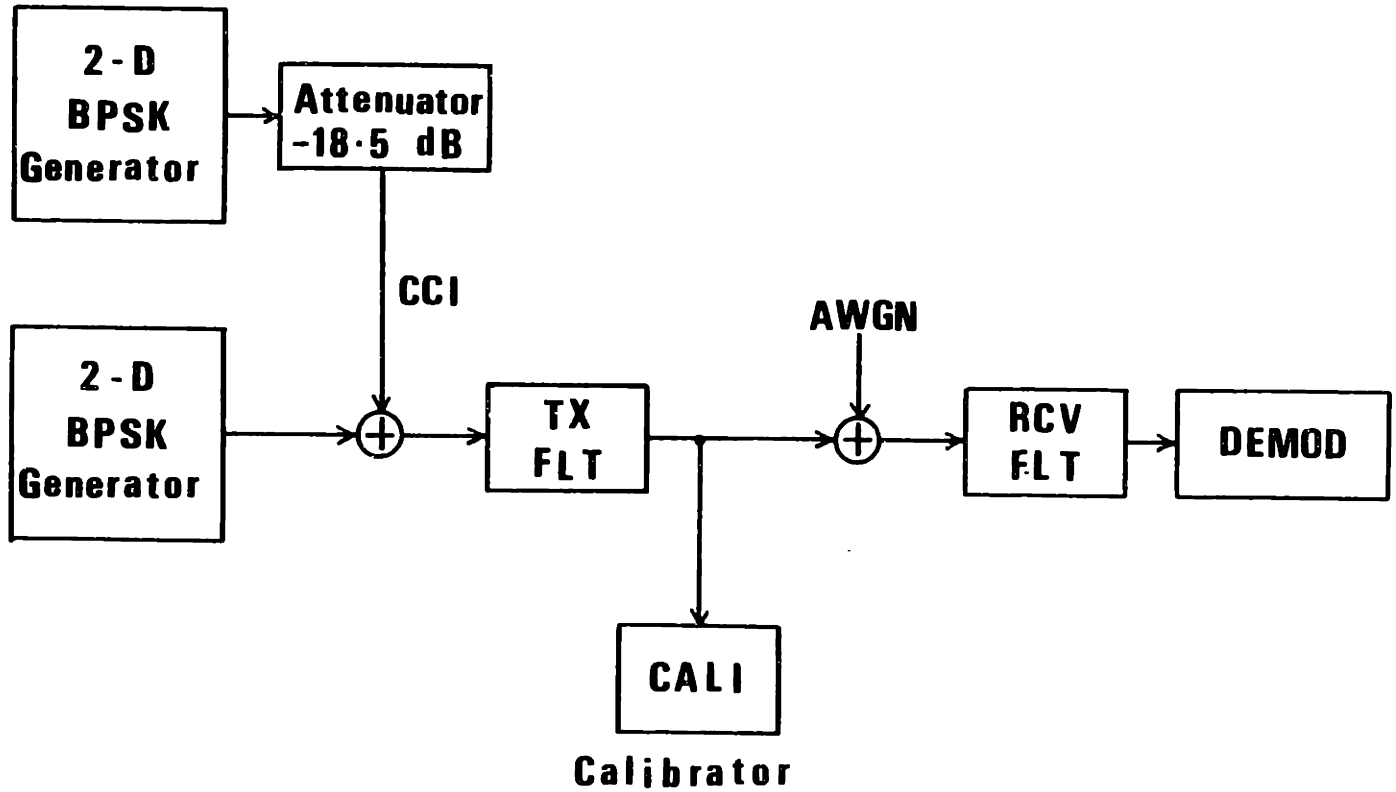

Figure 7-2. Simulation Block Diagram for 2-D Channel With AWGN, CCI and ISI

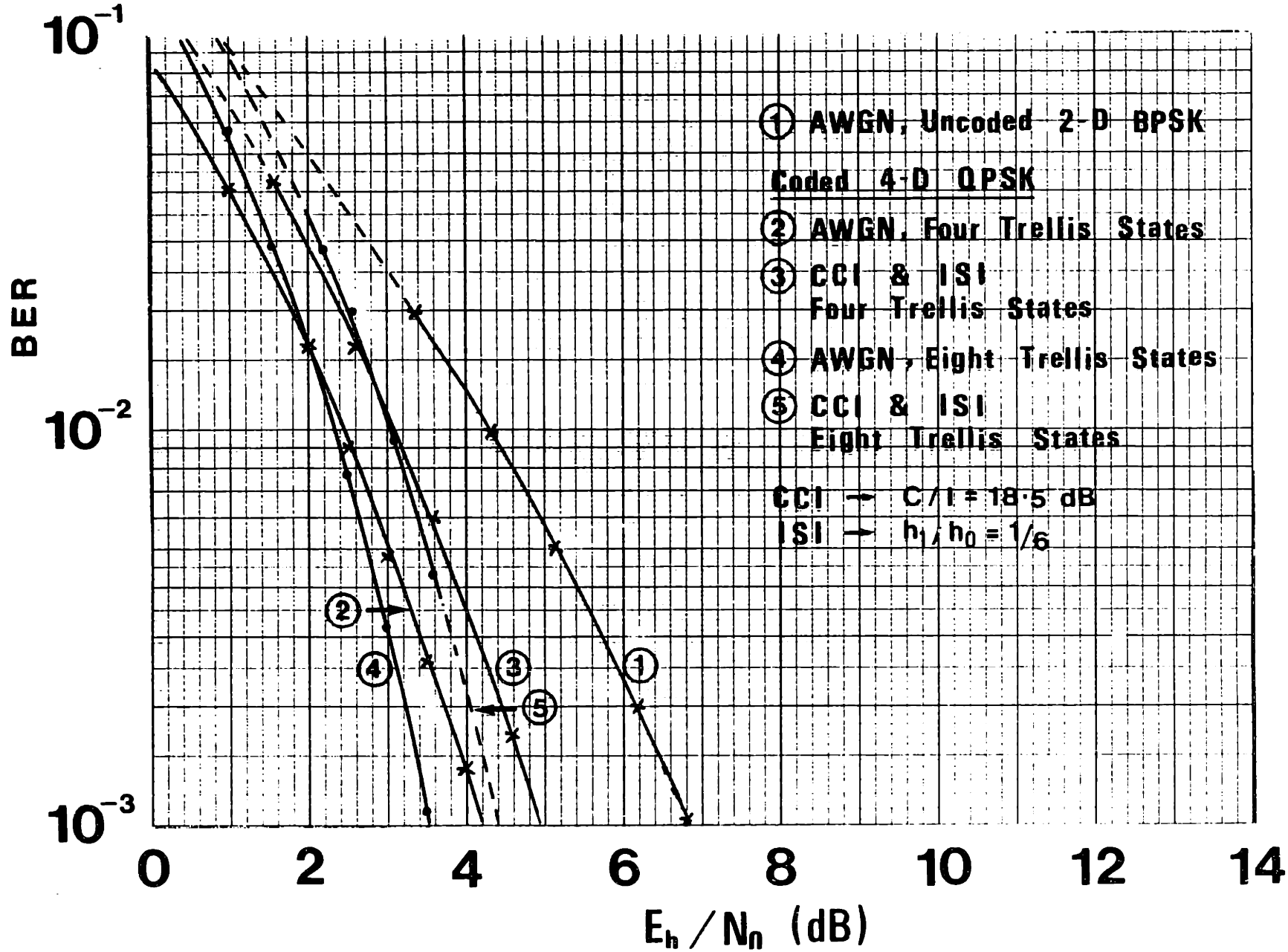

Figure 7-3. Performance of Coded 4-D QPSK for 4 and 8 Trellis States

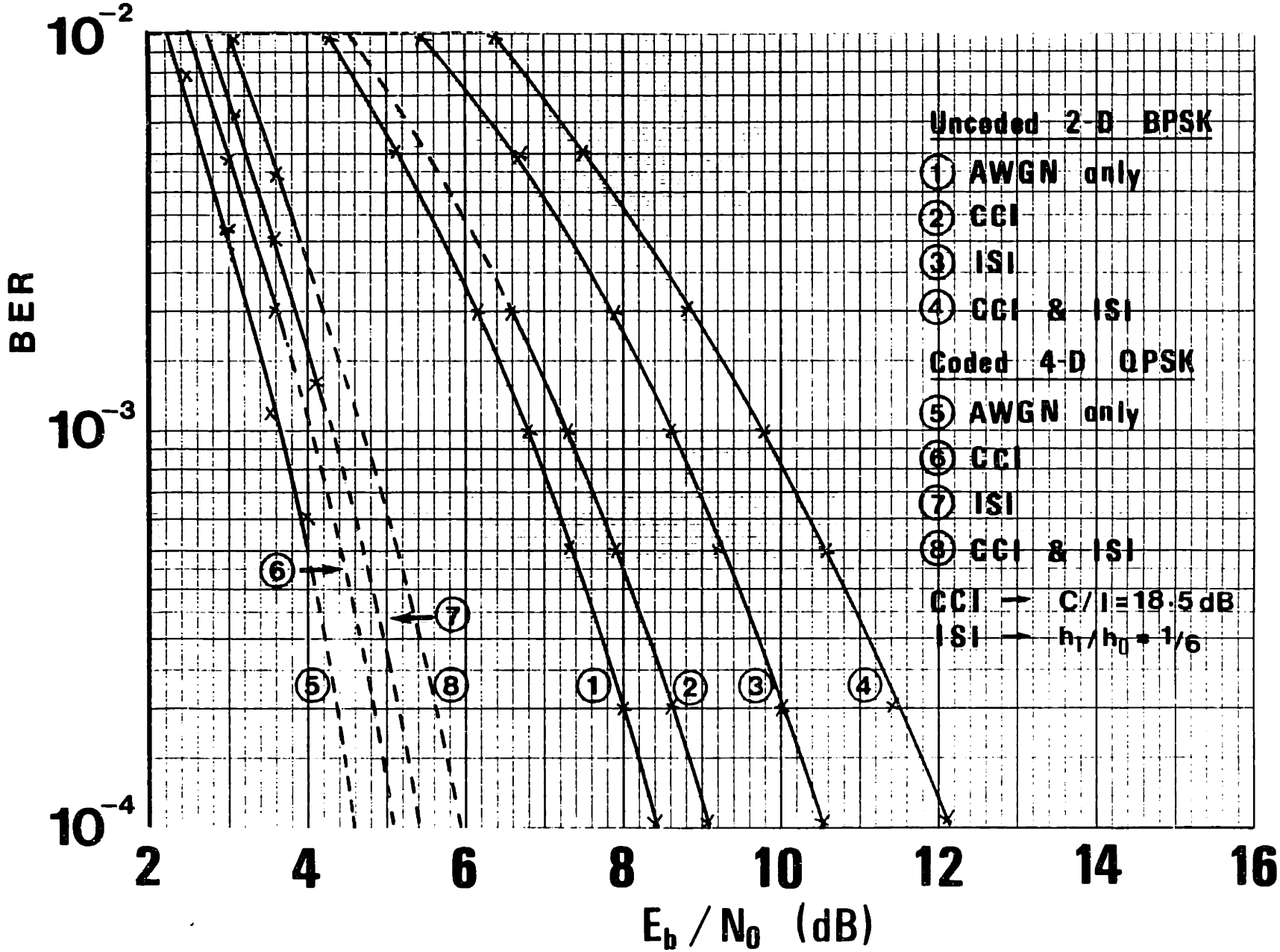

Figure 7-4. Performance of Coded 4-D QPSK (8 Trellis States) Over AWGN Channel With CCI and ISI

terms of peak power. The simulation block diagram is shown in Figure 7-5. The transmit and receive filters in the main channel have a raised cosine impulse response. Controlled intersymbol interference with $h_1/h_0 = 1/6$ has been included. We have assumed that there is co-channel interference in the up-link, with carrier-to-interference ratio of 18.5 dB. AWGN is added in the down-link.

The four-dimensional QPSK signals are transmitted at the rate of 120 Mbit/s. The upper and lower adjacent channels are respectively located at 80 MHz above and below the carrier frequency of the main channel. The transmit filters in the adjacent channels are assumed to be square-root Nyquist filters with 40 percent roll-off. The inputs to the square-root Nyquist filters are rectangular pulses. The outputs of all the transmit filters are amplified by nonlinear high-power amplifiers before they are transmitted to the satellite. The high-power amplifiers are assumed to be operated at an input backoff of 10 dB from saturation. The satellite is modeled as a cascade of an input filter, a nonlinear traveling-wave-tube amplifier, and an output filter. The satellite traveling-wave-tube amplifiers have an input backoff of 2 dB from saturation. The received signals are equalized and filtered before they are demodulated. The automatic gain controls normalize the signals to unity. The Viterbi decoder is the same as the one used in the previous simulations.

The performance of the uncoded two-dimensional BPSK systems in the nonlinear INTELSAT V channel has also been simulated. The configuration is more or less the same except for the encoder/modulator and the decoder.* The non-asymptotic

*The filters used are also different, as explained in Subsection 7.4.

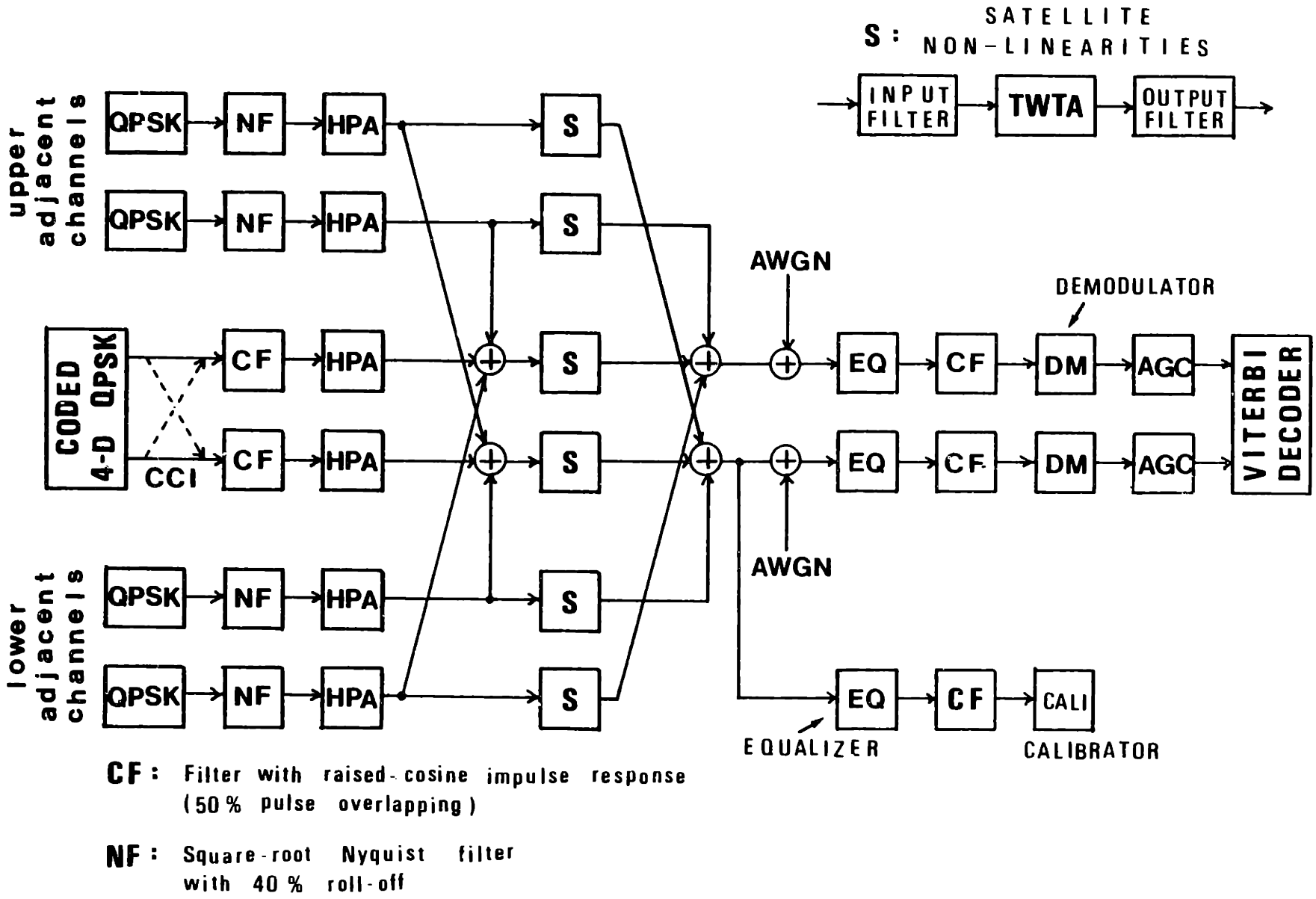

Figure 7-5. Simulation Block Diagram for INTELSAT V Channel

performance of the simulated systems over the nonlinear INTELSAT V channel is summarized on the graph shown in Figure 7-6.

7.4 DISCUSSION OF THE RESULTS

The results from the simulations agree fairly well with our theoretical predictions. Our theory predicts coding gains of 3.010 dB and 4.771 dB with respect to uncoded BPSK in AWGN for 4 and 8 trellis states, respectively. We can see from Figure 7-3 that at BER = 10^{-3}, the coding gains are about 2.5 dB and 3 dB for 4 trellis states and 8 trellis states, respectively. At high E_b/N_o, we can expect that the coding gains will tend towards their respective asymptotic values. Note that at moderate E_b/N_o, both the coded four-dimensional QPSK with 4 trellis states and that with 8 trellis states have similar performance.

Simulation results for the coded four-dimensional QPSK with 8 trellis states show that at BER = 10^{-3}, there is a degradation of about 0.4 dB due to co-channel interference, and about 1.2 dB due to both co-channel and intersymbol interference. From the bounds on squared free distances, we have evaluated the asymptotic degradation to be no greater than 0.62 dB and 1.35 dB, respectively. Again, the simulation results agree remarkably well with our theory.

Note that the coded four-dimensional QPSK systems not only have significant coding gains with respect to uncoded two-dimensional BPSK, they also have more robust performance in the presence of co-channel and intersymbol interference than the uncoded two-dimensional BPSK.

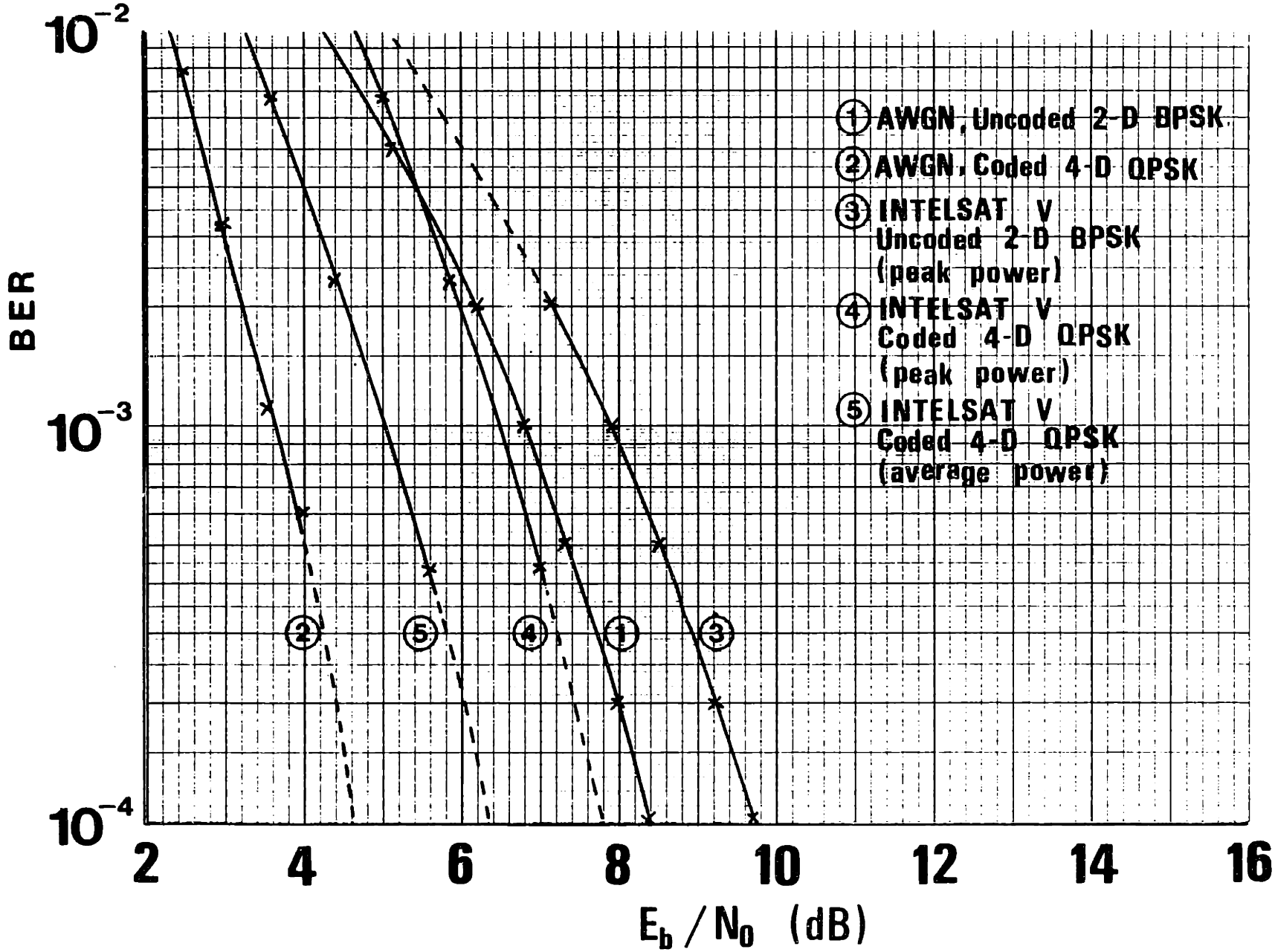

Figure 7-6. Performance of Coded 4-D QPSK (8 Trellis States) Over AWGN and INTELSAT V Channels

In the nonlinear INTELSAT V channel, the coded four-dimensional QPSK has a superior performance compared to the uncoded two-dimensional BPSK. However, note that the coded four-dimensional QPSK is degraded more by the channel nonlinearities than the uncoded two-dimensional BPSK. This is not surprising because the transmit and receive filters of the two-dimensional BPSK system are square-root Nyquist filters, whereas the corresponding filters in the four-dimensional system are filters which have been used to introduce controlled intersymbol interference. The average-power calibrated performance curve for the four-dimensional system in the INTELSAT V channel has been included for a comparison with that for the same system in AWGN only. The small degradation reflects the robustness of the system performance in the presence of satellite channel nonlinearities.

8. CONCLUSION AND SUGGESTIONS FOR FURTHER RESEARCH

8.1 CONCLUSION FROM THE RESEARCH

This research has been motivated by the belief, due to the results of an information theoretic study of the channel capacity regions, that there exist four-dimensional systems which perform more reliably than two-dimensional systems in the presence of cross-channel interference [86]-[98].

A combined coding and modulation scheme has been proposed for four-dimensional PSK systems. Significant coding gains with respect to uncoded two-dimensional PSK systems are achieved by concatenating a convolutional encoder with a four-dimensional signal mapper which maps the outputs of the encoder onto an expanded set of channel signals.

A family of four-dimensional QPSK systems with rate 2/3 convolutional coding have been designed. Some simple codes have been selected using Ungerboeck's "set-partitioning method" described earlier. Bounds on squared free distances have been derived, and used to evaluate the asymptotic performance of the four-dimensional QPSK systems.

Non-asymptotic performance of the systems in the presence of AWGN, co-channel, and intersymbol interference has been simulated on digital computers. The results are quite consistent with the theoretically predicted performance. The coded four-dimensional QPSK systems achieve coding gains of about 3 to 4 dB with respect to uncoded two-dimensional BPSK. Co-channel interference with carrier-to-interference ratio of 18.5 dB, together with intersymbol interference with $|h_1|/h_0 = 1/6$, only degrades the performance by a signal-to-noise ratio of 1 to 2 dB

with respect to its performance in AWGN only. The degradation is less for the coded four-dimensional systems than for the uncoded two-dimensional systems.

The system performance in nonlinear INTELSAT V channels has also been simulated, and compared to current uncoded two-dimensional BPSK systems without intersymbol interference. It is clear from the results that the coded four-dimensional QPSK systems with rate 2/3 convolutional coding and a four-dimensional signal mapping, have indeed a fairly robust performance in nonlinear channels with co-channel and intersymbol interference.

Perfect measurements of co-channel interference have been assumed in the design of our coded four-dimensional systems. Perturbation studies can be carried out to investigate the sensitivity of the system performance under imperfect knowledge of the co-channel interference parameters. Nevertheless, an examination of the squared free distance bound in the presence of both co-channel and intersymbol interference suggests that the systems are not very sensitive to small variations in the interference parameters.

In conclusion, when there is cross-channel interference, the method of four-dimensional modulation and coding is generally more desirable than lower dimensional systems.

8.2 SUGGESTIONS FOR FURTHER RESEARCH

It has been shown by this study that a combined design of two two-dimensional systems provides a larger degree of freedom in the selection of signal sets and coding schemes, and therefore can give rise to superior four-dimensional systems. Nonetheless, it is not very clear whether it is worthwhile to consider higher dimensional systems in the same manner. It is

conceivable that as the number of dimensions increases beyond 4, the design of signals and coding schemes will become increasingly complicated and be subject to diminishing returns.

We have considered the four dimensions in time, and in space or polarizations. Similar design techniques may be applied to other types of dimensions, such as frequencies. The coding schemes presented in this study are particularly useful when the channels in different dimensions are not perfectly orthogonal to one another.

It can be verified easily that the simple trellis codes obtained according to Ungerboeck's signal assignment rules have the largest possible free Euclidean distance in the absence of interference. However, whether the more complicated codes obtained according to the same rules are optimal remains a question to be answered. The bounds on squared free distances could have been used to design algorithms for searching more complicated codes and codes that are optimal in the presence of interference. However, this is beyond the scope of this research.

The issue of pulse-shaping to reduce bandwidth requirement, at the expense of introducing intersymbol interference, has been left out completely. In the computer simulation, controlled intersymbol interference, with 50 percent pulse-overlapping, has been achieved by simulating filters whose impulse response is a raised-cosine with user-specified pulse width.

It has been shown that the coded four-dimensional systems can be further improved by extending the states of the Viterbi decoder, in order to account for the dependence of the log likelihood functions on the intersymbol interference parameters. This was not done in the simulation in order to study the coding gains due to the coding scheme alone. Further simulation studies of the coded four-dimensional systems may include

extended-state Viterbi decoding. At higher levels of intersymbol interference, more intersymbol interference parameters, in addition to h_1, may have to be included in the metrics. This corresponds to a decoder with a larger number of extended states.

Four-dimensionally coded PSK has been considered in this research. Four-dimensionally coded QAM has been studied by Welti [100],[101]. Other general signal constellations may lack the symmetry we have exploited, especially in four-dimensional PSK. Hence, a generalized four-dimensionally coded modulation may require more sophisticated signal design techniques.

9. REFERENCES

[1] T. Logsdon, "Unsnarling Signals In Space," Technology Review, August/September 1982.

[2] "Techniques For Frequency Reuse," and "Modulation And Multiple Access Techniques," extracted from A Review Of Satellite Systems Technology, 1972, (Communications Satellite Systems: An Overview Of The Technology, edited by R.G. Gould and Y.F. Lum).

[3] R. J. Eaton and A. L. Smith, "Frequency Re-use In The INTELSAT System, Satellite Communication Systems Technology, IEE Conference Publication No. 126, April 1975.

[4] P. A. Watson and C. J. Soutter, "Dual Polarization Frequency Re-use In Satellite Communications Systems At 11 GHz," Satellite Communication Systems Technology, IEE Conference Publication No. 126, April 1975.

[5] N. McAvoy, "Frequencies Above 10 GHz," (Communications Satellite Systems: An Overview Of The Technology, Ed: Gould and Lum).

[6] D. Jansky, "Factors Affecting Orbit Utilization," (Communications Satellite Systems: An Overview Of The Technology, Ed: Gould and Lum).

[7] D. C. Hogg and T. Chu, "The Role Of Rain In Satellite Communications," Proceedings of the IEEE, Vol. 63, No. 9, September 1975.

[8] C. E. Shannon, "A Mathematical Theory Of Communication," The Bell System Technical Journal, Vol.27, July 1948; continuation in Vol. 27, October 1948.

[9] C. E. Shannon, "Communication In The Presence Of Noise," Proceedings of the IRE, Vol. 37, January 1949.

[10] A. D. Wyner, "Recent Results In The Shannon Theory," IEEE Trans. on Information Theory, Vol. IT-20, No. 1, January 1974.

[11] D. Slepian, "Bounds On Communication," The Bell System Technical Journal, May 1963.

[12] A. D. Wyner, "The Capacity Of The Band-Limited Gaussian Channel," The Bell System Technical Journal, March 1966.

[13] M. Schwartz, Information Transmission, Modulation, and Noise, New York: McGraw-Hill, 1959.

[14] C. W. Helstrom, Statistical Theory of Signal Detection, New York: Pergamon Press, 1960.

[15] J. M. Wozencraft and I. M. Jacobs, Principles of Communication Engineering, New York: Wiley, 1965.

[16] H. L. Van Trees, Detection, Estimation, and Modulation Theory, Part I, New York: Wiley, 1968.

[17] E. Arthurs and H. Dym, "On The Optimum Detection Of Digital Signals In The Presence Of White Gaussian Noise - A Geometric Interpretation And A Study Of Three Basic Data Transmission Systems," IRE Trans. on Communications Systems, December 1962.

[18] C. S. Weaver, "A Comparison Of Several Types Of Modulation," IRE Trans. on Communications Systems, March 1962.

[19] J. J. Spilker, Jr., Digital Communications by Satellite, New York: Prentice-Hall, 1977.

[20] A. J. Viterbi and J. K. Omura, Principles of Digital Communication and Coding, New York: McGraw Hill, 1979.

[21] J. G. Proakis, Digital Communications, New York: McGraw-Hill, 1983.

[22] F. Amoroso, "The Bandwidth Of Digital Data Signals," IEEE Communications Magazine, November 1980.

[23] S. A. Gronemeyer and A. L. McBride, "MSK And Offset QPSK Modulation," IEEE Trans. on Communications, Vol. COM-24, No. 8, August 1976.

[24] C. L. Weber, Elements Of Detection And Signal Design, New York: McGraw-Hill, 1968.

[25] C. R. Cahn, "Combined Digital Phase And Amplitude Modulation Communication Systems," IRE Trans. on Communications Systems, September 1960.

[26] C. N. Campopiano and B. G. Glazer, "A Coherent Digital Amplitude And Phase Modulation Scheme," IRE Trans. on Communications Systems, March 1962.

[27] R. W. Lucky and J. C. Hancock, "On The Optimum Performance Of N-ary Systems Having Two Degrees Of Freedom," IRE Trans. on Communications Systems, June 1962.

[28] J. Salz, J. R. Sheehan and D. J. Paris, "Data Transmission By Combined AM And PM," The Bell System Technical Journal, Vol. 50, No. 7, September 1971.

[29] M. K. Simon and J. G. Smith, "Hexagonal Multiple Phase-And-Amplitude-Shift-Keyed Signal Sets," IEEE Trans. on Communications, Vol. COM-21, No. 10, October 1973.

[30] G. J. Foschini, R. D. Gitlin, and S. B. Weinstein, "On The Selection Of A Two-Dimensional Signal Constellation In The Presence Of Phase Jitter And Gaussian Noise," The Bell System Technical Journal, Vol. 52, No. 6, July-August 1973.

[31] B. W. Kernighan and S. Lin, "Heuristic Solution Of A Signal Design Optimization Problem," The Bell System Technical Journal, Vol. 52, No. 7, September 1973.

[32] V. K. Prabhu, "On The Performance Of Digital Modulation Systems That Expand Bandwidth," The Bell System Technical Journal, July-August 1970.

[33] G. Ungerboeck, "Channel Coding With Multilevel/Phase Signals," IEEE Trans. on Information Theory, Vol. IT-28, No. 1, January 1982.

[34] L. Zetterberg, "A Class Of Codes For Polyphase Signals On A Bandlimited Gaussian Channel," IEEE Trans. on Information Theory, July 1965.

[35] R. Gallager, Information Theory and Reliable Communication, New York: Wiley, 1968.

[36] E. R. Berlekamp, Algebraic Coding Theory, New York: McGraw-Hill, 1968.

[37] W. W. Peterson and E. J. Weldon, Error Correcting Codes, Cambridge, MA: MIT Press, 1972.

[38] R. W. Hamming, Coding and Information Theory, New York: Prentice-Hall, 1980.

[39] A. J. Viterbi, "Convolutional Codes And Their Performance In Communication Systems," IEEE Trans. on Communications Technology, October 1971.

[40] Andrew J. Viterbi, "Error Bounds For Convolutional Codes And An Asymptotically Optimum Decoding Algorithm," IEEE Trans. on Information Theory, Vol. IT-13, No. 2, April 1967.

[41] G. David Forney, Jr., "The Viterbi Algorithm," Proceedings of the IEEE, Vol. 61, No. 3, March 1973.

[42] Jim K. Omura, "On The Viterbi Decoding Algorithm," IEEE Trans. on Information Theory, January 1969.

[43] Jerrold A. Heller and Irwin Mark Jacobs, "Viterbi Decoding For Satellite And Space Communication," IEEE Trans. on Communication Technology, October 1971.

[44] G. David Forney, Jr., "Convolutional Codes I: Algebraic Structure," IEEE Trans. on Information Theory, November 1970.

[45] G. David Forney, Jr., "Convolutional Codes II: Maximum-Likelihood Decoding," Information and Control, 25, 1974.

[46] G. David Forney, Jr., "Convolutional Codes III: Sequential Decoding," Information and Control, 25, 1974.

[47] G. D. Forney, Jr., "Structural Analysis Of Convolutional Codes Via Dual Codes," IEEE Trans. on Information Theory, Vol. IT-19, No. 4, July 1973.

[48] Interference Analysis Of Communication Systems, edited by P. Stavroulakis, IEEE Press, 1980.

[49] R. Fang and O. Shimbo, "Unified Analysis of a Class of Digital Systems in Additive Noise and Interference," IEEE Trans. on Communications, Vol. COM-21, No. 10 October 1973.

[50] S. Benedetto, E. Biglieri, and V. Castellani, "Combined Effects of Intersymbol, Interchannel and Co-Channel Interferences in M-ary CPSK Systems," IEEE Transactions on Communications, September 1973.

[51] O. Shimbo and R. Fang, "Effects Of Co-Channel Interference And Gaussian Noise In M-ary PSK Systems," COMSAT Technical Review, Vol. 3, No. 1, Spring 1973.

[52] R. L. Olsen, "Cross Polarization During Precipitation On Terrestrial Links: A Review," Radio Science, Vol. 16, No. 5, September-October 1981.

[53] D. J. Fang, "Attenuation And Phase Shift Of Microwaves Due To Canted Raindrops," COMSAT Technical Review, Vol. 5, No. 1, Spring 1975.

[54] J. A. Morrison, M. J. Cross and T. S. Chu, "Rain-Induced Differential Attenuation And Differential Phase Shift At Microwave Frequencies," The Bell System Technical Journal, Vol. 52, No. 4, April 1973.

[55] T. Kobayashi, "Degradation Of Cross-Polarization Isolation Due To Rain," Journal of the Radio Research Labs., Vol. 24, No. 114, July 1977.

[56] F. T. Tseng, "Wave Depolarization Matrix," NTC 1976.

[57] T. Oguchi, "Rain Depolarization Studies At Centimeter And Millimeter Wavelengths: Theory And Measurement," Journal of the Radio Research Labs., Vol. 22, No. 109, 1975.

[58] T. S. Chu, "Microwave Depolarization of an Earth-Space Path," Bell System Technical Journal, Vol. 59, No. 6, July-August 1980.

[59] D. F. DiFonzo and W. S. Trachtman, "Antenna Depolarization Measurements Using Satellite Signals," COMSAT Technical Review, Vol. 8, No. 1, Spring 1978.

[60] R. A. Semplak, "Simultaneous Measurements Of Depolarization By Rain Using Linear And Circular Polarizations At 18 GHz," The Bell System Technical Journal, Vol. 53, February 1974.

[61] F. T. Tseng and C. S. Cheng, "Satellite Wave Polarization Measurement," NTC 1976.

[62] T. S. Chu, "Restoring The Orthogonality Of Two Polarizations In Radio Communication Systems, I," The Bell System Technical Journal, Vol. 50, No. 9, November 1971.

[63] T. S. Chu, "Restoring The Orthogonality Of Two Polarizations In Radio Communication Systems, II," The Bell System Technical Journal, Vol. 52, No. 3, March 1973.

[64] R. W. Kreutel, "The Orthogonalization Of Polarized Fields In Dual-Polarized Radio Transmission Systems," COMSAT Technical Review, Vol. 3, No. 2, Fall 1973.

[65] D. F. DiFonzo, W. S. Trachtman and A. E. Williams, "Adaptive Polarization Control For Satellite Frequency Reuse Systems," COMSAT Technical Review, Vol. 6, No. 2, Fall 1976.

[66] A. E. Williams, "A Dual-Polarized 4/6-GHz Adaptive Polarization Control Network," COMSAT Technical Review, Vol. 7, No. 1, Spring 1977.

[67] Lin-Shan Lee, "The Vector Space-Formulation Of The Rain Crosspolarization Problem And Its Compensations," IEEE Trans. on Communications, Vol. COM-27, No. 2, February 1979.

[68] L. Lee, "A Polarization Control System For Satellite Communications With Multiple Uplinks," IEEE Trans. on Communications, Vol. COM-26, No. 8, August 1978.

69] W. P. Overstreet And C. W. Bostian, "Crosstalk Cancellation On Linearly And Circularly Polarized Communications Satellite Links," Radio Science, Vol. 14, No. 6, November-December 1979.

[70] N. Amitay, "Signal-to-Noise Ratio Statistics For Nondispersive Fading In Radio Channels With Cross Polarization Interference Cancellation," IEEE Trans. on Communications, Vol. COM-27, No. 2, February 1979.

[71] A. F. Culmone, "Polarization Diversity With Adaptive Channel Decoupling," NTC, New Orleans, December 1975.

[72] H. Kannowade, "An Automatic Control System For Compensating Cross-Polarization Coupling In Frequency-Reuse Communication Systems," IEEE Trans. On Communications, Vol. COM-24, No. 9, September 1976.

[73] B. D. Cullen, A. Gianatasio, G. Pelchat and L. R. Young, "Spectrum-Reuse By Adaptive Polarization Separation," NTC, New Orleans, December 1975.

[74] J. T. Cordaro, Jr. and Terry J. Wagner, "Intersymbol Interference On A Continuous-Time Gaussian Channel," IEEE Trans. on Information Theory, Vol. IT-16, No. 4, July 1970.

[75] D. W. Tufts, "Nyquist's Problem -The Joint Optimization Of Transmitter And Receiver In Pulse Amplitude Modulation," Proceedings of the IEEE, March 1965.

[76] I. Gerst and J. Diamond, "The Elimination Of Intersymbol Interference By Input Signal Shaping," Proceedings of the IRE, July 1961.

[77] J. J. Jones, "Filter Distortion And Intersymbol Interference Effects On PSK Signals," IEEE Trans. on Communication Technology, Vol. COM-19, No. 2, April 1971.

[78] N. J. Bershad and P. A. Vena, "Eliminating Intersymbol Interference -A State-Space Approach," IEEE Trans. on Information Theory, Vol.IT-18, No. 2, March 1972.

[79] M. R. Aaron, D. W. Tufts, "Intersymbol Interference And Error Probability," IEEE Trans. on Information Theory, Vol. 12, No. 1, January 1966.

[80] G. David Forney, Jr., "Maximum-Likelihood Sequence Estimation Of Digital Sequences In The Presence Of Intersymbol Interference," IEEE Trans. on Information Theory, May 1972.

[81] F. L. Vermeulen and M. E. Hellman, "Reduced State Viterbi Decoders For Channels With Intersymbol Interference," Dept. Of Electrical Engineering, Stanford University, Stanford, California.

[82] David Chase, "A Combined Coding And Modulation Approach For Communication Over Dispersive Channels," IEEE Trans. on Communication Technology, June 1969.

[83] P. A. Bello and D. Chase, "A Combined Coding And Modulation Approach For High-Speed Date Transmission Over Troposcatter Channels," NTC 1975.

[84] J. F. Pieper, et al, "Design Of Efficient Coding And Modulation For A Rayleigh Fading Channel," IEEE Trans. on Information Theory, Vol. IT-24, No. 4, July 1978.

[85] J. B. Anderson and D. P. Taylor, "A Bandwidth-Efficient Class Of Signal-Space Codes," IEEE Trans. on Information Theory, Vol. IT-24, No. 6, November 1978.

[86] E. C. Van Der Meulen, "A Survey Of Multi-Way Channels In Information Theory: 1961-1976," IEEE Trans. on Information Theory, Vol. IT-23, No. 1, January 1977.

[87] T. M. Cover, "Broadcast Channels," IEEE Trans. on Information Theory, Vol. IT-18, No. 1, January 1972.

[88] T. M. Cover, "An Achievable Rate Region For The Broadcast Channel," IEEE Trans. on Information Theory, Vol. IT-21, No. 4, July 1975.

[89] T. Kasami and S. Lin, "Coding For A Multiple-Access Channel," IEEE Trans. on Information Theory, Vol. IT-22, No. 2, March 1976.

[90] E. J. Weldon, Jr., "Coding For A Multiple-Access Channel," Information and Control, 36, 1978.

[91] M. Ohkubo, "Universal Coding For Multiple-Access Channels," IEEE Trans. on Information Theory, Vol. IT-27, No. 6, November 1981.

[92] R. Peterson and D. J. Costello, Jr., "Binary Convolutional Codes For A Multiple-Access Channel," IEEE Trans. on Information Theory, Vol. IT-25, No. 1, January 1979.

[93] P. P. Bergmans and T. M. Cover, "Cooperative Broadcasting," IEEE Trans. on Information Theory, Vol. IT-20, No. 3, May 1974.

[94] D. Slepian and J. K. Wolf, "Noiseless Coding Of Correlated Information Sources," IEEE Trans. on Information Theory, Vol. IT-19, No. 4, July 1973.

[95] M. L. Ulrey, "The Capacity Region Of A Channel With S Senders And R Receivers," Information and Control, 29, 1975.

[96] R. Ahlswede, "The Capacity Region Of A Channel With Two Senders And Two Receivers," The Annals of Probability, Vol. 2, No. 5, 1974.

[97] H. Sato, "Two-User Communication Channels," IEEE Trans. on Information Theory, Vol. IT-23, No. 3, May 1977.

[98] H. Sato, "On The Capacity Region Of A Discrete Two-User Channel For Strong Interference," IEEE Trans. on Information Theory, Vol. IT-24, No. 3, May 1978.

[99] G. R. Welti and J. S. Lee, "Digital Transmission With Coherent Four-Dimensional Modulation," IEEE Trans. on Information Theory, Vol. IT-20, No. 4, July 1974.

[100] G. R. Welti, "PCM/FDMA Satellite Telephony With 4-Dimensionally-Coded Quadrature Amplitude Modulation," COMSAT Technical Review, Vol. 6, No. 2, Fall 1976.

[101] G. R. Welti, "SCPC Satellite Telephony With 4-Dimensionally-Coded Quadrature Amplitude Modulation," COMSAT Technical Review, Vol. 7, No. 1, Spring 1977.

[102] S. G. Wilson, P. J. Schottler and H. A. Sleeper, "Rate 3/4 16-PSK Phase Codes," IEEE International Conference on Communications, Philadelphia, June 1982, Vol. 3 of 3.

[103] W. L. Cook, "Interactive Computer Simulation of Satellite Transmission Systems," Proceedings of the Fifth Annual Pittsburgh Conference on Modeling and Simulation, Vol. 5, April 1974.

[104] L. C. Palmer and S. Lebowitz, "Including Synchronization in Time-Domain Channel Simulations," COMSAT Technical Review, Vol. 7, No. 2, Fall 1977.

[105] V. K. Prabhu and L. H. Enloe, "Interchannel Interference Considerations In Angle-Modulated Systems," The Bell System Technical Journal, September 1969.

[106] A. S. Rosenbaum, "PSK Error Performance With Gaussian Noise And Interference," The Bell System Technical Journal, February 1969.

[107] J. Hui, "Joint Coding And Modulation Designs For Band-limited Satellite Channels," Master's Thesis, Dept. of Electrical Engineering and Computer Science, Massachusetts Institute of Technology, 1981